



Graduate School of  
Systemic Neurosciences  
LMU Munich



LUDWIG-MAXIMILIANS-UNIVERSITÄT MÜNCHEN  
GRADUATE SCHOOL OF SYSTEMIC NEUROSCIENCES

PHD THESIS

---

**DISCOVERY AND CHARACTERIZATION OF NOVEL DRUGS  
FOR TREATMENT OF ALZHEIMER'S DISEASE FROM A HIGH-  
THROUGHPUT COMPOUND SCREEN**

---

KAMRAN HONARNEJAD

2014



---

**DISCOVERY AND CHARACTERIZATION OF NOVEL DRUGS  
FOR TREATMENT OF ALZHEIMER'S DISEASE FROM A HIGH-  
THROUGHPUT COMPOUND SCREEN**

---

Dissertation  
an der Graduate School of Systemic Neurosciences  
der Ludwig–Maximilians–Universität München

vorgelegt von

Kamran Honarnejad  
aus Teheran

München, 2014



Erstgutachter: Prof. Dr. Jochen Herms  
Zweitgutachter: Prof. Dr. Jacek Kuźnicki  
Tag der mündlichen Prüfung: 05.08.2014



## TABLE OF CONTENTS

<b>1</b>	<b><u>SUMMARY.....</u></b>	<b>1</b>
<b>2</b>	<b><u>INTRODUCTION.....</u></b>	<b>5</b>
2.1	ALZHEIMER'S DISEASE .....	5
2.2	CALCIUM SIGNALING IN HEALTH AND DISEASE .....	7
2.3	IMPAIRMENT OF CALCIUM HOMEOSTASIS IN ALZHEIMER'S DISEASE.....	7
2.4	APP PROCESSING AND AMYLOID PATHOLOGY IN AD .....	8
2.5	THE INTERPLAY BETWEEN CALCIUM AND AMYLOID PATHOLOGY IN AD.....	11
2.6	CONNECTION BETWEEN CALCIUM AND TAU PATHOLOGY IN AD .....	12
2.7	MITOCHONDRIAL DYSFUNCTION IN ALZHEIMER'S DISEASE .....	13
2.8	THE THERAPY OF ALZHEIMER'S DISEASE .....	15
2.8.1	SYMPTOMATIC THERAPY .....	15
2.8.2	DISEASE-MODIFYING THERAPY .....	16
2.8.2.1	AMYLOID-TARGETED THERAPIES .....	16
2.8.2.2	TAU-TARGETED THERAPIES.....	18
2.8.2.3	ALTERNATIVE THERAPIES .....	19
2.9	THE DEVELOPMENT STATUS OF CALCIUM SIGNALING-TARGETED THERAPIES FOR AD. 19	
2.9.1	PHARMACOLOGICAL MODULATION OF EXTRACELLULAR CALCIUM FLUX.....	19
2.9.1.1	RECEPTOR-OPERATED CALCIUM CHANNELS (ROCC) .....	19
2.9.1.2	VOLTAGE-GATED CALCIUM CHANNELS (VGCC).....	20
2.9.2	PHARMACOLOGICAL MODULATION OF ER CALCIUM SIGNALING.....	20
2.10	CALCIUM IMAGING .....	21
<b>3</b>	<b><u>PRESENILINS: ROLE IN CALCIUM HOMEOSTASIS .....</u></b>	<b>23</b>
3.1	ABSTRACT.....	24
3.2	INTRODUCTION.....	25
3.3	STRUCTURE .....	25
3.4	EXPRESSION, ACTIVATION AND TURNOVER .....	26
3.5	ROLE IN CALCIUM HOMEOSTASIS .....	26
3.6	PS AS A THERAPEUTIC TARGET FOR ALZHEIMER'S DISEASE TREATMENT .....	30
<b>4</b>	<b><u>AIM OF THE STUDY .....</u></b>	<b>33</b>
<b>5</b>	<b><u>INVOLVEMENT OF PRESENILIN HOLOPROTEIN UPREGULATION IN CALCIUM DYSHOMEOSTASIS OF ALZHEIMER'S DISEASE .....</u></b>	<b>35</b>
5.1	ABSTRACT.....	36
5.2	INTRODUCTION.....	37
5.3	MATERIALS AND METHODS .....	38
5.3.1	CELL CULTURE AND CELL LINES.....	38
5.3.2	CALCIUM IMAGING .....	38
5.3.3	TREATMENT WITH $\gamma$ -SECRETASE INHIBITORS .....	39

5.3.4	WESTERN BLOT .....	39
5.3.5	HUMAN SUBJECTS .....	40
<b>5.4</b>	<b>RESULTS.....</b>	<b>40</b>
5.4.1	EFFECT OF PS1 HOLOPROTEIN OVEREXPRESSION ON CALCIUM RELEASE FROM ER.....	40
5.4.2	EFFECT OF $\gamma$ -SECRETASE INHIBITORS ON CALCIUM RELEASE FROM ER .....	41
5.4.3	EFFECT OF PEN-2 KNOCKDOWN ON ER CALCIUM RELEASE.....	42
5.4.4	PS1 HOLOPROTEIN IN BRAINS OF FAD-PS1 PATIENTS.....	43
<b>5.5</b>	<b>DISCUSSION .....</b>	<b>43</b>

**6 DEVELOPMENT AND IMPLEMENTATION OF A HIGH-THROUGHPUT COMPOUND SCREENING ASSAY FOR TARGETING DISRUPTED ER CALCIUM HOMEOSTASIS IN ALZHEIMER'S DISEASE .....** **55**

<b>6.1</b>	<b>ABSTRACT .....</b>	<b>56</b>
<b>6.2</b>	<b>INTRODUCTION .....</b>	<b>57</b>
<b>6.3</b>	<b>MATERIALS AND METHODS .....</b>	<b>58</b>
6.3.1	CELL CULTURE AND CELL LINES .....	58
6.3.2	COMPOUND LIBRARY .....	58
6.3.3	HIGH-THROUGHPUT CALCIUM IMAGING ASSAY AND AUTOMATED IMAGE ANALYSIS .....	58
6.3.4	DATA MINING .....	60
6.3.5	CYTOTOXICITY ASSAY .....	60
6.3.6	AB MEASUREMENTS .....	60
6.3.7	SAPPA AND SAPPB MEASUREMENTS.....	61
6.3.8	AMPK ACTIVITY ASSAY .....	62
6.3.9	STATISTICAL DATA ANALYSIS.....	62
<b>6.4</b>	<b>RESULTS.....</b>	<b>63</b>
6.4.1	FAD-PS1 MUTATIONS ENHANCE THE AMPLITUDE OF CCh-INDUCED CALCIUM RELEASE AND THE NUMBER OF RESPONSIVE CELLS .....	63
6.4.2	HIGH-THROUGHPUT COMPOUND SCREENING ASSAY ENABLES THE DISCOVERY NOVEL LEAD STRUCTURES .....	63
6.4.3	EFFECT OF BEPRIDIL ON CCh-EVOKED CALCIUM RELEASE FROM ER.....	66
6.4.4	EFFECT OF BEPRIDIL ON APP PROCESSING AND AB GENERATION .....	67
6.4.5	EFFECT OF BEPRIDIL ON AMPK ACTIVITY .....	67
<b>6.5</b>	<b>DISCUSSION .....</b>	<b>68</b>

**7 IDENTIFICATION OF TETRAHYDROCARBAZOLES AS NOVEL MULTIFACTORIAL DRUG CANDIDATES IN THE TREATMENT OF ALZHEIMER'S DISEASE .....** **91**

<b>7.1</b>	<b>ABSTRACT .....</b>	<b>92</b>
<b>7.2</b>	<b>INTRODUCTION .....</b>	<b>93</b>
<b>7.3</b>	<b>MATERIAL AND METHODS.....</b>	<b>94</b>
7.3.1	CELL CULTURE AND CELL LINES .....	94
7.3.2	AUTOMATED HIGH-THROUGHPUT FRET-BASED CALCIUM IMAGING AND IMAGE ANALYSIS .....	94
7.3.3	MITOCHONDRIAL MEMBRANE POTENTIAL TMRM ASSAY .....	96
7.3.4	AB MEASUREMENTS .....	96
7.3.5	SAPPA AND SAPPB MEASUREMENTS.....	97
7.3.6	STATISTICAL DATA ANALYSIS.....	97
<b>7.4</b>	<b>RESULTS.....</b>	<b>98</b>
7.4.1	DISCOVERY OF A NOVEL LEAD STRUCTURE FROM A HIGH-THROUGHPUT COMPOUND SCREEN TARGETING DISRUPTED ER CALCIUM HOMEOSTASIS .....	98



7.4.2	TETRAHYDROCARBAZOLES ATTENUATE THE FAD-PS1 MEDIATED EXAGGERATED ER CALCIUM RELEASE .....	99
7.4.3	TETRAHYDROCARBAZOLES INCREASE THE MITOCHONDRIAL MEMBRANE POTENTIAL .....	99
7.4.4	TETRAHYDROCARBAZOLES LOWER Aβ PEPTIDE PRODUCTION .....	100
7.5	DISCUSSION .....	101
7.6	SUPPLEMENTARY MATERIAL.....	122
<b>8</b>	<b><u>GENERAL DISCUSSION.....</u></b>	<b>123</b>
8.1	THE ROLE OF PRESENILIN HOLOPROTEIN UPREGULATION IN AD-ASSOCIATED CALCIUM DYSHOMEOSTASIS .....	123
8.2	DEVELOPMENT OF A HIGH-THROUGHPUT FRET-BASED CALCIUM IMAGING ASSAY FOR DRUG SCREENING IN AD .....	125
8.3	HIGH-THROUGHPUT SCREENING OF COMPOUND LIBRARIES, DISCOVERY AND CHARACTERIZATION OF NOVEL DRUGS FOR TREATMENT OF AD .....	128
<b>9</b>	<b><u>REFERENCES.....</u></b>	<b>131</b>
<b>10</b>	<b><u>ACKNOWLEDGMENTS.....</u></b>	<b>159</b>
<b>11</b>	<b><u>CURRICULUM VITAE .....</u></b>	<b>161</b>



تقدیم بہ پدر و مادرم

**TO MY PARENTS**

WITHOUT WHOM NONE OF MY SUCCESS WOULD HAVE BEEN

POSSIBLE



## 1 Summary

Alzheimer's disease (AD) is a progressive neurodegenerative brain disorder and the most frequent cause of dementia. To date, there are few approved symptomatic drugs for treatment of AD, which show little or no effect on disease progression. Impaired intracellular calcium homeostasis is one of the underlying mechanisms responsible for synaptic dysfunction. In addition, calcium dysregulation is believed to occur early in the cascade of events leading to AD. Mutations in presenilins (PS1 and PS2) account for the vast majority of early onset familial Alzheimer's disease cases (FAD). Beside the well-investigated role of presenilins as the catalytic unit in  $\gamma$ -secretase complex, their involvement in regulation of intracellular calcium homeostasis has recently gained growing attention in AD research.

In brief, within this study we characterized the role of presenilin mutations in AD-associated impairment of endoplasmic reticulum (ER) calcium homeostasis. Based on those findings, we examined the possibility of pharmacologically reversing the disrupted calcium homeostasis in the ER as an innovative approach for AD drug discovery. Therefore, we developed a fully automated high-throughput calcium imaging assay utilizing a genetically-encoded calcium sensor and subsequently screened a large collection of compounds. High-throughput drug screening led to the identification of a number of novel drug candidates that were characterized and validated for their relevance in AD therapy using a number of secondary assays.

In the first part of this work, we reveal that the overexpression of PS1 full-length holoprotein, in particular familial Alzheimer's disease-causing forms of PS1 (FAD-PS1), result in significantly attenuated calcium release from thapsigargin- and bradykinin-sensitive ER calcium stores. Interestingly, treatment of HEK293 cells with  $\gamma$ -secretase inhibitors also lead to decreased amount of calcium release from ER accompanying elevated PS1 holoprotein levels. Similarly, the knockdown of PEN-2 that is associated with deficient PS1 endoproteolysis and accumulation of its holoprotein form also leads to decreased ER calcium release. Notably, we detected enhanced PS1 holoprotein levels in postmortem brains of patients harboring FAD-PS1 mutations. Taken together, the

conditions in which the amount of full-length PS1 holoprotein is enhanced often resulted in decreased calcium release from ER. Based on these results and the proposed leak channel activity of presenilins in the ER, we suggest that the disturbed ER calcium homeostasis mediated by the elevation of PS1 holoprotein levels may be a contributing factor to the pathogenesis of AD.

On the other hand, we also found that FAD-PS1 mutations cause remarkably enhanced muscarinic agonist-evoked calcium release from ER, a mechanism that may potentially compensate for the lowered ER calcium content. In the second part of the work, we aimed at screening compounds that can reverse the potentiated muscarinic agonist-evoked calcium release in FAD-PS1-expressing cells, as a robust phenotypic readout. Accordingly, we developed a fully automated high-throughput calcium imaging assay utilizing a FRET-based calcium indicator at single-cell resolution for compound screening. Initially, we employed the developed assay for a pilot screen with a library of 72 known ion channel ligands. This led to the identification of Bepridil, a calcium channel antagonist drug, which was capable of partially reversing the potentiated FAD-PS1-induced ER calcium release from ER. We detected increased AMPK activity upon treatment of cells with Bepridil in a dose-dependent manner. AMPK activation by Bepridil is most likely a calcium-dependent phenomenon, since CaMKK inhibition by STO-609 abolishes the Bepridil-induced AMPK activation. In accordance with another study, we detected lowered Amyloid- $\beta$  ( $A\beta$ ) peptide production, increased sAPP $\alpha$  and decreased sAPP $\beta$  levels upon Bepridil treatment. Therefore, based on the results here, we propose a novel calcium-dependent mode of action for Bepridil that through activation of AMPK can shift the balance of downstream APP processing from amyloidogenic  $\beta$ -cleavage towards non-amyloidogenic  $\alpha$ -cleavage.

In the third and final part of this work, we performed a truly high-throughput compound screen with a diverse library of 20,000 small molecules. This novel screen yielded five lead structures identified upon structure-activity-relationship analysis. Amongst them were tetrahydrocarbazoles, a novel multifactorial class of compounds that can reverse the impaired ER calcium homeostasis. We found that tetrahydrocarbazole lead structure, firstly, dampens the potentiated calcium release from ER in HEK293 cells expressing FAD-PS1 mutations. Secondly, the lead structure also improves mitochondrial function, measured by increased mitochondrial membrane potential. Thirdly, the same lead

structure also attenuates the production of A $\beta$  peptides by decreasing the cleavage of Amyloid Precursor Protein (APP) by  $\beta$ -secretase, without notably affecting  $\alpha$ - and  $\gamma$ -secretase cleavage activities. Considering tetrahydrocarbazoles' multiple modes of action by addressing three key pathological aspects of AD, this compound class holds promise for development of a potentially effective AD drug candidate.



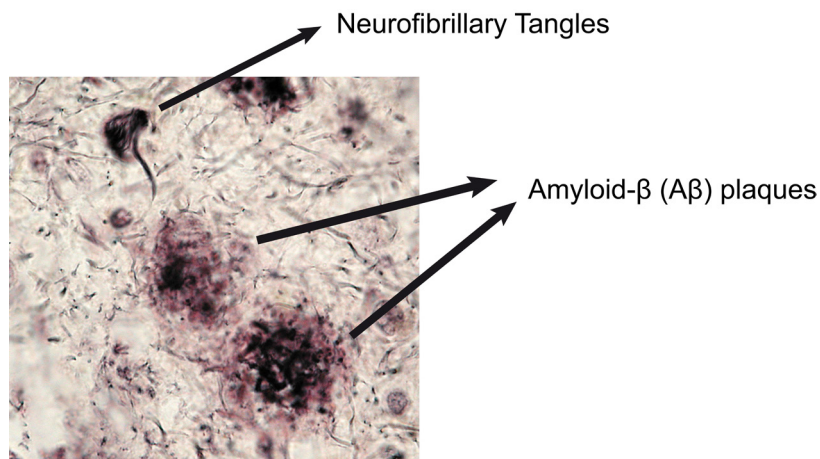


## 2 Introduction

### 2.1 Alzheimer's disease

Alzheimer's disease (AD) is the most common form of dementia and a growing threat to our aging society [1]. This progressive neurodegenerative disorder is characterized by global cognitive decline involving memory, orientation, judgment, and reasoning [2]. The estimations suggest that currently over 22 million patients are suffering from AD worldwide [1]. AD was described for the first time over a hundred years ago by Alois Alzheimer, a German psychiatrist and neuropathologist as "*eine eigenartige Erkrankung der Hirnrinde*" (a peculiar disease of the cerebral cortex) [3]. That work was based on monitoring the long-term clinical course of his first AD case Mrs. Auguste Deter, a 51-year-old lady whom was admitted to Frankfurt community psychiatric hospital for paranoia, progressive sleep and memory disturbance, aggression, and confusion [4]. After the death of the patient 5 years later, in the microscopic preparations of her brain autopsies, Dr. Alzheimer detected the presence of distinctive deposits, which he would describe them as "miliary bodies" and "dense bundles of fibrils", that later respectively became known as amyloid plaques and neurofibrillary tangles [3, 5].

The majority of AD cases are sporadic with no obvious implication of genetic factors and the typical age of onset older than 65 [6]. Age is the principal risk factor of developing sporadic AD [7]. After the age of 65, the overall prevalence of AD doubles every five years [8]. However, in less than 1% of AD patients, known as familial Alzheimer's disease (FAD) cases, the dominantly inherited mutations in Amyloid Precursor Protein (APP), Presenilin-1 and Presenilin-2 (PS1 and PS2) genes lead to early-onset cases of AD [9]. While sporadic and familial AD follow a very similar course, in the case of familial AD the disease progression rate is much faster [10].



**Figure 2.1. Original microscopic brain preparation of the first AD case described by A. Alzheimer**

The presence of amyloid plaques and neurofibrillary tangles in brain autopsies of Auguste Deter, the first AD case described by Alois Alzheimer (Source: Archives of Center for Neuropathology and Prion Research, Ludwig Maximilian University of Munich).

Today after more than a century from the discovery of AD, despite the countless breakthroughs in understanding the underlying mechanisms governing the disease progression, the etiology of AD (in particular sporadic AD) remains largely unknown [11]. The latter is thought to be one of the reasons for the very little success in the development of effective AD therapies [12]. The current AD treatments are very insufficient and the few approved AD drugs in the market show symptomatic relief at the best and only delay the progression of the disease temporarily [1, 13]. The major hallmarks of AD are the accumulation of intracellular neurofibrillary tangles and extracellular plaques of amyloid beta ( $A\beta$ ) protein in the brain [5]. In accordance, the current AD drug development strategies mainly focus on targeting these two major disease hallmarks [14-16]. However, those events correspond to late stages of AD during which the irreversible brain damage has likely already occurred [17]. In view of the unsuccessful outcome of all clinical trials with  $A\beta$ -targeted drug candidates so far, it is suggested that in future clinical trials, drugs should be administered early enough to asymptomatic patients as a preventative measure [18-21]. In addition, it is not fully understood whether  $A\beta$  plaque and tangle pathologies are the actual causes or rather the symptoms of AD [22]. Those are some of the possible reasons for the consistent recent failure of disease-modifying drug candidates targeting  $A\beta$  and tangle pathologies in late clinical phases.

## 2.2 Calcium signaling in health and disease

Calcium is a key second messenger involved in regulation of many physiological and pathological processes. Learning and memory, muscle contraction, synaptic transmission, secretion, motility, membrane trafficking, excitability, gene expression, and cell division are examples of processes that are being regulated by calcium signaling [23]. Therefore regulation of calcium homeostasis in space, time and magnitude is essential for the cellular function and viability [24]. Neurons maintain this tight regulation through a set of machinery consisting of calcium buffers, binding proteins, pumps and sequestering mechanisms [25]. The cytosolic calcium concentration is particularly regulated by the action of receptor-operated, voltage-gated, and store-operated calcium channels located in the plasma or ER membrane. The calcium concentration in the ER lumen is more than 1000-fold higher than in the cytosol [26]. The basal cytosolic concentration is maintained at very low levels (50-300 nM) and only after activation by extracellular influx or from intracellular stores, it rapidly reaches low micromolar levels [22]. Too high cytosolic calcium concentrations lead to cell death, whereas too low levels impair neuronal function [27]. Liberation of calcium from ER into the cytosol is mediated through two major calcium channels on the ER membrane, one being inositol-1,4,5- triphosphate receptors (IP<sub>3</sub>R) and the other one Ryanodine receptors (RyR). The IP<sub>3</sub>R are activated by binding of IP<sub>3</sub> molecule, which is generated by stimulating G-protein-coupled receptors on the plasma membrane by agonists (Figure 3.2). Only in the presence of IP<sub>3</sub>, calcium ions can potentiate the calcium release from IP<sub>3</sub>R [28]. In addition, RyRs are activated directly by calcium ions through a process known as “calcium-induced calcium release” (CICR), while substances like caffeine can enhance the sensitivity of RyR to its native activator calcium [22, 24, 29, 30]. The tight regulation of ER calcium release is crucial for rapid neuronal responses to synaptic inputs, action potentials and synaptic plasticity [31].

## 2.3 Impairment of calcium homeostasis in Alzheimer’s disease

Among many different hypotheses, it is believed that calcium dysregulation plays a key role in the pathophysiology of AD [22, 32]. Disrupted cellular calcium homeostasis impairs synaptic plasticity, mitochondrial function, membrane excitability, APP processing, Tau phosphorylation and increases susceptibility to apoptosis, practically all

being features of AD [33]. The involvement of calcium dyshomeostasis in the pathogenesis of AD has been acknowledged over the last 2 decades [34, 35]. In late 80s and early 90s, Zaven Khachaturian postulated a role for disrupted calcium homeostasis in aging and pathogenesis of AD. He suggested that lifelong impairment of calcium homeostasis eventually results in neurodegeneration [31]. Even prior to that, indirect cues indicated the activation of calcium-dependent proteins in postmortem brains of AD patients, pointing towards the involvement of calcium in AD pathogenesis [36]. Interestingly, Memantine, one of the only few approved drugs for treatment of moderate-to-severe AD, is an NMDA receptor antagonist, which by inhibition of sustained calcium influx leads to stabilization of intracellular calcium homeostasis [37].

Long preceding the manifestation of pathological hallmarks and cognitive deficits in AD [25], the intracellular neural calcium homeostasis is likely to be altered due to either aging or alternatively by familial Alzheimer's disease linked mutations in the Presenilin genes (FAD-PS) [38-41, 42; discussed in section 3]. It is suggested that age-dependent alterations in the calcium homeostasis may lead to altered neuronal excitability, a phenomenon similar the effect of FAD-PS mutations [42-45]. Moreover, impaired calcium signaling in peripheral tissues was proposed as diagnostic biomarkers of mild AD [46, 47]. Notably, alterations in ER calcium channels were found to correlate with neurofibrillary and A $\beta$  pathology in AD brain [48]. Furthermore, the long-term disruption of calcium homeostasis triggers and accelerates both A $\beta$  and tangle pathologies [39, 49, 50]. Essentially, AD is believed to be primarily a disorder of synaptic failure [51]. In AD, calcium dysregulation is a proximal event in disease progression which plays a key role in synaptic failure and neuronal loss [52]. Notably, the latter irreversible pathological events correlate best with cognitive loss and the stages of dementia [53, 54].

## **2.4 APP processing and amyloid pathology in AD**

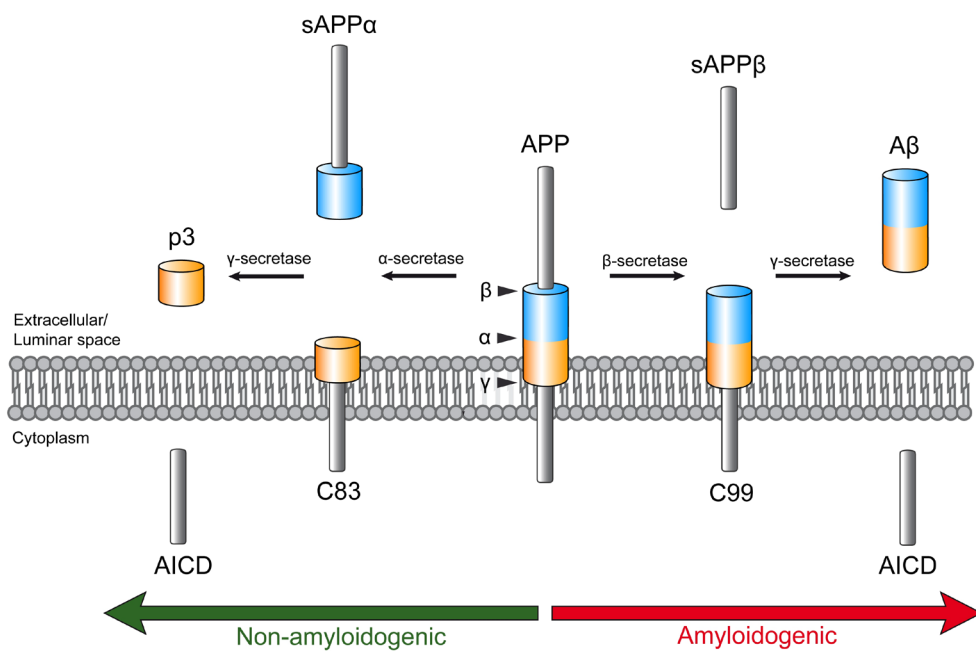
As indicated in section 2.1, one of the AD hallmarks is the generation of amyloid plaques, the extracellular insoluble protein deposits found in the brains of AD patients [55]. The major constituent of the amyloid plaques is a 4 kDa peptide called A $\beta$  which can be ranging from 36-43 amino acids in length [7]. However, A $\beta$  peptides with 40 or 42 amino acids are the most prevalent species [7, 56]. In “amyloid hypothesis”, the accumulation of

A $\beta$  because of imbalanced A $\beta$  production, clearance and aggregation, is believed to initiate a pathogenic cascade ultimately leading to AD [55].

After over 20 years since it was proposed, amyloid hypothesis still dominates the AD field [57]. However, poor correlation between A $\beta$  deposits and the course of AD, substantial differences between early- and late-onset AD cases, pathological assessments indicating the secondary nature of lesions/proteins/cascades, poor reproducibility of soluble species in the lab, and the irrelevance of synaptic assessment to pathological interpretation, are some of the issues which altogether have resulted in a debate as to how far this hypothesis shall be pursued in the drug discovery of AD [58].

A $\beta$  is the product of regulated intramembrane proteolysis (RIP) of Amyloid Precursor Protein (APP) [55, 59]. APP is a type I transmembrane protein which can be cleaved by three different enzymes:  $\alpha$ -secretase and  $\beta$ -secretase in the extracellular domain and  $\gamma$ -secretase in the transmembrane region [60]. In the amyloidogenic pathway, A $\beta$  is generated from the sequential proteolytic cleavage of APP, first at  $\beta$ -site by a  $\beta$ -secretase called BACE ( $\beta$ -site APP cleaving enzyme), followed by PS-containing  $\gamma$ -secretase complex at the  $\gamma$ -site of APP [32]. Alternatively, in a competing non-amyloidogenic pathway,  $\alpha$ -secretase can cleave APP at  $\alpha$ -site within the A $\beta$  domain to preclude A $\beta$  generation [60] (Figure 2.2).

The  $\beta$ -cleavage takes place within the ectodomain of APP in close proximity of the transmembrane domain. Soluble APP ectodomain (sAPP $\beta$ ) and membrane-bound C-terminal fragment C99 are the products of APP cleavage with  $\beta$ -secretase. Subsequently, C99 is cleaved by  $\gamma$ -secretase resulting in secretion of A $\beta$  in the extracellular and the formation of the APP intracellular domain (AICD). Alternatively, in the non-amyloidogenic pathway, from the cleavage of APP with metalloprotease  $\alpha$ -secretase, soluble APP ectodomain (sAPP $\alpha$ ) and a C-terminal fragment (C83) are produced. Next, C83 is cleaved by  $\gamma$ -secretase resulting in secretion of p3 peptide (3 kDa) and generation of AICD [61, 62] (Figure 2.2).



**Figure 2.2. APP processing by  $\alpha$ -,  $\beta$ - and  $\gamma$ -secretase**

In amyloidogenic processing of APP, A $\beta$  is generated from the sequential cleavage by  $\beta$ -secretase and  $\gamma$ -secretase. However, in non-amyloidogenic pathway, the cleavage of APP with  $\alpha$ -secretase within the A $\beta$  domain precludes the formation of A $\beta$  [Adapted from Lichtenthaler et al., Reference number 61].

Currently most attempts in AD drug development are targeted at A $\beta$  pathology [63]. These approaches aim at inhibition or modulation of the proteolytic cleavage of APP in order to decrease the neurotoxic A $\beta$  formation, enhance A $\beta$  clearance using immunotherapy, influence A $\beta$  aggregation, neutralize A $\beta$  toxicity, or remove existing A $\beta$  aggregates [14, 57].

While our understanding of pathological versus physiological roles of APP and A $\beta$  are rather limited [64, 65], there seems to be also a certain level of uncertainty as to which type of A $\beta$  is the most relevant species to be targeted in anti-A $\beta$  therapy [66]. In addition, it is not fully understood how much decrease in A $\beta$  burden is optimal to yield clinical efficacy. Furthermore, many AD clinical trials so far did not address disease modification at the right progression stage and with the right AD patient population category [67].

## 2.5 The interplay between calcium and amyloid pathology in AD

The connection between calcium and A $\beta$  pathology is mutual. Calcium triggers A $\beta$  pathology, but also gets triggered by it [49]. The maintenance of low cytosolic calcium concentration with respect to extracellular environment and intracellular stores is essential for the neuronal function [68]. High cytosolic calcium concentrations, originated either from extracellular calcium influx or from intracellular stores increase A $\beta$  production, aggregation, and A $\beta$ 42:A $\beta$ 40 ratio [22, 50, 69-76]. The knockdown of two main components of ER calcium homeostasis, namely IP<sub>3</sub>R and SERCA2b, was shown to mediate decreased A $\beta$  generation [69, 72]. How disrupted calcium homeostasis exactly contributes to amplified A $\beta$  pathology is not yet fully understood. Nevertheless, it seems that calcium affects several factors involved in APP processing. For example, it has been demonstrated that calcium can enhance the BACE1 proteolytic activity [39].

On the other hand, already in early 90s, Mattson and colleagues could show that A $\beta$  causes destabilization of neuronal calcium homeostasis and consequently vulnerability to excitotoxicity [77]. The role on A $\beta$  in disrupting cellular calcium homeostasis is mainly attributed to the stimulated calcium influx from extracellular [78]. Several modes of action have been proposed to explain the A $\beta$ -dependent enhanced calcium influx. For example A $\beta$  oligomers have been shown to directly form pores on lipid bilayers [79-81], disrupt membranes [82, 83], form ROS causing lipid peroxidation [84] or impair membrane ATPase activity [85]. A $\beta$  oligomers have been also shown to modulate the activity of NMDA receptors [86] and thus lead to NMDA-mediated excitotoxicity [87], while on the other hand suppress the activity of P/Q-type voltage-gated calcium channels [88]. 2-photon *in vivo* calcium imaging in AD mouse models has revealed that there are clusters of hyperactive neurons and calcium overload in neurites in close proximity of senile plaques [89, 90]. On the other hand, a recent study found no correlation between the evoked calcium responses and the distance from A $\beta$  plaques in pyramidal hippocampal CA1 neurons of an APP/PS1 mouse model of AD [91].

Interestingly upon exposure of cortical neurons with extracellular A $\beta$ 42, a specific upregulation in RyR3 levels can be detected [92]. The latter seems to play a protective role, since the knockdown of RyR3 led to increased neuronal cell death [93]. In contrast,

treatment of PC12 expressing FAD-PS cells with dantrolene an inhibitor of RyR attenuates glutamate and A $\beta$ -induced toxicity [94, 95]. Remarkably, RyR2 isoform is densely expressed in the same brain regions that are most vulnerable in AD pathology, particularly hippocampus, whereas the RyR3 isoform has a diffuse and sparse expression pattern [96]. Furthermore, a recent study also shows that intracellular application A $\beta$ 42 soluble oligomers (but not monomers) causes release of calcium from IP<sub>3</sub>Rs, a mechanism which may contribute to the cytotoxic effects of A $\beta$  [97].

In 6-8 week old presymptomatic 3xTg-AD mice, already a selective upregulation of RyR2 isoform can be detected [98]. Interestingly at this young age, these mice do not show any cognitive or neurophysiological impairment [99]. In agreement with these data, RyR2 mRNA levels were shown to be increased in brain samples from patients with mild-cognitive-impairment (MCI) compared to individuals with no cognitive impairment [100]. Therefore, the upregulation of RyR2 might reflect a compensatory mechanism to normalize the disrupted ER calcium homeostasis in order to maintain a healthy neuronal transmission and plasticity during presymptomatic stages of the disease. However, maintaining this balance over the course of years might influence the disease process. Once the chronic calcium assaults overwhelm those neuronal compensatory mechanisms, the impairments in synaptic plasticity and LTP become apparent and neurodegeneration is likely to occur [101]. On the other hand, high levels of A $\beta$ 42 resembling the later stages of the disease induce specific upregulation of RyR3 isoform [92]

## **2.6 Connection between calcium and tau pathology in AD**

Another hallmark of AD is the accumulation of neurofibrillary tangles in the brain, which are common filamentous inclusions in tauopathies [5, 102]. A strong correlation is found between the neurofibrillary tangle pathology and the severity of AD [103, 104]. These tangles are mainly composed of paired helical filaments of abnormally hyperphosphorylated tau, a microtubule-associated protein [105, 106]. Under physiological conditions soluble tau protein is involved in stabilization of axonal microtubules, however under pathological conditions tau undergoes aggregation due to hyperphosphorylation as a result of imbalanced activity of tau kinases and phosphatases [107, 108]. The activity of many kinases associated with tau hyperphosphorylation is



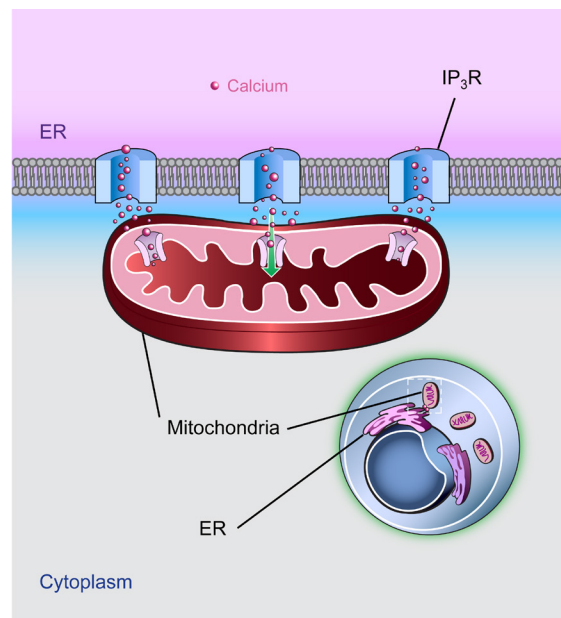
calcium-dependent. For example  $\text{Ca}^{2+}$ /calmodulin-dependent protein kinase II (CaMKII) and its downstream target AMP-activated protein kinase (AMPK) are implicated in Tau phosphorylation [109]. In addition, calcium ions stimulate proteolytic cleavage of p35 to p25 which leads to aberrant activation of kinase 5 (Cdk5), yet another kinase involved in tau phosphorylation [110]. Notably, Memantine can inhibit and reverse tau hyperphosphorylation [111], presumably by stabilization of disrupted cellular calcium homeostasis. Interestingly several proteins involved in calcium signaling are associated with tauopathies. Calpains [112], calcineurin [113], transglutaminase [114] and a novel EF-hand domain-containing calcium-binding protein [115] are examples of that. Similar to the feed-forward relationship between  $\text{A}\beta$  and calcium, there is also a feed-forward relationship between tau hyperphosphorylation and increased intracellular calcium concentrations. It is suggested that extracellular tau by interacting with muscarinic receptors can also promote the release of calcium from ER [116]. This would result in a vicious cycle in which the excess calcium triggers the calcium-activated kinases and tau hyperphosphorylation, compromising the integrity of neuronal processes, altering signaling cascades, and upregulating cholinergic receptor activation coupled to calcium release [41, 117].

## 2.7 Mitochondrial dysfunction in Alzheimer's disease

Mitochondria are dynamic ATP-generating organelles which are responsible for more than 90% of cellular energy production [118]. In particular, due to the limited glycolytic capacity of neurons and their strong dependence on aerobic oxidative phosphorylation, mitochondrial energy production plays an important role in the brain [119]. Mitochondria are implicated in many cellular functions including intracellular calcium homeostasis, alteration of cellular reduction-oxidation potentials, free radical scavenging and activation of caspase-mediated apoptosis [120]. Mitochondria buffer the changes in the local calcium concentration proximal to plasma membrane and ER, regulate calcium flux and modulate the frequency of calcium oscillations [121]. The mitochondrial calcium uptake particularly plays an important role in synaptic transmission at presynapses [122].

Both functionally and physically, ER and mitochondria are interdependent. The interaction between them is mainly through the zones where the two organelles come into

close contact [123]. These zones known as ER-mitochondria-associated-membranes (MEM) are loci of calcium shuttling between ER and mitochondria [124], playing an important role in many fundamental biological processes [125] (Figure 2.3). Particularly, calcium release from IP<sub>3</sub>R to mitochondria is essential for the maintenance of mitochondrial functions [126]. Importantly presenilin mutations have been shown to also modulate the shuttling of calcium between ER and mitochondria [127]. Therefore, it is plausible that the disruption in the ER calcium homeostasis also affects mitochondrial activity. Furthermore, mitochondrial calcium overload is proposed to underlie the oligomeric A $\beta$ -induced toxicity, a phenomenon which can be reversed by non-steroidal anti-inflammatory drugs (NSAIDs) [128].



**Figure 2.3. Shuttling of calcium between ER and mitochondria**

Calcium ions are shuttled between ER and mitochondria at the junctions between the two organelles, known as ER-mitochondria-associated-membranes (MEM). The shuttling is mediated by the IP<sub>3</sub>R at the ER membrane and the calcium uniporter in the inner mitochondrial membrane [Adapted from Collins et al., Reference number 129].

Mitochondrial dysfunction is a key early event in the course of aging and in the pathogenesis many neurodegenerative disorders, including AD [120, 130-135]. Examples of AD-associated mitochondrial dysfunctions are decreased number of neuronal mitochondria, increased mitochondrial DNA content, lowered glucose metabolism, imbalanced mitochondrial fission and fusion, impaired mitochondrial trafficking, and

reduced mitochondrial membrane potential [136-140]. The functions of several crucial mitochondrial enzymes have been demonstrated to be inhibited by A $\beta$  exposure in brain or in isolated mitochondria [141, 142]. Moreover, mitochondrial dysfunction is believed to be implicated in the dysfunction and loss of synapses as well as neuronal apoptosis in AD [51, 143, 144]. In this context, A $\beta$  has been demonstrated to induce mitochondrial dysfunction and morphological changes accompanied by decreased amount of synaptic proteins [145]. Morphological studies indicate a strong correlation between mitochondrial pathology with dystrophic dendrites, loss of dendritic branches and the pathological alteration of the dendritic spines [146]. Therefore, improving mitochondrial function by itself is considered as a viable approach in AD drug development [133, 147-149]. Recently a drug known as Dimebon (Latrepidine) made its way to clinical phase III trials for AD [150]. Despite its late-stage failure, the beneficial biological effects of Dimebon were mainly attributed to improving mitochondrial function [151, 152].

## **2.8 The therapy of Alzheimer's disease**

Currently, all of the AD drugs in the market are symptomatic, whereas the drugs in development are mostly disease-modifying, in the sense that these novel treatments are targeted at the pathological steps leading to AD, with the aim of interfering with the evolution of the disease [15].

### **2.8.1 Symptomatic therapy**

The first drugs developed for AD were acetylcholinesterase inhibitors (AChEI) [15]. These drugs were developed on the basis of the cholinergic hypothesis of AD which argues that the cholinergic deficits, in particular decreased acetylcholine levels and the loss of basal forebrain cholinergic neurons, are implicated in the pathogenesis of AD [153]. Currently there are 3 approved AChEIs in the market for treatment of mild-to-moderate AD patients: Donepezil (Pfizer), Rivastigmine (Novartis) and Galantamine (Janssen) [154]. Tacrine (First Horizon Pharmaceuticals) was the first AChEI approved drug for treatment of AD in 1993, which is not anymore being used due to the damage it causes to the liver [155]. Donepezil is now also approved for treatment of severe AD patients in the US [156]. The development of further cholinergic drugs is still ongoing.

Apart from AChEIs, Memantine (Merz, Forest, and Lundbeck) is a further symptomatic therapeutic option for treatment of moderate-to-severe AD [154]. Memantine is an uncompetitive, moderate-affinity NMDA receptor antagonist, which is believed to protect neurons from excitotoxicity [15, 154].

### **2.8.2 Disease-modifying therapy**

In contrast to the partial success in development of symptomatic drugs for treatment of AD, in spite of huge investments towards the development of Alzheimer's disease-modifying therapies, the field has faced the consistent failure of disease-modifying approaches for AD in preclinical and clinical phases [20].

#### **2.8.2.1 Amyloid-targeted therapies**

On the basis of the widely accepted amyloid hypothesis of AD and its central role in the diagnosis of the disease, the majority of disease-modifying approaches have largely focused on the development of medicines targeting A $\beta$  pathology [154]. In essence, such approaches suggest that excessive levels of A $\beta$  in its different forms, e.g. plaques, soluble oligomers, fibrils, protofibrils... play a causative role in the pathogenesis of AD. Therefore, the removal of such neurotoxic A $\beta$  should result in clinical efficacy. Here, we try to summarize the most important therapeutic interventions targeting A $\beta$  pathology.

##### **2.8.2.1.1 $\beta$ -secretase inhibitors**

Since the first step in APP processing is the  $\beta$ -secretase cleavage, several BACE1 inhibitors have been developed as potential therapeutics for AD. However, BACE1 inhibition turns out to be a challenging approach for two major reasons: Firstly, BACE1 cleaves many substrates beside APP with important physiological roles. Therefore, BACE1 inhibition may cause undesired toxic side effects. Secondly, BACE1 has a relatively wide active site. Therefore, BACE1 inhibitors are often bulky molecules that do not readily cross the blood-brain barrier [14, 154].

Due to such difficulties, only a small number of BACE1 inhibitors entered early clinical trials while the majority of  $\beta$ -secretase inhibitors are still in preclinical stages [157].

#### 2.8.2.1.2 *$\gamma$ -secretase inhibitors and modulators*

$\gamma$ -secretase is a multiprotein complex inside of which presenilins (PS1 and PS2) are responsible for the final enzymatic cleavage of APP that results in formation of A $\beta$ . Similar to  $\beta$ -secretase,  $\gamma$ -secretase also cleaves many transmembrane protein substrates. Accordingly,  $\gamma$ -secretase inhibition was shown to be associated with side-effects which are often related to Notch signaling [158]. Although, several  $\gamma$ -secretase inhibitors reached clinical trials, their late clinical trials were often prematurely interrupted due to toxicity and detrimental effects on cognition and functionality of treated patients. Those side effects are believed to be caused by impaired Notch processing and accumulation of neurotoxic APP-CTF [159]. More recently,  $\gamma$ -secretase inhibitors with high selectivity to APP are being developed [160].

In addition, a particular focus has been put towards the development of  $\gamma$ -secretase modulators (GSMs). GSMs specifically lower the production of amyloidogenic A $\beta$ 42 peptides, while increasing the production of shorter A $\beta$  species (e.g. A $\beta$ 38) [158, 159, 161]. Importantly, GSMs alter APP processing without the Notch-based adverse effects [14]. A subset of non-steroidal anti-inflammatory drugs (NSAIDs), including ibuprofen, indomethacin, and sulindac sulfide, were shown to possess the properties of GSMs [14, 15, 154].

#### 2.8.2.1.3 *$\alpha$ -secretase activators*

Enhancing  $\alpha$ -secretase activity and shifting APP processing towards non-amyloidogenic pathway results in decreased A $\beta$  production and increased levels of neuroprotective sAPP $\alpha$  peptide [64, 162]. Therefore, stimulating  $\alpha$ -secretase activity has been regarded as a valuable approach in AD drug development [163]. Although several  $\alpha$ -secretase activators failed to show desired clinical efficacy, encouraging safety results support the development of further  $\alpha$ -secretase activators with improved clinical efficacies [15, 164].

#### 2.8.2.1.4 *Anti A $\beta$ aggregation drugs*

The hypothesis that A $\beta$  aggregation leads to formation of oligomeric A $\beta$  species that impair synaptic function and plasticity has led to development of drugs which are aimed at preventing A $\beta$  aggregation or destabilizing A $\beta$  oligomers [14]. Glycosaminoglycans

that binds to A $\beta$  monomers and prevent oligomer formation [165], zinc- and copper-chelating compounds which dissolve amyloid deposits [14, 15, 166], and scyllo-inositols which directly bind to A $\beta$  oligomers and promote the dissociation of A $\beta$  aggregates are examples of such drugs [167, 168]. Based on the lack of clear-cut clinical efficacy results, large-scale phase 3 clinical studies are required in order to better evaluate the potential of anti-A $\beta$  aggregation agents as AD therapeutics [14, 15, 154, 162, 168].

#### **2.8.2.1.5 Immunotherapy**

Both active immunization (vaccination) and passive immunization (monoclonal antibodies) are regarded as promising approaches that aim at increasing A $\beta$  clearance which may potentially affect A $\beta$  production, aggregation and deposition [162, 169]. In active immunization, the immune system is stimulated to promote formation of antibodies against pathogenic forms of A $\beta$ , whereas in passive immunotherapy antibodies are delivered exogenously [169]. Although a number of immunotherapy approaches were associated with adverse side effects [14, 170-172], currently several antibodies are under investigation in clinical and preclinical phases for AD [14, 15, 154, 173].

#### **2.8.2.2 Tau-targeted therapies**

On the basis of the hypothesis that tau pathology strongly contributes to the pathogenesis of AD and its strong correlation with the stage of the disease, a number of tau-targeted AD therapeutic approaches are being developed [107, 174]. Amongst them are drugs in clinical trials which are interfering with either tau aggregation or phosphorylation [154, 175-178]. Based on recent immunization studies in AD mouse models, both tau vaccination and the use of tau antibodies were proposed as potential AD therapeutic modalities [179-181]. However, given the fact that tau is an intracellular protein, development of a successful tau immunotherapy appears to be rather challenging [15].

### 2.8.2.3 Alternative therapies

Stem cells, neurotrophins, enhancers of mitochondrial function, anti-inflammatory medications, antioxidants, neuroprotective agents, as well as drugs modulating cholesterol and vascular-related risk factors are some of the alternative approaches currently being investigated in preclinical and clinical stages for AD therapy [14, 154, 162].

## 2.9 The development status of calcium signaling-targeted therapies for AD

### 2.9.1 *Pharmacological modulation of extracellular calcium flux*

#### 2.9.1.1 Receptor-operated calcium channels (ROCC)

Despite efforts in drug discovery and development of ion channel blockers and their promising results in AD animal models, memantine remains to be the first and only clinically approved drug in Europe and North America for treatment of moderate-to-severe AD patients [37, 182, 183]. The beneficial effects of memantine are only marginal [184], however, they are attributed to blockage of NMDA receptor and thus restoring the excess calcium influx to physiological levels. This results in lowered cytosolic calcium concentration, enhanced CCE and increased ER calcium load and in turn potentiated agonist-induced calcium release [185]. EVT 101, a NR2B-selective NMDA receptor antagonist, is currently in clinical trials for AD [186].

A $\beta$ 42 (but not A $\beta$ 40), has been shown to interact and exert inhibitory effects on synaptic AMPA receptors, a phenomenon which may contribute to AD-associated memory impairments [187]. This finding provides an explanation for the observed downscaling of AMPA receptor activity accompanied with memory impairments in APP/PS1 double knock-in AD mouse model [188, 189]. Indeed AMPA receptor activators have been shown to reverse the age-associated memory loss and improve learning in rats, however with no efficacy in AD patients [190]. Interestingly, Dimebon apart from improving mitochondrial activity was shown to block NMDA receptors and potentiate the activity of AMPA receptors as well [191].

### 2.9.1.2 Voltage-gated calcium channels (VGCC)

The involvement of VGCCs in AD is known for quite some time. A $\beta$  has been shown to enhance calcium influx through L-type VGCCs [192]. Therefore blocking VGCC is an interesting target for AD therapy [193]. Nimodipine (an L-type calcium channel antagonist) has been shown to attenuate the neurotoxicity mediated by A $\beta$ -induced potentiation of calcium influx [192] and A $\beta$  accumulation caused by neuronal depolarization and increased cytosolic calcium concentration [74]. However due to mixed results in terms of clinical efficacy of Nimodipine in AD and other dementias, its usefulness still a matter of debate [194]. MEM 1003 is a Nimodipine-related compound, which is currently in late clinical trials for AD [195, 196].

Nimmrich *et al.* demonstrated that A $\beta$  oligomers can impair presynaptic P/Q-type calcium currents at both GABAergic and glutamatergic synapses [88]. Roscovitine is a drug which was shown to enhance the P/Q-type calcium currents [197] and rescue the impaired vesicle trafficking in hippocampal neurons induced by A $\beta$  oligomers [88].

### 2.9.2 Pharmacological modulation of ER calcium signaling

Manipulating ER calcium homeostasis in the context of clinical therapeutics has been so far only rarely investigated and never examined for neurodegenerative diseases. Modulation of the elements involved in the ER calcium homeostasis has been tested in cell culture. Blockade of SERCA pump with Thapsigargin led to increased cytosolic calcium concentration through blocking calcium uptake into ER, caspase-3 activation and thus enhanced apoptosis. Similarly, A $\beta$ -induced apoptosis is also associated with increased cytosolic calcium concentration and caspase-3 activity [198]. However, SERCA2b loss of function by siRNA knockdown or pharmacologically by Thapsigargin or CPA was shown to lower A $\beta$  levels [72, 199]

Blockade of IP<sub>3</sub>R with Xestosponginn B or C, and RyR with dantrolene restores the elevated cytosolic calcium concentrations and protects against A $\beta$ -induced apoptosis [200, 201]. On the other hand, treatment with Caffeine sensitizes FAD-PS1 expressing neurons to A $\beta$ -induced apoptosis [202]. Genetic ablation of IP<sub>3</sub>R in cells expressing FAD-PS1 also results in remarkable reduction in A $\beta$  levels [69]. Indeed, pharmacological



normalization of disrupted ER calcium signaling by blocking hyperactivated RyR channels with dantrolene was demonstrated to restore synaptic transmission and synaptic plasticity, reduce memory deficits and A $\beta$  burden, increase PSD-95 expression, and improve learning and memory in different AD mouse models [203-205]. By contrast, another study shows that long-term feeding of dantrolene to APP/PS1 mice [206], results in increased A $\beta$ -load accompanied with synaptic marker loss and atrophies in hippocampus and cortex [207]. Notably, dantrolene has been already used for treatment of malignant hypothermia, neuroleptic malignant syndrome, muscle spasticity and ecstasy intoxication. Procaine and tetracaine, two other inhibitors of RyR have been used as local anesthetics. Benzothiazepine K201, a RyR-stabilizing compound is being tested for treatment of defective RyR channel gating conditions, such as heart failure and kidney disease [208]. Therefore, therapeutic modalities aiming at manipulation of ER calcium homeostasis present a novel strategy for treatment a wide range of diseases.

## 2.10 Calcium Imaging

Calcium imaging is technique to monitor and quantify the calcium concentrations and calcium dynamics in the living cells. This is achieved through the use of either synthetic organic molecules with selective affinity to calcium (calcium dyes) or genetically engineered calcium indicators (GECIs) [209]. Both of these methods rely on the changes in fluorescence properties of the indicator upon calcium binding. Calcium indicators can be either single-wavelength or ratiometric. The advantage of ratiometric indicators is the distinct emission (or excitation) properties in calcium-free and calcium-bound states, which minimizes the risk of artifacts.

The concept of using Green Fluorescent Protein (GFP) as biosensors was employed in development of genetically engineered calcium indicators as well. Two important classes of GECIs are either FRET (Förster Resonance Energy Transfer)-based or single-emission calcium indicators [210]. Cameleons are a subclass of FRET-based calcium sensor fusion proteins that consist of cyan (CFP) and yellow (YFP) fluorescent protein domains, which are linked by calmodulin (CaM), the calmodulin-binding peptide M13 (Figure 6.2a). Binding of calcium to CaM results in the conformational change of CaM causing wrapping around the M13 domain and thus increasing the FRET between CFP and YFP

[211]. In single-emission calcium indicators, the change in the fluorescence intensity of a single fluorescent protein is proportional to the amount and change in the calcium concentration [210]. Yellow Cameleon 3.6. (YC3.6) is a bright FRET-based calcium indicator with about 6-fold wide dynamic range and thus an enhanced signal-to-noise ratio [212]. It is photostable and absorbs a great amount of light.

The advantage of genetically engineered calcium probes compared to synthetic organic dyes is the possibility to perform long-term calcium imaging without the drawbacks involved in dye loading, washing and leakage, therefore making it ideal for high-throughput calcium imaging. In addition, in contrast to synthetic calcium dyes, it possible to target GECIs to specific compartments and generate stable lines or transgenic animals expressing the calcium sensor.

Opera<sup>®</sup>, a high-throughput confocal laser scanning imaging system (PerkinElmer), was used for calcium imaging in the present work. It combines high sub-cellular resolution and speed, in combination with flexible image analysis software, Acapella<sup>®</sup> [213]. The system includes an on-board dispensing unit suitable for applying small drug volumes while imaging live cells under environmental control of temperature, CO<sub>2</sub> and humidity. High resolution is achieved by using confocal imaging and water immersion lenses creating an optimal reader for calcium imaging based high-throughput screening. We equipped the Opera<sup>®</sup> system with Bravo<sup>®</sup> (Agilent technologies), an automated liquid handling robot, which works under a laminar flow hood and suitable for sterile cell based assays.

CUMULATIVE THESIS: PAPER I – REVIEW**3 Presenilins: Role in calcium homeostasis**

Kamran Honarnejad<sup>1,2,3</sup> and Jochen Herms<sup>1,2</sup>

<sup>1</sup> Department of Translational Brain Research, DZNE – German Center for Neurodegenerative Diseases, Munich, Germany

<sup>2</sup> Center for Neuropathology and Prion Research, Ludwig Maximilian University, Munich, Germany

<sup>3</sup> Graduate School of Systemic Neurosciences, Ludwig Maximilian University, Munich, Germany

*This manuscript has been peer-reviewed and published under the indicated citation:  
Honarnejad K, Herms J.; Int J Biochem Cell Biol. 2012 Nov; 44(11):1983-6;  
doi: 10.1016/j.biocel.2012.07.019.*

*Author's rights to reuse and post their own articles published by Elsevier (e.g. for inclusion in a thesis or dissertation) are acknowledged by Elsevier's copyright policy.*

*The author of this doctoral thesis has majorly contributed to this review paper by completely writing the manuscript and preparing the figures.*

Abbreviations used:

AD, Alzheimer's disease; FAD, familial Alzheimer's disease; ER, endoplasmic reticulum; PS, presenilin; PS1, presenilin 1; PS2, presenilin 2; CTF, C-terminal fragment; NTF, N-terminal fragment; PS1-FL, presenilin 1 full-length holoprotein; PS-DKO, presenilin double-knockout; IP<sub>3</sub>, inositol 1,4,5-triphosphate; RyR, ryanodine receptor; SERCA, sarco/endoplasmic reticulum calcium-ATPase; TMD, transmembrane domain; LTP, long-term potentiation; CCE, capacitative calcium entry; CICR, calcium-induced calcium release; SOCC, store-operated calcium channel; FAD-PS, familial Alzheimer's disease presenilin; A $\beta$ ,  $\beta$ -amyloid; NMDA receptor, N-methyl-D-aspartate receptor; 3xTg-AD, triple-transgenic model of AD.

### 3.1 Abstract

Mutations in presenilins are responsible for the vast majority of early-onset familial Alzheimer's disease cases. Full-length presenilin structure is composed of nine transmembrane domains, which are localized on the endoplasmic reticulum membrane. Upon endoproteolytic cleavage, presenilins assemble into the  $\gamma$ -secretase multiprotein complex and subsequently get transported to the cell surface. There is a wealth of knowledge around the role of presenilins as the catalytic component of  $\gamma$ -secretase, their involvement in amyloid precursor protein processing and generation of neurotoxic  $\beta$ -amyloid species. However, recent findings have revealed a wide range of  $\gamma$ -secretase-independent presenilin functions, including involvement in calcium homeostasis. Particularly, familial Alzheimer's disease presenilin mutations have been shown to interfere with the function of several molecular elements involved in endoplasmic reticulum calcium homeostasis. Presenilins modulate the activity of IP<sub>3</sub> and Ryanodine receptor channels, regulate SERCA pump function, affect capacitative calcium entry and function *per se* as endoplasmic reticulum calcium leak conductance pores.

**Keywords:** Presenilin, Calcium, Endoplasmic reticulum, Alzheimer's disease

## 3.2 Introduction

Presenilin (PS) mutations account for over 90% of human familial Alzheimer's disease (FAD) cases. Beyond the intensively characterized role of PS as the catalytic core of  $\gamma$ -secretase multimeric enzyme complex [214], presenilins have been shown to be implicated also in a wide range of  $\gamma$ -secretase-independent functions including  $\beta$ -catenin regulation, signal transduction, cell adhesion, protein trafficking and turnover, apoptosis, synaptic function, tau phosphorylation and calcium homeostasis [215].  $\gamma$ -secretase is responsible for the regulated intramembrane proteolysis (RIP) of over 60 different substrates, including amyloid precursor protein (APP) and Notch. Yet,  $\gamma$ -secretase is best known for its involvement in formation of  $\beta$ -amyloid (A $\beta$ ) peptide, which is generated from sequential proteolytic cleavage of APP in Alzheimer's disease (AD) [214]. The discovery of PS came from the work of Sherrington and colleagues in 1995. Their genome-wide screen revealed that missense mutations in the PS1 gene (originally known as S182) lead to early-onset FAD cases [216]. This finding was shortly complemented by an independent study which reported that the PS1 homologous gene in *Caenorhabditis elegans* (*sel-12*) is implicated in Notch signaling [217]. Meanwhile, PS homologues have been identified in several other species, ranging from mammals to frogs, flies, worms, fish and plants [218]. PS1 and PS2 are the two highly homologous forms of PS in mammals which are respectively located on chromosomes 14q24.3 and 1q42.2 [214]. In this review article, we mainly highlight the role of PS in the context of calcium signaling, particularly in relation to disrupted calcium homeostasis implicated in the pathogenesis of Alzheimer's disease (AD).

## 3.3 Structure

Although the crystal structure of PS is not yet resolved, there is strong evidence in favor of a nine transmembrane domain (TMD) structure model (Figure 3.1). PS holoprotein is ~50 kDa in size which undergoes endoproteolysis within a putatively large intracellular loop between TMD6 and TMD7 to generate a ~30 kDa N-terminal fragment (NTF) and a ~20 kDa C-terminal fragment (CTF) which remain associated as a heterodimer [214].

NMR studies could only determine the structure of PS1-CTF, containing a half-membrane-spanning helix, a severely kinked helical structure toward the carboxyl terminus as well as a soluble helix in the unstructured amino-terminal loop of the CTF [219]. Despite the lack of NMR structure for PS1-NTF, it is generally agreed upon that the PS1-NTF has a classical transmembrane topology consisting of six  $\alpha$ -helices.

### **3.4 Expression, activation and turnover**

The expression of both PS1 and PS2 is detectable throughout the brain, in most adult human tissues and regulated during development [218]. PS is primarily localized to the ER and Golgi apparatus, but also a small fraction is located at the cell surface [218] (Figure 3.2). In the brain, endogenous PS is predominantly present as N- and C-terminal fragments, while the immature precursor full-length PS holoprotein (PS-FL) is only faintly detectable. This is also reflected by the short half-life (~1.5 h) and rapid turnover of PS-FL compared to its more stable endoproteolytic fragments with longer half-lives (~24 h) [220]. However, upon PS overexpression, the NTF and CTF levels reach a saturation threshold, beyond which PS-FL gets accumulated [218]. The proteasomal pathway is responsible for the degradation of PS-FL [221]. Endoproteolytic cleavage of PS-FL occurs primarily within the ER. Upon association of PS proteolytic fragments with three other ER transmembrane proteins (Nicastrin, Aph-1 and Pen-2), a complex is formed and subsequently transported to the Golgi through several vesicular transport cycles and trafficked to the plasma membrane where it functions as  $\gamma$ -secretase [214].

### **3.5 Role in calcium homeostasis**

In 1994, the involvement of PS in ER calcium signaling was demonstrated for the first time. Ito and colleagues observed exaggerated agonist-evoked calcium release from IP<sub>3</sub> receptor (IP<sub>3</sub>R) channels in fibroblasts from AD patients harboring FAD-PS mutations [222]. Guo and colleagues confirmed those data in neuronal-like cells. They observed remarkably enhanced IP<sub>3</sub>R-evoked calcium responses in PC12 cells expressing FAD-PS1 compared to those expressing wildtype PS1 [223]. Numerous follow-up studies have confirmed FAD-PS-mediated excessive ER calcium release in other models including

*Xenopus* oocytes [224], primary neuronal culture [202], acutely dissociated neurons [225] and brain slices of adult FAD-PS1 mice [226]. In addition to the greater magnitude of IP<sub>3</sub>R-evoked calcium release, remarkable increase in the percentage of stimuli-responsive cells accompanied expression of FAD-PS1 [226]. Using PS-DKO MEF cells (PS1 and PS2 double knock out mouse embryonic fibroblasts) of the same origin, inconsistent results have been obtained describing either attenuated [227] or amplified [228] calcium release from ER. Etcheberrigaray *et al.* detected an altered IP<sub>3</sub>R-mediated calcium release in fibroblasts from a large proportion of AD family members prior to the appearance of overt AD clinical symptoms, but not in family member subjects who failed to develop AD [229]. These data supported the “calcium hypothesis” of AD and led to many follow-up studies, which aimed to mechanistically explore the role of FAD-PS mutations in potentiating ER calcium release, which will be discussed later.

Interestingly, calcium release from Ryanodine receptors (RyR) was also potentiated as a consequence of FAD-PS expression (Figure 3.2). In PC12 cells and primary hippocampal neurons, upregulation of RyR expression level and enhanced RyR-evoked calcium release by caffeine was observed [202]. Likewise, RyR-evoked calcium responses were amplified in slices from young, adult and aged FAD-PS1 knock-in mice, accompanying increased RyR expression [230]. This effect was most remarkable in dendrites and particularly in dendritic spines, but also detectable in soma and perinuclear regions [98]. From the earlier studies taken together, the “calcium overload” hypothesis was proposed arguing that the ER calcium overload is the cause of excessive ER calcium release. The interesting finding of the Bezprozvanny group, that PS holoprotein forms passive calcium leak channels on planar lipid bilayers and the leak activity to be impaired by FAD-PS mutations, came in support of the “calcium overload” hypothesis [228]. They argue that RyR upregulation in FAD-PS cells is a neuroprotective compensatory mechanism to normalize the overloaded ER calcium levels [207]. They hypothesize that the hydrophilic water-filled catalytic cavity of PS may function as a low conductance calcium-permeable pore [231]. They also demonstrated a correlation between the effects of FAD-PS mutations in terms of the leak activity and different AD clinical phenotypes by calcium imaging of patient-derived lymphoblasts [40]. However, more recent data have challenged the PS “leak channel” theory [232] and “calcium overload” hypothesis. [69, 233]. Using several different cell lines and various calcium imaging protocols and indicators, the Foskett team investigated ER calcium filling rates, steady-state ER calcium

levels and calcium leak rates from ER. However, they could not provide consistent supporting evidence in favor of “leak channel” hypothesis [232]. The results from their study and several other recent works indicate that FAD-PS mutations lead to an unchanged or even attenuated ER calcium level by directly monitoring the absolute calcium content of the ER [69, 232-234].

The FAD-PS mutations do not seem to change the abundance or distribution of IP<sub>3</sub> receptors. However, single IP<sub>3</sub>R channel recordings in FAD-patient-derived lymphoblasts and Sf9 cells have revealed that through physical and functional interaction of IP<sub>3</sub>R channels with FAD-PS holoprotein, IP<sub>3</sub>Rs become more sensitive. The direct consequence of this is the excessive calcium release from ER even under resting conditions and sub-threshold IP<sub>3</sub> molecule levels, i.e. calcium leakage in the absence of muscarinic receptor agonists [69] (Figure 3.2). FAD-PS mutations exert their stimulatory effect by enhancing the modal gating activity of IP<sub>3</sub>R and shifting the balance towards burst mode with high open-probability and repetitive openings and away from closed-probability mode with only brief openings [69, 235]. Similarly, PS2-NTF facilitates the single channel activity of mouse brain RyR through its direct physical interaction with RyR at the cytosolic side of the ER membrane [236]. This interaction seems to play a role in modulating neurotransmitter release in hippocampus, as it was shown that specific inactivation of PS at presynapses (but not postsynapses) impairs glutamate release, synaptic facilitation and LTP, suggesting a primary role for presynaptic pathomechanisms in AD initiation [237]. Intracellular store calcium handling plays a crucial role in synaptic function. Indeed, several genetic and electrophysiological studies have pointed towards the role of PS in synaptic plasticity. Since PS associates with NMDA receptors, PS-DKO mice present lowered synaptic NMDA receptor levels, synaptic and memory deficits as well as neurodegeneration with increasing age [238]. In young presymptomatic 3xTg-AD mouse model, enhanced calcium release from RyRs accompanies subtle alterations in mechanisms underlying hippocampal synaptic transmission, which are typically masked by compensatory factors in early disease stages and only detectable under RyR blockade conditions [98]. Moreover, hippocampal neuronal cultures from PS1 knockout and PS1-M146V mice show disrupted homeostatic synaptic scaling of excitatory synapses, which reflects disturbances in the neuronal ability to tune with changes in the network activity [239]. Furthermore, we have demonstrated that PS1 influences the structural plasticity of postsynaptic dendritic spines in the somatosensory cortex [240].



Calsenilin and calmyrin are further proteins involved in ER calcium homeostasis, which have been also shown to interact with presenilins [241, 242]. Coexpression of calsenilin reverses the FAD-PS specific potentiation of IP<sub>3</sub>R-evoked calcium release [243]. FAD-PS mutations have been shown to increase the neuronal vulnerability to A $\beta$  and glutamate through activation of caspase-3 as a result of RyR3 isoform upregulation and enhanced RyR-mediated calcium release [244].

FAD-PS mutations have been shown to increase the neuronal vulnerability to A $\beta$  and glutamate through caspase-3 activation as a result of RyR3 isoform upregulation and enhanced RyR-mediated calcium release in PC12 cells [244]. Notably, the FAD-PS mediated vulnerability and apoptosis can be normalized by pharmacologically or functionally inhibiting the IP<sub>3</sub>R-CaMKIV-CREB pathway in SH-SY5Y cells [201]. In PS-DKO MEFs, the expression of IP<sub>3</sub>R was remarkably upregulated [227]. Moreover, FAD-PS mutations lead to enhanced basal activity of phospholipase C (PLC) in SH-SY5Y cells, which in turn result in increased production of IP<sub>3</sub> molecule, mediating amplified calcium release from IP<sub>3</sub>R channels [200] (Figure 3.2). Therefore, it is crucial to distinguish the FAD-PS-mediated excessive calcium release as a result of IP<sub>3</sub>R/RyR hyperactivity from ER “calcium overload”.

In fibroblasts, the interaction of PS and SERCA2b was demonstrated by their colocalization and coimmunoprecipitation [72]. This interaction is required for the regulation of the SERCA pump activity. The same study shows that *Xenopus* oocytes harboring FAD-PS1 more effectively sequester calcium from cytosol into the ER than oocytes expressing wildtype PS1 protein [72] (Figure 3.2). In contrast, another study in MEFs and SH-SY5Y cells claims that both wildtype PS2 and FAD-PS2 reduce the SERCA2b activity [233].

Capacitive calcium entry (CCE) is the process of refilling intracellular calcium stores through store-operated calcium channels (SOCC) on the plasma membrane. Calcium imaging in SH-SY5Y cells and primary neurons revealed that CCE is attenuated as a result of FAD-PS mutations and potentiated as a result of PS knockout or deficiency [245, 246] (Figure 3.2). Bojarksi *et al.* found altered expression levels of STIMs, key proteins involved in CCE, in PS-DKO MEFs and patient-derived B-lymphocytes expressing FAD-PS mutations [247].

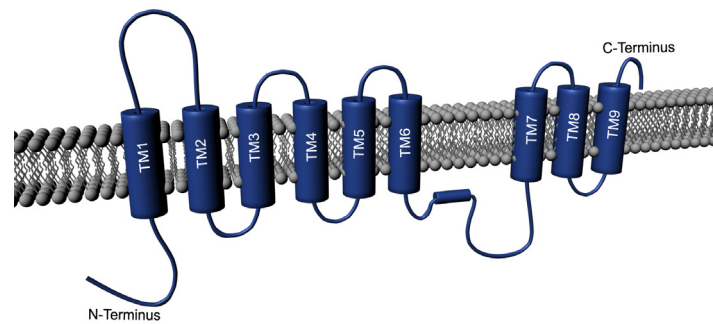
As reviewed, the exact mechanism responsible for the FAD-PS mediated amplified ER calcium release is still controversial. However, the consequence of this phenomenon is the elevation of cytosolic calcium concentration and enhanced neuronal vulnerability to stressors. Because calcium itself is the co-agonist of both IP<sub>3</sub>R and RyR, the elevated cytosolic calcium concentration in turn initiates a long-term feed-forward mechanism causing a vicious cycle in which the calcium waves and calcium-induced calcium release (CICR) become increasingly exaggerated in space, time, and amplitude.

### **3.6 PS as a therapeutic target for Alzheimer's disease treatment**

Since PS forms the catalytic component of  $\gamma$ -secretase, inhibition or modulation of its function serves as the prime therapeutic target for AD drug candidates interfering with A $\beta$  generation. However, in view of the unexceptional failures of recent A $\beta$ -focused therapies in clinical trials and the emerging non-proteolytic PS functions, future PS-targeted therapies should not only focus on interfering with  $\gamma$ -secretase proteolytic activity, but rather address the broad spectrum of PS functions, particularly those implicated in the pathogenesis of AD (e.g. disrupted calcium homeostasis).

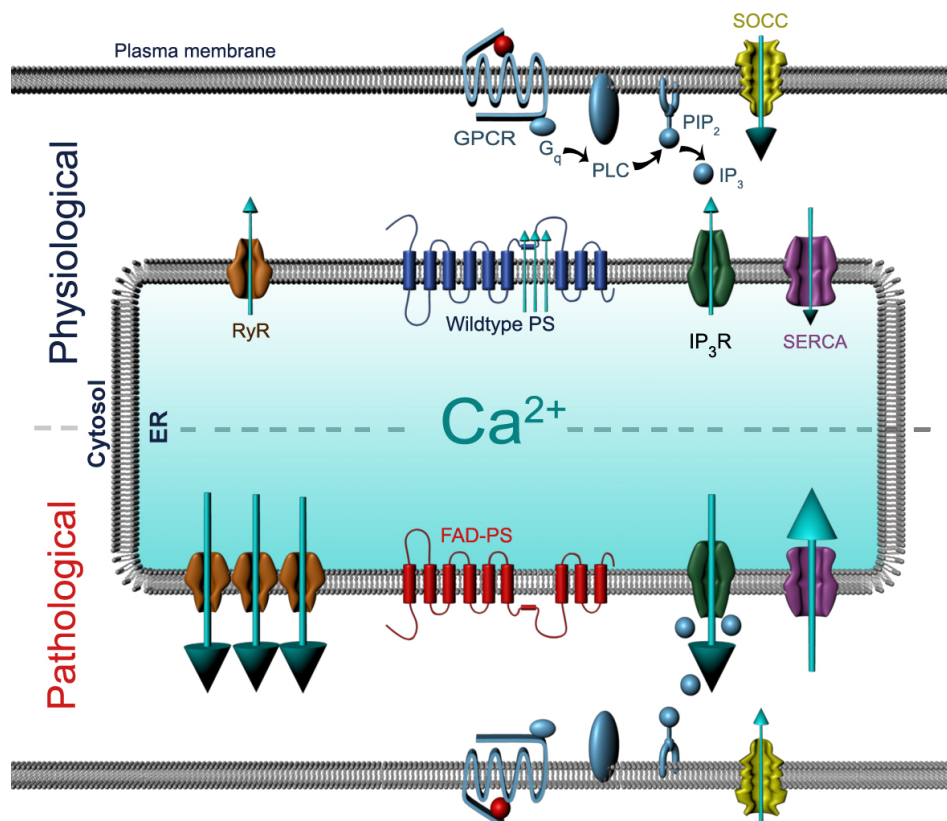
#### **Acknowledgments**

This work was supported by the German-Polish grant from the German Federal Ministry for Education and Research Council (BMBF — 01GZ0713). We are grateful to Ramin Rastin for excellent graphical support. The authors declare no conflict of interest.



**Figure 3.1. Schematic representation of human PS1 structure**

PS1 holoprotein is proposed to consist of nine TM domains on the ER membrane. PS1 undergoes endoproteolytic cleavage at a large cytosolic loop between TMD6 and TMD7 to generate N- and C-terminal fragments.



**Figure 3.2. Physiological versus pathological FAD-PS-mediated ER calcium homeostasis**

Calcium concentration in the ER is approximately 1000 folds higher than cytosol. FAD-PS mutations (lower panel) potentiate the IP<sub>3</sub>R- and RyR-induced calcium release, upregulate RyR expression, increase PLC basal activity and IP<sub>3</sub> molecule generation, enhance SERCA pump function and attenuate CCE, as compared to wildtype PS (upper panel). Moreover, PS-FL holoprotein *per se* may function as passive calcium leak channel on the ER membrane, while most FAD-PS mutations lead to the loss of this activity. The direction and the size of the arrows respectively represent the direction and amount of calcium mobilization.



## 4 Aim of the study

Alzheimer's disease (AD) is a progressive neurodegenerative brain disorder and the most frequent cause of dementia. The current AD drugs in the market are purely symptomatic, with little or no effect on the disease progression. Moreover, the recent failure in development of disease-modifying therapies for AD (which were largely targeted at amyloid and tangle pathologies) justifies the importance of a shift towards alternative novel drug targets. Based on the hypothesis that impaired intracellular calcium homeostasis is an early event in AD progression, which is also likely to underlie the AD-associated synaptic dysfunction, here we aimed at development of calcium signaling-targeted therapeutic modalities for treatment and/or prevention of AD.

In brief, the goal of this project was to characterize the disturbances in the endoplasmic reticulum (ER) calcium homeostasis in AD, and to address the latter pathophysiological phenomenon as a therapeutic target for disease-modifying drug discovery of AD. To that end, the specific aims of this thesis were:

- (i) Investigation of the role presenilin (PS) holoprotein upregulation in the impairment of ER calcium homeostasis in AD.
- (ii) Development of a novel FRET-based high-throughput calcium imaging assay for a phenotypic drug screening targeted at ER calcium dyshomeostasis. Screening aimed at identification of compounds that reverse the impaired ER calcium signaling phenotype associated with FAD-linked PS mutations.
- (iii) Implementation of the high-throughput calcium imaging assay for a large-scale primary compound screen with a library of over 20,000 small molecules and identification active hits and lead structures.
- (iv) Validation and characterization of the identified lead structures using multiple AD-relevant secondary assays.



CUMULATIVE THESIS: PAPER II**5 Involvement of presenilin holoprotein upregulation in calcium dyshomeostasis of Alzheimer's disease**

Kamran Honarnejad<sup>1,2,3</sup>, Christian K.E. Jung<sup>1,2</sup>, Sven Lammich<sup>4</sup>, Thomas Arzberger<sup>2</sup>, Hans Kretzschmar<sup>2</sup>, Jochen Herms<sup>1,2,5</sup>

<sup>1</sup> Department of Translational Brain Research, DZNE – German Center for Neurodegenerative Diseases, Munich, Germany

<sup>2</sup> Center for Neuropathology and Prion Research, Ludwig Maximilian University, Munich, Germany

<sup>3</sup> Graduate School of Systemic Neurosciences, Ludwig Maximilian University, Munich, Germany

<sup>4</sup> Adolf Butenandt Institute - Biochemistry, Ludwig Maximilian University, Munich, Germany

<sup>5</sup> Munich Cluster for Systems Neurology (SyNergy), Munich, Germany

*This manuscript has been peer-reviewed and published under the indicated citation:  
Honarnejad K, Jung CK, Lammich S, Arzberger T, Kretzschmar H, Herms J.; J Cell Mol Med. 2013 Feb;17(2):293-302. doi: 10.1111/jcmm.12008.*

*This article was published under a Creative Commons Attribution License (CC-BY).*

*The author of this doctoral thesis has majorly contributed to this work by conceiving, designing and performing the experiments, analyzing the data, writing the entire manuscript and designing all the figures.*

## 5.1 Abstract

Mutations in presenilins (PS1 and PS2) account for the vast majority of early onset familial Alzheimer's disease cases. Beside the well investigated role of presenilins as the catalytic unit in  $\gamma$ -secretase complex, their involvement in regulation of intracellular calcium homeostasis has recently come into more focus of Alzheimer's disease research. Here we report that the overexpression of PS1 full-length holoprotein forms, in particular familial Alzheimer's disease-causing forms of PS1, result in significantly attenuated calcium release from thapsigargin- and bradykinin-sensitive stores. Interestingly, treatment of HEK293 cells with  $\gamma$ -secretase inhibitors also leads to decreased amount of calcium release from endoplasmic reticulum (ER) accompanying elevated PS1 holoprotein levels. Similarly, the knockdown of PEN-2 which is associated with deficient PS1 endoproteolysis and accumulation of its holoprotein form also leads to decreased ER calcium release. Notably, we detected enhanced PS1 holoprotein levels also in postmortem brains of patients carrying familial Alzheimer's disease PS1 mutations. Taken together, the conditions in which the amount of full length PS1 holoprotein is increased result in reduction of calcium release from ER. Based on these results, we propose that the disturbed ER calcium homeostasis mediated by the elevation of PS1 holoprotein levels may be a contributing factor to the pathogenesis of Alzheimer's disease.

**Keywords:** Presenilin, Holoprotein, Calcium, Alzheimer's disease, Endoplasmic Reticulum



## 5.2 Introduction

Alzheimer's disease (AD) is the most common form of adult dementia characterized by the extracellular accumulation of amyloid beta ( $A\beta$ ) protein and formation of intracellular neurofibrillary tangles leading to neuronal dystrophy and loss [13, 248]. Mutations in presenilins (PS) account for the majority of early onset familial Alzheimer's disease (FAD) cases [249]. Upon undergoing endoproteolytic processing and forming N- and C-terminal fragments (NTF and CTF), PS functions as the catalytic subunit of  $\gamma$ -secretase multiprotein complex on the cell surface, comprising PS, Nicastrin, Aph-1, and PEN-2 [250]. Among over 60 different type I transmembrane protein substrates,  $\gamma$ -secretase sequentially cleaves amyloid precursor protein (APP) after  $\beta$ -secretase cleavage to generate  $A\beta$  [251]. FAD mutations in PS have been shown to alter the cleavage of APP in favor of neurotoxic  $A\beta_{42}$  generation [252]. However growing body of evidence also indicates that FAD-PS mutations impair several intracellular calcium signaling mechanisms, particularly endoplasmic reticulum (ER) calcium homeostasis [22, 253]. Uncleaved full-length (FL) PS holoprotein is approximately 50 kDa in size and primarily located on the ER membrane [254]. ER calcium store has approximately 1000-fold higher calcium concentration than cytosol [26]. The exact molecular mechanism as to how FAD-PS mutations cause ER calcium dyshomeostasis is not fully resolved. Yet PS have been shown to affect multiple components of ER calcium handling [255]. PS holoprotein has been proposed to form passive calcium leak channel on the ER membrane [228, 256] through its hydrophilic catalytic cavity [231], regulate Inositol 1,4,5-triphosphate ( $InsP_3$ ) receptor gating [69, 235], Ryanodine receptor (RyR) channel activity [236, 257] and abundance [202]. PS have also been shown to interact with Sarco/endoplasmic reticulum calcium-ATPase (SERCA) pump which actively transfers calcium from cytosol into the ER [258], and to modulate this function [72, 233]. Capacitative calcium entry (CCE) – the process of refilling intracellular calcium stores through plasma membrane channels – has been shown to be attenuated in cells expressing FAD PS mutants [246, 259]. Moreover, PS2 modulates calcium shuttling between ER and mitochondria [127]. Here we aimed to examine the potential role of impaired PS endoproteolysis leading to accumulation of PS holoprotein on the ER membrane [260, 261] in the context of disrupted ER calcium homeostasis in AD.

## 5.3 Materials and Methods

### 5.3.1 Cell culture and cell lines

Human embryonic kidney 293 (HEK293) cells were cultured in Dulbecco's modified eagle medium (DMEM) supplemented with 10% fetal bovine serum and 1% penicillin/streptomycin while being incubated at 37°C, 5% CO<sub>2</sub> and 90% humidity. PS1-overexpressing and PEN-2 knockdown HEK293 lines were generously provided by Dr. H. Steiner. HEK293 cells stably expressing either PS1 wild type or mutant variants, or AChR $\alpha$ 1 were generated by transfection of HEK293 cells with the respective cDNA cloned into pcDNA3.1/Zeo (+) (Invitrogen, Carlsbad, CA, USA) and subsequent selection for zeocin (100  $\mu$ g/ml) resistance. Likewise, RNA interference-mediated PEN-2 stable knockdown clone was generated by stable transfection of pSUPER/PEN-2-163 and pcDNA3.1/Hygro(-) (Invitrogen) into HEK293 cells and subsequent selection for hygromycin (100  $\mu$ g/ml) resistance [262].

### 5.3.2 Calcium imaging

One day prior to the experiment, HEK293 cells were plated in a 96-well collagen coated microplate (Greiner BioOne GmbH, Frickenhausen, Germany) at 40,000 cells/well. Cytosolic calcium concentration was measured using the Fluo-4 NW kit (Invitrogen Corporation, Madison, WI, USA) according to manufacturer's instructions. Briefly, the growth medium was exchanged with a freshly mixed calcium-free assay buffer. The cells were incubated at 37°C for 30 minutes, then for an additional 30 minutes at room temperature. Fluorimetric calcium measurements were performed utilizing a confocal laser-scanning system (Carl Zeiss AG, Jena, Germany) equipped with a climate control chamber (EMBL, Heidelberg, Germany). Cells were then imaged using a 40x oil immersion objective (Zeiss Plan-Apochromat, Zeiss; 40x NA 1.3). Excitation of the cells was performed at 488 nm with an Argon Laser (Zeiss) and the emission was collected using band pass filter (500–550 nm). Time-lapse fluorescence images were acquired at 5 s interval for Thapsigargin (TP; 1  $\mu$ M) and 1 s interval for Bradykinin (BK; 300 nM) and Carbachol (CCh; 10  $\mu$ M). Subsequently images were analyzed by defining typically 20-

30 regions of interest (ROI) for individual cells in each well using the Zeiss LSM 510 Meta Software. Data analysis was performed using Microsoft EXCEL (Microsoft, Seattle, WA, USA), Sigma Plot (SPSS, Chicago, IL, USA) and GraphPad Prism 5.0b (GraphPad Software, San Diego, CA, USA). All fluorescence data are expressed as  $\Delta F/F_0 = (F - F_0)/F_0$ , where  $F$  is the measured fluorescence signal at any given time and  $F_0$  is the average fluorescence from the scans preceding stimulation.

If not otherwise stated, values represent mean  $\pm$  standard error of the mean (SEM). To test significance, student's t-test (two tailed) was performed and differences were considered statistically significant if  $p < 0.05$ .

### 5.3.3 Treatment with $\gamma$ -secretase inhibitors

HEK293 cells were grown to 60-70% confluency inside of 10 cm petri dishes.  $\gamma$ -secretase inhibitors (all from Calbiochem, Darmstadt, Germany) were added to the growth medium and incubated for 24 hours at concentrations which were reported to inhibit the  $\gamma$ -secretase activity. DAPT, Gamma IV and Gamma XXI were used respectively at 10  $\mu$ M, 2.7  $\mu$ M and 300 nM concentration. Controls were treated in parallel with DMSO vehicle instead of inhibitors.

### 5.3.4 Western blot

HEK293 cells were lysed in “complete lysis-M buffer” with protease inhibitor mix (Roche, Molecular Biochemicals, Indianapolis, IN, USA) according to the manufacturer’s instructions. Similarly for human brain material, a small piece from frozen postmortem frontal cortex of FAD as well as control cases were cut and homogenized in sucrose/hepes buffer with PMSF. Protein concentrations were measured using BCA assay. Equal amounts of protein samples were separated in a 10% tris-glycine SDS-PAGE and transferred to PVDF-membrane (Millipore, Corporation, Bedford, MA, USA). For detection of presenilin holoprotein, a rabbit polyclonal antibody against a MBP/PS1-loop (aa 263-407) fusion protein was used at 1:500 dilution (antibody 5023; a kind gift from Dr. H. Steiner [263]). Mouse monoclonal anti-Tubulin (Santa Cruz Biotechnology, Santa Cruz, CA, USA) was used at 1:1000 dilution for loading control and corresponding AP-coupled secondary antibodies (Thermo Scientific, Waltham, MA, USA) at 1:5000

dilution. Chemiluminescent reaction was performed with CDP-Star (Roche Molecular Biochemicals) and detected with a Chemocam Imager (INTAS Science Imaging Instruments GmbH, Göttingen, Germany). Western blot bands were quantified using Advanced Image Data Analyzer/2D Densitometry 3.52 (Raytest GmbH, Straubenhardt, Germany).

### 5.3.5 *Human subjects*

In total seven frontal cortex samples comprising three FAD-PS1 and one FAD-APP mutation carrying patients as well as three control individuals were collected from BrainNet Europe. The staging of samples was determined according to Braak & Braak during routine postmortem tissue diagnostics by skilled neuropathologists [264]. The use of human tissue samples was approved by the institutional review board of the University of Munich (BrainNet: Brain Banking Center Munich).

## 5.4 Results

### 5.4.1 *Effect of PS1 holoprotein overexpression on calcium release from ER*

To assess the role of increased PS1 holoprotein levels in the ER calcium homeostasis, we used HEK293 cells stably expressing either wild type or several different mutant forms of PS1. Typically the endogenous PS1 holoprotein level is relatively low, being on the border line of detection [265]. We confirmed remarkable increase in PS1 holoprotein expression level by western blotting protein lysates from PS1 stable lines (Figure 5.1a). Densitometric analysis indicate 6-7 fold increase in the PS1 full length holoprotein levels in all stable clones compared to the wild type HEK293 cells (Figure 5.1b). Likewise the PS1-CTF levels were increased in all the clones, except for PS1-DeltaE9 and PS1-D385N which both lack the endoproteolytic cleavage site (Figure 5.1a). Overexpression of wild type PS1 and to a higher degree various FAD-PS1 mutants led to significantly lowered calcium release from ER in comparison to the untransfected controls. The ER calcium responses were generated by applying Bradykinin (BK). Application of BK leads to liberation of calcium from  $\text{InsP}_3$ -sensitive ER stores. The peak amplitude of the BK-evoked calcium release alone in wild type PS1 (wtPS1) overexpressing cells was

decreased to  $71 \pm 2.2\%$  of control wild type HEK293 cells. All FAD-PS1 mutants further lowered the amplitude of BK-evoked calcium release peak size as follows: PS1-DeltaE9 to  $41 \pm 2.5\%$ , PS1-M146L to  $38 \pm 3.4\%$ , PS1-G384 to  $35 \pm 1.2\%$  and PS1-L166P to  $25 \pm 1.4\%$  of the wild type HEK293 controls (Figure 5.1d). These results were confirmed using Thapsigargin (TP) as well. TP is an inhibitor of SERCA pump that blocks calcium uptake into ER, causing the diffusion of calcium from ER into the cytosol due to a very strong calcium gradient. Following a similar trend, the peak amplitude of TP-evoked calcium release in wtPS1 overexpressing cells was reduced to  $65 \pm 1.9\%$ , in PS1-DeltaE9 to  $29 \pm 2.1\%$ , in PS1-M146L to  $49 \pm 2.9\%$ , in PS1-G384 to  $35 \pm 3.2\%$  and in PS1-L166P to  $47 \pm 2.1\%$  of the wild type HEK293 controls (Figure 5.1f). Importantly, overexpression of a mutant form of PS1 being functionally inactive for  $\gamma$ -secretase substrate cleavage (PS1-D385N) [266], also resulted in lowered BK-evoked (to  $28 \pm 1.6\%$  of wild type) and TP-evoked (to  $45 \pm 3.3\%$  of wild type) calcium liberation from ER, indicating that the observed effects are independent of  $\gamma$ -secretase substrate cleavage activity (Figure 5.1d and 5.1f). Moreover, there was no correlation observed between the PS1-CTF levels and the attenuated calcium response from ER. PS1-DeltaE9 and PS1-D385N mutants, which do not undergo endoproteolysis and thus do not generate PS1-CTF, showed comparable attenuation of ER calcium release as to the rest of FAD-PS1 mutants which generate approximately proportionate levels of PS1-CTF. Conversely, the amplitude of calcium release upon activation of muscarinic receptors with carbachol (CCh) was enhanced in FAD-PS1 mutant and PS1-D385N expressing cells (Figure 5.1h). On a note, the overexpression of rat nicotinic acetylcholine receptor subunit alpha 1 (rAChR $\alpha$ 1), an unrelated protein which also localizes to the ER did not alter the amplitude of BK-evoked calcium release in HEK293 cells (Figure 5.1i).

#### **5.4.2 Effect of $\gamma$ -secretase inhibitors on calcium release from ER**

Next, we investigated the effect of acute  $\gamma$ -secretase inhibition on the ER calcium release. After treatment of HEK293 cells for 24 hours with three different  $\gamma$ -secretase inhibitors, we measured BK-evoked calcium responses. Treatment with each of the three  $\gamma$ -secretase blockers, resulted in significantly lowered BK-evoked calcium response compared to vehicle treated controls. The peak amplitude for BK-evoked calcium release for cells treated with DAPT, Gamma IV and Gamma XXI were respectively  $80 \pm 2.5\%$ ,  $58 \pm 3.3\%$  and  $75 \pm 2.8\%$  of that for DMSO treated cells (Figure 5.2a). As another parameter

proportional to the amount of released ER calcium, the area under the curve (AUC) of BK-evoked calcium responses were calculated. Following a similar trend, the AUC for cells treated with DAPT, Gamma IV and Gamma XXI were respectively  $61 \pm 5.1\%$ ,  $42 \pm 6.1\%$  and  $48 \pm 6.1\%$  of DMSO-treated cells (Figure 5.2b). Likewise, the amplitude of TP- and CCh-evoked calcium responses were attenuated in  $\gamma$ -secretase inhibitor treated HEK293 cells (Figure 5.2c and 5.2d). However, treating wtPS1- and PS1-D385N-overexpressing cells with DAPT did not further potentiate the reduction of BK-evoked calcium release (Figure 5.2g and 5.2h).  $\gamma$ -secretase inhibitors were used at concentrations which were previously described to inhibit the  $\gamma$ -secretase activity. Based on the literature that suggest  $\gamma$ -secretase activity is required for endoproteolysis of PS [267], we postulated that the treatment with  $\gamma$ -secretase blockers might inhibit the endoproteolysis of PS1 itself as well. Despite the expected faint expression of PS1 holoprotein at endogenous levels which could only be detected at longer exposures, we could indeed detect a modest increase in the PS1 holoprotein levels upon 24 hours treatment of cells with each of the three  $\gamma$ -secretase inhibitors by western blotting (Figure 5.2e). Treatment with DAPT, Gamma IV and Gamma XXI respectively led to  $48 \pm 4.1\%$ ,  $45 \pm 5.4\%$  and  $34 \pm 4.6\%$  increase in detected PS1 holoprotein levels by western blot (Figure 5.2f).

#### 5.4.3 *Effect of PEN-2 knockdown on ER calcium release*

PEN-2 (Presenilin enhancer 2) is a key regulatory component of the  $\gamma$ -secretase complex [268]. PEN-2 is necessary for the proper assembly of active  $\gamma$ -secretase complex and the knockdown of PEN-2 is associated with deficiency in PS endoproteolysis leading to stabilization and accumulation of PS holoprotein [269, 270]. Here we used RNA interference-mediated PEN-2 stable knockdown (PEN-2 KD) in HEK293 cells [262]. The cell line was previously characterized by Prokop and colleagues. In this cell line, increased PS1 holoprotein levels accompanying the downregulation of PEN-2 was demonstrated [262]. The interaction of PS holoprotein with PEN-2 is a key step for PS holoprotein to adopt a conformation which allows its endoproteolytic cleavage [262]. The PS1 holoprotein increase was confirmed in PEN-2 KD cells (Figure 5.3e). Here we report that BK-evoked calcium release is attenuated in PEN-2 knockdown cells relative to wild type controls, similar to the observation made in PS1 overexpressing cells. The peak amplitude and the area under the curve in PEN-2 KD cells were respectively  $42 \pm 4.9\%$  and  $55 \pm 6.6\%$  of those for wild type cells (Figure 5.3a and 5.3b). Similarly, the amplitude

of TP- and CCh-evoked calcium responses were also decreased in PEN-2 KD cells (Figure 5.3c and 5.3d).

#### **5.4.4 PS1 holoprotein in brains of FAD-PS1 patients**

To assess the physiological relevance of the finding that the accumulation of PS holoprotein is associated with the attenuated ER calcium release in the context of AD pathogenesis, we compared the PS1 holoprotein levels in the postmortem frontal cortices of FAD patients relative to non-demented control cases. As expected, the amount of PS1 holoprotein level in control individuals was relatively low. However we observed on average 1.7 fold significant increase in PS1 holoprotein levels in three FAD-PS1 patient cases. In contrast, the level of PS1 holoprotein in a FAD-APP patient was comparable to the controls (Figure 5.4a and 5.4b). Table 5.1 summarizes the patient data from which the samples were collected.

## **5.5 Discussion**

Here we report that the conditions causing an enhancement in the amount of PS1 holoprotein, result in attenuated calcium release from the ER. Only very little is known about the exact mechanism of PS holoprotein endoproteolysis. Despite the controversial findings, some FAD-PS mutations have been shown to impair the PS endoproteolysis leading to accumulation of PS holoprotein primarily on the ER membrane [260, 261].

Although there exists evidence in favor of FAD-PS mediated “ER calcium overload” theory [271], the results presented here and several other studies show that the FAD-PS and to a lesser extent wild type PS lead to either attenuated or unchanged ER calcium [69, 127, 233-235, 259, 272-274]. The reason behind such discrepancies is not completely clear. However, in comparing such data one has to critically discriminate between the FAD-PS mediated hyperactivity of InsP<sub>3</sub>R or RyR channels from “ER calcium overload”. Those exaggerated calcium responses may simply be a result of enhanced receptor gating and/or density [69, 202, 235, 257], increased basal phospholipase C (PLC) activity and the consequent overproduction of InsP<sub>3</sub> molecule [200, 275], or a combination of those,

while being independent from ER calcium content. While previous studies have demonstrated the biochemical interaction between PS1 and InsP<sub>3</sub>R [69], it is established that the overexpression of FAD-PS does not alter the abundance of InsP<sub>3</sub> receptors [276]. Notably, we have also observed augmented carbachol (CCh)-evoked calcium responses in FAD-PS1 mutant bearing cells (Figure 5.1g and 5.1h). While calcium release upon stimulation with both BK and CCh is associated with G-protein coupled receptor (GPCR) activation and InsP<sub>3</sub> generation, in spite of sharing the same calcium pools, such differential effects between BK- and CCh-evoked calcium responses have been previously described in airway smooth muscle and neuroblastoma cells and proposed to be regulated by differences in the specific PLC involvement and the expression of muscarinic receptors [277, 278]. Furthermore, activation of muscarinic receptors with CCh is associated with remarkably higher InsP<sub>3</sub> generation as to the activation of bradykinin receptors by BK [279]. Therefore it is possible that in CCh-evoked calcium release experiments (but not BK-evoked), the contribution of FAD-PS1 mediated hyperactivity of InsP<sub>3</sub> receptors [69, 235], can mask the lowered ER calcium content. Although CCh has been reported to induce calcium release also from RyRs in an InsP<sub>3</sub>R-dependent manner [280], due to extremely low expression levels of RyR in HEK293 cells, the contribution of RyRs in the observed differential effects is rather unlikely [281]. Further work is needed to comprehensively elucidate the differences between BK- and CCh-evoked calcium responses in the context of FAD-PS expression.

It has been proposed that the holoprotein form of PS can function as passive calcium leak channels on the ER membrane allowing the leakage of calcium into the cytoplasm [207, 228, 256]. Majority of FAD-PS mutations lead to loss of this function, some do not affect and others even cause a further gain of this function [40]. Independently from how FAD-PS mutations modulate the leak activity, it is plausible that the increase in PS holoprotein amounts may directly increase the degree of passive calcium leakage from ER to cytoplasm. This can explain our observation that conditions increasing the amount of PS1 holoprotein result in reduced ER calcium. Constant enhanced calcium leakage from ER into cytoplasm as a result of PS holoprotein accumulation will in turn affect the calcium equilibrium between ER and cytoplasm in which the reached steady state of ER calcium level is relatively low. Similar to FAD-PS1 mutants, a loss of function mutant for  $\gamma$ -secretase activity (PS1-D385N) [266] showed reduced calcium release from ER. This observation is in line with another finding showing that  $\gamma$ -secretase cleavage activity is



dispensable for the reduction of ER calcium levels, demonstrated using a different  $\gamma$ -secretase inactive mutant (PS2-D366A) [272]. The PS-mediated attenuation of ER calcium release seems to be a specific effect and not caused by ER stress or protein overload, since the overexpression of rAChR $\alpha$ 1 which also accumulates at the ER [282], did not alter the amplitude of BK-evoked calcium release.

We demonstrated that treatment with  $\gamma$ -secretase inhibitors lowers the magnitude of calcium release from ER in HEK293 cells. A similar finding has been previously described by others as well [283]. However here we propose an alternative explanation for this phenomenon which is independent from  $\gamma$ -secretase substrate cleavage activity and the suggested functional role for APP intracellular domain (AICD) in calcium signaling [283]. We reveal convincing evidence that treatment of HEK293 cells with  $\gamma$ -secretase blockers results in enhanced PS1 holoprotein levels. This is not very surprising given that  $\gamma$ -secretase blockers may also simultaneously inhibit the PS autocatalytic activity. The elevated PS1 holoprotein levels would in turn lead to enhanced leakage of calcium from ER into cytosol and consequently lowered ER calcium content. Further support for this hypothesis comes from the work of Fukumori and colleagues which nicely demonstrate that the PS holoprotein endoproteolysis is indeed autolytic [267]. Although the detected increase in PS holoprotein was only marginal, in view of extremely low levels of endogenously expressed PS holoprotein as well as the tremendous calcium gradient between ER and cytosol [26], even such minor but sustained enhancements in passive calcium leakage through PS holoprotein may heavily impact the calcium equilibrium between ER and cytosol. In both wtPS1 and PS1-D385N overexpressing cells, treatment with DAPT did not further reduce the amplitude of BK-evoked calcium release. These findings are indeed in line with our hypothesis, since PS1-D385N mutant is deficient for endoproteolysis and a marginal increase in PS1 holoprotein levels caused by DAPT treatment in wtPS1 cells would be negligible in the presence of constitutive PS1 overexpression which accompany abounding PS1 holoprotein levels. In view of therapeutic applications, the finding that  $\gamma$ -secretase inhibitors can elevate the PS holoprotein levels reflects yet another potential undesirable side-effect associated with the use of  $\gamma$ -secretase inhibitors (apart from unspecifically blocking the processing of several substrates other than APP) which should be taken into consideration [284].

Likewise, we demonstrated that the knockdown of PEN-2 leads to attenuated ER calcium release. Prokop and colleagues have shown that the knockdown of PEN-2 is associated

with deficiency in PS1 endoproteolysis and accumulation of PS1 holoprotein [262]. Using the same cell line, here we show reduced BK-, TP- and CCh-evoked ER calcium responses as well. These findings reinforce an inverse correlation between the PS holoprotein levels and the amount of calcium release from ER.

In previous studies utilizing AD patient post-mortem brains, the activation of calcium-dependent proteases and the alterations in the activity and abundance of proteins involved in calcium homeostasis were detected [285-287]. In this study, in spite of limited number of human postmortem brains from FAD-PS1 cases, we reveal convincing indication that the amount of PS1 is upregulated in the brains of patients harboring different FAD-PS1 mutations. Evidence exists that even in brains of sporadic late-onset AD cases, PS1 protein and mRNA levels and  $\gamma$ -secretase activity are upregulated [288]. Li *et al.* have postulated that presenilin upregulation may contribute to sporadic AD as a risk factor in the context of  $\gamma$ -secretase activity [289]. However, more detailed studies are needed to address whether the disturbed calcium homeostasis associated with PS holoprotein accumulation plays a role in the pathogenesis of late onset sporadic AD cases too. PS holoprotein is quite unstable with a relatively short half-life (~1.5 hours) and a rapid turnover [220]. Indeed, FAD-PS1 DeltaE9 mutant was shown to possess relatively higher stability and a longer half-life (~40 hours) [220]. Weihl and colleagues have suggested that FAD-PS mutations can alter the stability of PS holoprotein in a cell-type and differentiation-state dependent manner [290]. Given the emerging roles for PS outside of  $\gamma$ -secretase complex, increased stability and/or accumulation of PS holoprotein may have direct implications in pathophysiology of AD, particularly through their involvement in disruption of ER calcium homeostasis.

The disturbances in ER calcium homeostasis have been observed in both familial and sporadic AD cases long preceding the disease hallmarks, i.e. senile plaque and tangle pathology [98, 116]. While increasing age is the main risk factor for development of sporadic AD, indications suggest that age-dependent alterations in the calcium homeostasis may contribute to the pathogenesis of sporadic AD as well [291]. Moreover calcium dysregulation plays a key role in synaptic failure and neuronal loss [52]. Notably, the latter pathological events correlate best with the stages of dementia [53]. Therefore, better understanding the underlying mechanisms responsible for the disruption of ER

calcium homeostasis would be valuable in development of therapies targeting calcium dyshomeostasis as an early event in AD pathogenesis.

There are controversies in the literature as to how FAD-PS mutations alter ER calcium handling. These variations were mainly attributed to differences in methodologies used, different cells types and mutations. However based on the results here, we suggest that in the experimental setups where either wild type or mutant PS forms are overexpressed, possible differences in the PS expression levels may potentially give rise to the inconsistencies between independent studies. This point becomes even more critical taking into account that the expression level of PS holoprotein is quite low under physiological conditions. Given the fact that only a fraction of PS can incorporate into  $\gamma$ -secretase complex [292], constitutive overexpression might be suitable for studying the effect of PS mutations on  $\gamma$ -secretase activity. However when FAD-PS-dependent alterations in the ER calcium homeostasis are investigated, overexpression of PS might not fully resemble their role in pathophysiological circumstances. Therefore the use of patient derived FAD-PS cells (e.g. fibroblasts, lymphocytes, etc) which express PS holoprotein at endogenous levels may be more appropriate. On the other hand, since FAD-PS mutations alter the stability of PS holoprotein in a cell-type and differentiation-state dependent manner [290], calcium homeostasis in periphery might not exactly correspond to the FAD-PS-mediated disruption of calcium homeostasis in the brain. Despite the mentioned drawbacks associated with the use of overexpression and secondary cell models, HEK293 cells were suitable for the purpose of this study. Regulation of calcium homeostasis in neurons is a very complex mechanism which is tightly controlled by the functions of multiple molecular elements. The existence of compensatory mechanisms which by masking studied effect can efficiently restore balanced calcium homeostasis makes the manipulation of calcium signaling in neurons for studying cause-effect relationships rather challenging. By contrast, in simpler cell models (e.g. HEK293 cells), in shortage of such efficient compensatory mechanisms, directly assessing the effect of PS1 holoprotein accumulation on ER calcium homeostasis was more readily possible.

Taken together our results reinforce the notion that the accumulation of full length forms of PS (as a result of e.g. impaired PS autoendoproteolysis) result in reduced ER calcium content. Therefore future studies are necessary to examine whether the adverse FAD-PS-

mediated effects on the functions of several ER calcium handling elements, including described loss of PS calcium leak channel activity [228], enhanced InsP<sub>3</sub> [69, 235], and RyR channel activity [236, 257] and abundance [202, 230] could be secondary mechanisms to compensate for the PS holoprotein-associated attenuation of ER calcium load.

### **Acknowledgments**

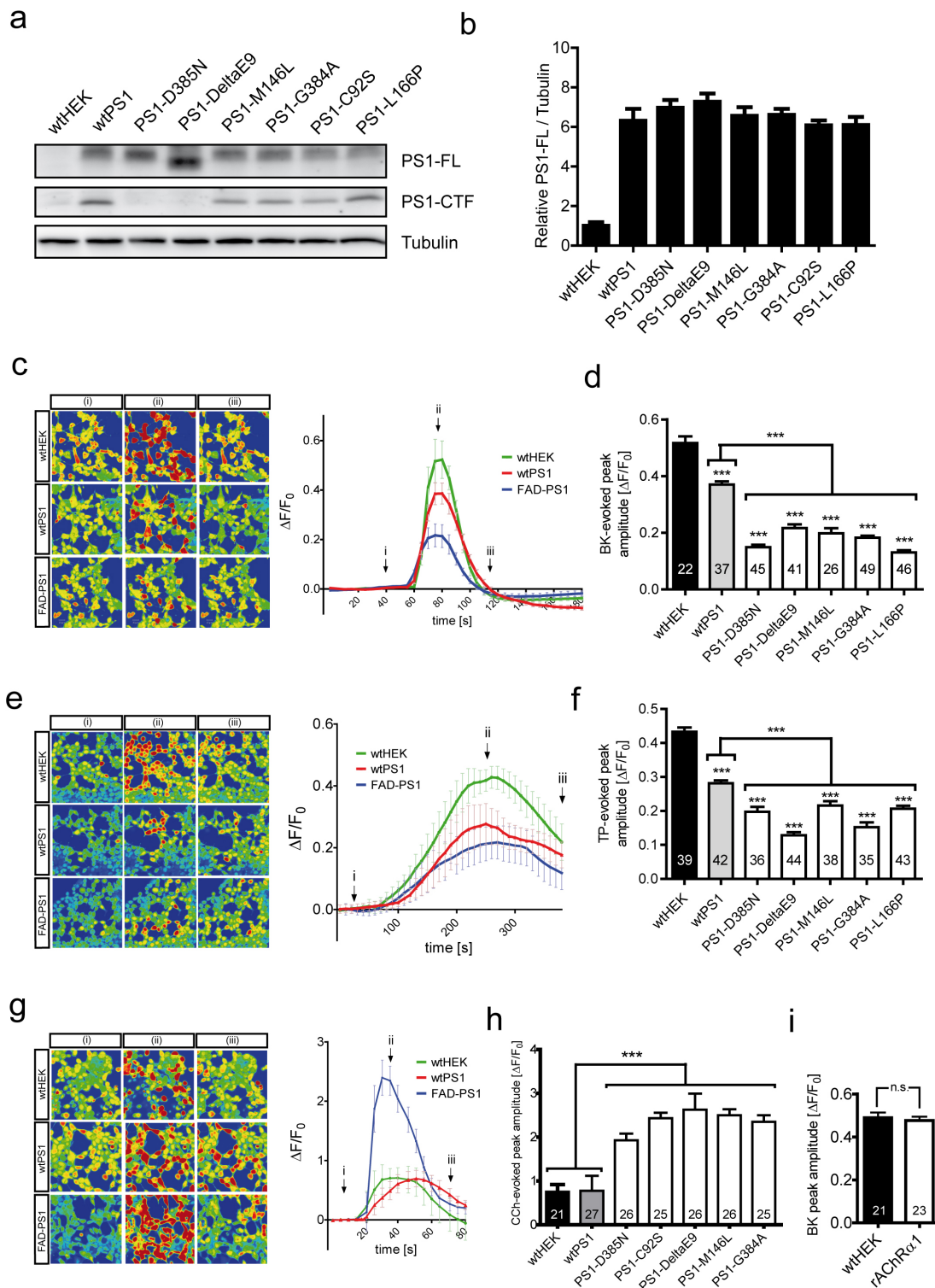
This work was supported the German-Polish grant from the German federal ministry for education and research council (BMBF — 01GZ0713). The authors are grateful to Drs. H. Steiner and C. Haass for kindly providing us with PS1 stable cell lines, PEN2-KD line and MBP/PS1-loop antibody, to Dr. Christoph Kaether for the rAChR $\alpha$ 1 line, and to BrainNet Europe for the human brain materials. We also would like to thank T. Kares, J. Knörndel and O. Stelmakh for their excellent technical assistance.

### **Conflict of Interest:**

The authors confirm that there are no conflicts of interest.

**Table 5.1: Human frontal cortex postmortem brain materials examined for PS1 holoprotein levels**

<b>Sample Number</b>	<b>Diagnosis</b>	<b>Age (years)</b>	<b>Sex</b>	<b>Postmortem interval (hours)</b>	<b>Braak&amp;Braak Stage</b>
RZ145	Control	85	F	20	I
RZ340	Control	54	M	9.5	0
RZ342	Control	83	F	22	II
RZ179	PS1 Leu286Val	57	M	44	VI
RZ265	PS1 Leu174Arg	57	F	34	VI
RZ272	PS1 Ile143Thr	39	M	7	VI
RZ421	APP Thr714Ile	49	M	48	VI



**Figure 5.1. Altered calcium release from ER in PS1-overexpressing HEK293 cells**

**(a)** Representative immunoblot indicating the expression of PS1 in HEK293 cells. The expression of PS1-FL holoprotein and PS1-CTF protein were analyzed using MBP/PS1-loop (aa 263-407) antibody on western blot using the protein lysates from wild type cells, cells stably overexpressing wild type PS1, several FAD-PS1 mutants and a  $\gamma$ -secretase inactive mutant (PS1-D385N). 5  $\mu$ g of protein lysate was loaded into each lane on the gel.

**(b)** Densitometric quantification of PS1-FL band intensity normalized to loading control Tubulin (n=3).

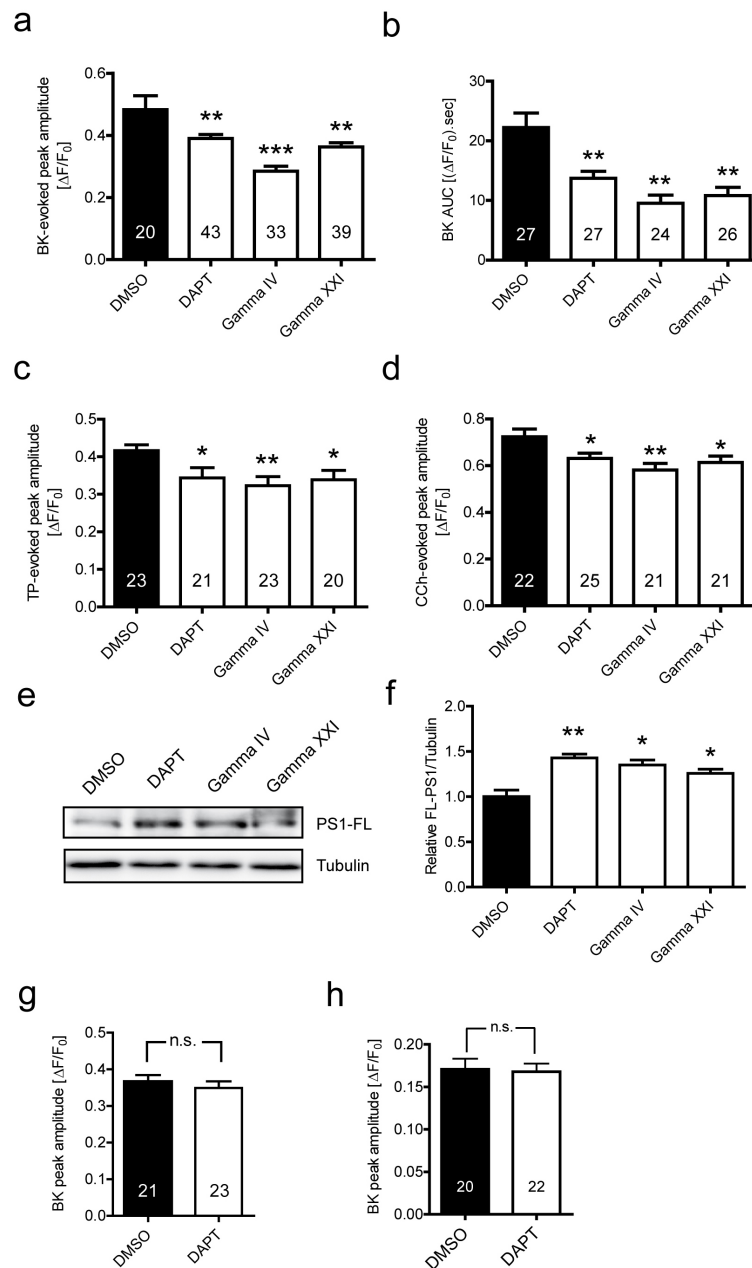
**(c)** Representative traces of BK-evoked, **(e)** TP-evoked and **(g)** CCh-evoked calcium releases for wild type HEK293 cells, HEK293 cells stably overexpressing wild type or mutant PS1 and the corresponding calcium images for the time points indicated with arrows displayed in pseudocolors.

**(d)** Average peak amplitude of BK-evoked and **(f)** TP-evoked calcium release from ER are significantly reduced in cells stably expressing wild type PS1 versus wild type HEK293 cells. Furthermore BK- and TP-evoked calcium responses are significantly attenuated in cells overexpressing mutants form of PS1 in comparison to both wild type PS1-overexpressing and plain wild type HEK293 cells.

**(h)** Average peak amplitude of Carbachol (CCh)-evoked calcium release from ER is significantly amplified in HEK293 cells stably expressing mutant forms of PS1 relative to cell stably expressing wild type PS1 and plain wild type HEK293 cells (\*\* $P < 0.001$ ).

**(i)** Average peak amplitude of BK-evoked calcium release from ER is unchanged in HEK293 cells stably overexpressing rAChR $\alpha$ 1 relative to wild type HEK293 cells.

(n.s.: non-significant)



**Figure 5.2. Attenuated calcium release from ER after treatment of HEK293 cells with  $\gamma$ -secretase inhibitors**

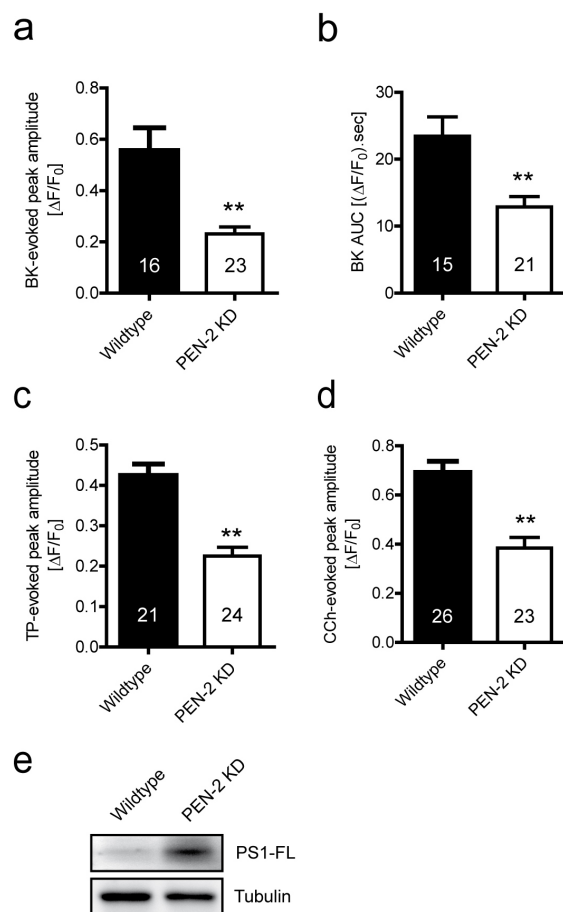
(a) Average peak amplitude and (b) the area under the curve (AUC) of BK-evoked calcium release and (c) the average peak amplitude of TP- and (d) CCh-evoked calcium release from ER are significantly reduced in HEK293 cells treated with  $\gamma$ -secretase inhibitors for 24 hours. DAPT, Gamma IV and Gamma XXI were used respectively at 10  $\mu\text{M}$ , 2.7  $\mu\text{M}$  and 300 nM concentration (\*  $P < 0.05$ , \*\*  $P < 0.01$  and \*\*\*  $P < 0.001$ ).

(e) Increase in PS1-FL (holoprotein) levels were detected by western blot in HEK293 cells. (f) Densitometric quantification of PS1-FL band intensities normalized to loading control Tubulin in (e) ( $n=3$ ). 10  $\mu\text{g}$  of protein lysate was loaded into each lane on the gel (\*  $P < 0.05$  and \*\*  $P < 0.01$ ).

Average peak amplitude of BK-evoked calcium response in (g) wild type PS1- and (h) PS1-D385N-overexpressing HEK293 cells is unchanged after treatment with DAPT for 24 hours.

(n.s.: non-significant)

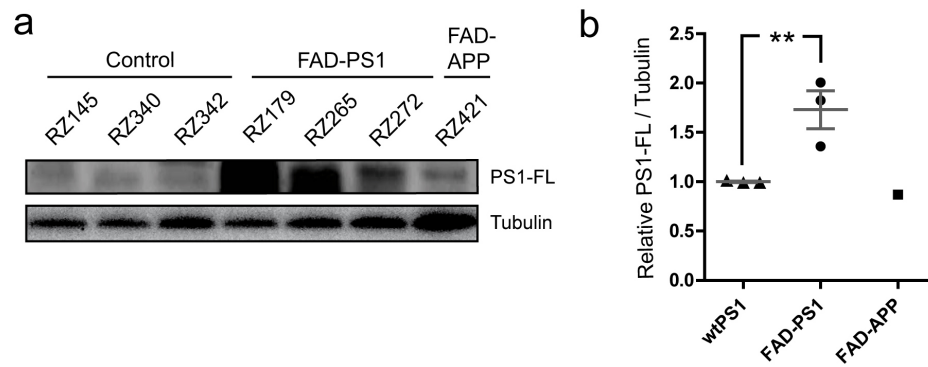




**Figure 5.3. Attenuated calcium release from ER in PEN-2 KD cells**

(a) Average peak amplitude and (b) the area under the curve (AUC) of BK-evoked calcium release and (c) the average peak amplitude of TP- and (d) CCh-evoked calcium release from ER are significantly reduced in PEN-2 KD cells compared to wild type HEK293 cells (\*\*  $P < 0.01$ ).

(e) Increased PS1-FL (holoprotein) levels detected by western blot in PEN-2 KD cells. 10  $\mu$ g of protein lysate was loaded into each lane.



**Figure 5.4: Elevation of PS1 holoprotein levels in frontal cortices of FAD-PS1 patients**

(a) Significant increase in PS1-FL (holoprotein) levels was detected by western blot in postmortem frontal cortex samples from FAD-PS1 cases (RZ179, RZ265 and RZ272), but not in a FAD-APP case (RZ421), compared to control cases (RZ145, RZ340 and RZ342). 15  $\mu$ g of brain homogenate was loaded in each lane on the gel (\*\*  $P < 0.01$ ).

(b) Densitometric quantification of PS1-FL band intensities normalized to loading control Tubulin in (a).

CUMULATIVE THESIS: PAPER III**6 Development and Implementation of a High-throughput Compound Screening Assay for Targeting Disrupted ER Calcium Homeostasis in Alzheimer's Disease**

Kamran Honarnejad<sup>1,2,3</sup>, Alexander Daschner<sup>1,2</sup>, Armin Giese<sup>2</sup>, Andrea Zall<sup>4</sup>, Boris Schmidt<sup>4</sup>, Aleksandra Szybinska<sup>5</sup>, Jacek Kuznicki<sup>5</sup>, Jochen Herms<sup>1,2,6</sup>

<sup>1</sup> Department of Translational Brain Research, DZNE – German Center for Neurodegenerative Diseases, Munich, Germany

<sup>2</sup> Center for Neuropathology and Prion Research; Ludwig Maximilian University, Munich, Germany

<sup>3</sup> Graduate School of Systemic Neurosciences, Ludwig Maximilian University, Munich, Germany

<sup>4</sup> Clemens Schöpf Institute of Chemistry and Biochemistry, Technische Universität Darmstadt, Darmstadt, Germany

<sup>5</sup> Laboratory of Neurodegeneration, International Institute of Molecular and Cell Biology, Warsaw, Poland

<sup>6</sup> Munich Cluster for Systems Neurology (SyNergy), Munich, Germany

**Keywords:** High-throughput screening; Drug Discovery; Alzheimer's disease; Bepridil; Endoplasmic Reticulum; Calcium

*This manuscript has been peer-reviewed and published in its essence under the indicated citation:*

*Honarnejad K, Daschner A, Giese A, Zall A, Schmidt B, Szybinska A, Kuznicki J, Herms J.; PLoS One. 2013 Nov 15;8(11):e80645. doi: 10.1371/journal.pone.0080645*

*This article was published under a Creative Commons Attribution License (CC-BY).*

*The author of this doctoral thesis has majorly contributed to this work by conceiving, designing and performing the experiments, analyzing parts of the data, preparing the figures and entirely writing the manuscript.*

## 6.1 Abstract

Disrupted intracellular calcium homeostasis occurs early in the cascade of events leading to Alzheimer's disease (AD) pathology. Particularly familial AD mutations linked to Presenilins result in exaggerated agonist-evoked calcium release from endoplasmic reticulum (ER). Here we report the development of a fully automated high-throughput calcium imaging assay utilizing a genetically-encoded FRET-based calcium indicator at single cell resolution for compound screening. The established high-throughput screening assay offers several advantages over conventional high-throughput calcium imaging technologies. We employed this assay for drug discovery in AD by screening compound libraries consisting of over 20,000 small molecules followed by structure-activity-relationship analysis. This led to the identification of Bepridil, a calcium channel antagonist drug in addition to four further lead structures capable of normalizing the potentiated FAD-PS1-induced calcium release from ER. We detected increased AMPK activity upon treatment of cells with Bepridil in a dose-dependent manner. AMPK activation by Bepridil is most likely a calcium-dependent phenomenon, since CaMKK inhibition by STO-609 abolishes the Bepridil-induced AMPK activation. Interestingly, it has recently been reported that Bepridil can reduce A $\beta$  production by lowering BACE1 activity. Indeed, we also detected lowered A $\beta$ , increased sAPP $\alpha$  and decreased sAPP $\beta$  fragment levels upon Bepridil treatment. Therefore based on the results here, we propose a novel calcium-dependent mode of action for Bepridil which through activation of AMPK can shift the balance of downstream APP processing from amyloidogenic  $\beta$ -cleavage towards non-amyloidogenic  $\alpha$ -cleavage.

## 6.2 Introduction

Alzheimer's disease (AD) is the most common form of dementia [293]. Major breakthroughs in understanding the underlying pathomechanisms of AD within the last few decades have not yet yielded effective disease-modifying therapies. The major hallmarks of AD are the accumulation of intracellular neurofibrillary tangles of hyperphosphorylated tau protein and extracellular plaques of  $\beta$ -amyloid ( $A\beta$ ) protein in brain [293]. Current AD drug development mainly focuses on targeting these two major pathological features. However, there is evidence that long before the manifestation of those hallmarks and cognitive deficits in AD, the neuronal calcium homeostasis is disturbed as a result of aging or due to missense mutations in Presenilin genes – the most common cause of early onset familial AD (FAD) [25, 40-42, 52, 255]. Long-term disruption of calcium homeostasis has been shown to both trigger and accelerate  $A\beta$  and tangle pathologies [49, 50, 294-296]. Moreover, calcium dysregulation as an early event in AD progression plays a key role in synaptic failure and neuron loss [53, 297]. Notably, the latter irreversible pathological events correlate best with the stages of dementia [53, 298]. Calcium alterations in peripheral tissues have been even proposed as diagnostic markers for mild AD [47]. Interestingly, Memantine, one of the only few approved drugs for treatment of moderate-to-severe AD patients, is an NMDA receptor antagonist which by inhibition of sustained calcium influx leads to stabilization of intracellular calcium homeostasis [37]. Therefore, restoring disrupted calcium homeostasis as an early event leading to cellular dysfunction may open novel avenues to more efficient treatment of AD patients. Hence, we examined the possibility of stabilizing intracellular store calcium homeostasis, particularly in the endoplasmic reticulum (ER), as an innovative target for AD drug discovery. To that end, we developed a high-throughput compound screening assay and screened over 20,000 small molecules which led to the identification of lead structures which can stabilize the familial Alzheimer's disease linked mutant Presenilin 1 (FAD-PS1) mediated disruption of ER calcium homeostasis.

## 6.3 Materials and Methods

### 6.3.1 Cell culture and cell lines

Human embryonic kidney 293 (HEK293) cells were cultured in Dulbecco's modified eagle medium (DMEM) supplemented with 10% fetal bovine serum and 1% penicillin/streptomycin while being incubated at 37°C, 5% CO<sub>2</sub> and 90% humidity. All stable PS1 lines (generously provided by Dr. S. Lammich) were carrying PS1 variants that were cloned into pcDNA3.1/Zeo(+) and selected via Zeocin antibiotic resistance. The PS1 lines were then stably transfected with YC3.6/pcDNA3 construct (kindly provided by Dr. A. Miyawaki) and respectively isolated by G418 antibiotic resistance leading to generation of double stable lines. The APP-, C99- and APPsw/PS1-M146L-overexpressing HEK293 lines were kindly provided by Dr. S. Lichtenthaler and Dr. H. Steiner and cultured as it has been previously described [299, 300].

### 6.3.2 Compound Library

DIVERSet™ 1 and 2 libraries (ChemBridge Corp., San Diego, CA, USA), each containing a diverse collection of 10,000 hand-synthesized small molecules (in total 20,000 compounds) as well as a medium size ion channel ligand library (Enzo Life Sciences GmbH, Lörrach, Germany) comprising 72 further structures were used for high-throughput compound screening. Compounds fulfilled the "Lipinski's rule of 5", indicating their high druglikeness potential [301].

### 6.3.3 High-throughput calcium imaging assay and automated image analysis

For the primary screen, HEK293 cells stably expressing PS1-M146L and Yellow Cameleon 3.6. (YC3.6) were seeded at 13,000 cells/well in 40 µl of growth medium on collagen-coated 384-well CellCarrier plates (PerkinElmer, Rodgau, Germany). After 6 h, using an automated pipetting robot (Bravo®; Agilent Technologies, Santa Clara, CA, USA), library compounds were added to each well at the final concentration of 10 µM in 1% DMSO, each in 4 replicates. All plates contained Thapsigargin (TP; 1 µM; Calbiochem, Darmstadt, Germany), Cyclopiazonic acid (CPA; 20 µM; Calbiochem) and

3,4,5-trimethoxybenzoic acid 8-(diethylamino)octyl ester (TMB-8; 50  $\mu\text{M}$ ; Sigma-Aldrich, Taufkirchen, Germany) as positive controls, as well as untreated and DMSO vehicle-treated wells. After 24 h using the pipetting robot, DRAQ5 (Biostatus Ltd, Leicestershire, UK), a far-red fluorescent nuclear dye, was added to each well at the final concentration of 500 nM. After 2 h, plates were measured for Carbachol (CCh)-induced calcium release using the Opera<sup>®</sup> high-throughput confocal imaging platform (PerkinElmer Cellular Technologies GmbH, Hamburg, Germany). Throughout imaging of the entire plate, 37°C temperature, 5% CO<sub>2</sub> and 90% humidity was maintained in the plate chamber. Using a 442 nm laser, YC3.6 was excited and its CFP and YFP emissions were separated respectively using 483/35 nm and 540/75 nm filters. Additionally, using a 640 nm laser DRAQ5 dye was excited and its emission was collected by 690/50 nm filter in order to locate the nuclei. Imaging was performed with a 20x water immersion autofocus objective. The duration of the entire time-lapse calcium imaging for each well was 23.5 s. This was achieved by imaging at 2.5 s interval resolution prior to dispensing CCh (for 5 s) to monitor the basal calcium levels. Next, the CCh-induced calcium rise and decay was monitored for 18.5 s post dispensing. Imaging was performed first at 1 s interval resolution immediately after dispensing (for 5 s) and subsequently at 2.5 s interval resolution (for 12.5 s). During dispensing, 10  $\mu\text{l}$  of CCh (Calbiochem) diluted in HBSS (10  $\mu\text{M}$ ) was injected to each well concurrent with calcium imaging by an automated dispensing unit which is part of the Opera<sup>®</sup> platform. Imaging was performed sequentially for all 384 wells. Using Acapella<sup>®</sup> software (PerkinElmer Cellular Technologies GmbH), an automated image analysis tool was developed to translate fluorescent signals to numerical values. Here, DRAQ5 and YC3.6 signals were used respectively to detect single cell nuclei and single cell boundaries over the entire course of time-lapse calcium imaging. After assigning each cell to its segmented nuclei and excluding the cells positioned at the edges of the imaging frames, calcium transients for every cell were monitored by plotting the kinetics of YFP/CFP versus time and normalizing the signals using the equation,  $\Delta F/F_0 = (F - F_0)/F_0$ , where F is the measured fluorescence signal at any given time and F<sub>0</sub> is the average fluorescence signal of the time points preceding CCh application. The peak amplitude of calcium rise upon CCh injection was the output of automated image analysis at single cell level. Non-responsive cells to CCh were excluded from analysis by setting an arbitrarily defined threshold. The average peak amplitude of all responsive cells in each well was calculated as the final readout in this assay.

#### 6.3.4 Data mining

Data mining, clustering and identification of the lead structures were performed with the Benchware DataMiner software (Tripos, St. Louis, MO, USA).

#### 6.3.5 Cytotoxicity assay

The cytotoxicity of the compounds was assessed *in vitro* using the 3-(4,5-dimethylthiazol-2-yl)-2,5-diphenyltetrazolium bromide (MTT) cell proliferation assay kit (Roche Diagnostics GmbH, Mannheim, Germany) according to manufacturer's instructions and previously described protocols [302]. In brief, HEK293 cells were cultured at a density of 35,000 cells/well in 96-well cell culture plates (Nunc GmbH, Langenselbold, Germany). On the next day, compounds (10  $\mu$ M) were added to separate wells in triplicates. Cells viability was analyzed after 24 h incubation with the compounds. For this purpose, 10  $\mu$ l of MTT (5 mg/ml in PBS) was pipetted to each well, followed by 4 h incubation at 37°C. The formed formazan crystals were dissolved by adding 100  $\mu$ l of 10% SDS (dissolved in 0.01 M HCl) to each well and the plates were shaken vigorously to ensure complete solubilization. The absorbance was measured at 560 nm using a microtiter-plate reader (FLUOstar Optima, BMG Labtech GmbH, Ortenberg, Germany). Values are presented as percentage of viable cells.

#### 6.3.6 A $\beta$ measurements

Levels of three different A $\beta$  species (A $\beta$ 38, A $\beta$ 40 and A $\beta$ 42) were measured using sandwich ELISA. Pools of HEK293 cells stably transfected with APP<sub>sw</sub>/PS1-M146L or APP were used to study the effect of compounds on A $\beta$  generation. According to Page et al. [300], cells were seeded at a density of 200,000 cells/well in collagen/poly-L-lysine (PLL)-coated 24-well plates and incubated for 24 h in growth medium. Next, the medium was exchanged with 500  $\mu$ l of fresh medium containing either Bepridil (3 - 30  $\mu$ M, Sigma-Aldrich), STO-609 (50  $\mu$ M, Calbiochem) or the positive controls DAPT (10  $\mu$ M, Calbiochem) and Sulindac sulfide (50  $\mu$ M, Sigma-Aldrich) or vehicle. After 16 h conditioned medium was collected and the levels of secreted A $\beta$ 38, A $\beta$ 40 and A $\beta$ 42 fragments were quantified using "Human (6E10) Abeta 3-Plex" sandwich ELISA



immunoassay kit (Meso Scale Discovery, Rockville, MD, USA) according to the instructions of the manufacturer. In brief, 150  $\mu$ l of blocker reagent was added to each well of the ELISA plate and incubated for 1 h at room temperature, followed by 3x washing using TRIS wash buffer. Next, 25  $\mu$ l of detection antibody was added to each well. At appropriate dilution, each of the samples or calibration standards were added to separate wells of ELISA plate and incubated for 2 h at room temperature, followed by 3x washing using TRIS wash buffer. Finally 150  $\mu$ l of read buffer was added to the wells. The light emission after electrochemical stimulation was measured using Sector Imager 2400 reader (Meso Scale Discovery). Based on the values generated with calibration standards, corresponding concentrations of A $\beta$  species were calculated using the Meso Scale Discovery Workbench software. All measurements were performed in four replicates.

#### 6.3.7 *sAPP $\alpha$ and sAPP $\beta$ measurements*

Levels of sAPP $\alpha$  and sAPP $\beta$  fragments were measured using sandwich ELISA. HEK293 cells stably expressing APP or APP<sup>sw</sup>/PS1-M146L were seeded at a density of 200,000 cells/well in collagen/poly-L-lysine (PLL)-coated 24-well plates and incubated for 24 h in growth medium. Next, the medium was exchanged with 500  $\mu$ l of fresh medium containing either compounds or vehicle. After 16 h conditioned medium was collected and the levels of secreted sAPP $\alpha$  and sAPP $\beta$  fragments were quantified using sAPP $\alpha$ /sAPP $\beta$  sandwich ELISA immunoassay kit (Meso Scale Discovery) according to the instructions of the manufacturer. In brief, 150  $\mu$ l of blocker reagent was added to each well of the ELISA plate and incubated for 1 h at room temperature, followed by 3x washing using TRIS wash buffer. Next, 25  $\mu$ l of samples or calibration standards were added to separate wells of ELISA plate and incubated for 1 h at room temperature, followed by 3x washing using TRIS wash buffer. Then 25  $\mu$ l of detection antibody was added to each well and incubated for 1 h at room temperature, followed by 3x washing using TRIS wash buffer. Finally, 150  $\mu$ l of read buffer was added to the wells. The light emission after electrochemical stimulation was measured using Sector Imager 2400 reader (Meso Scale Discovery). Based on the values generated with calibration standards, corresponding concentrations of sAPP $\alpha$  and sAPP $\beta$  were calculated using the Meso Scale Discovery Workbench software. All measurements we performed in four replicates.

### 6.3.8 AMPK activity assay

The AMP-activated protein kinase (AMPK) activity was determined by means of measuring pThr172AMPK levels using sandwich ELISA immunoassay (Invitrogen Corp., Camarillo, CA, USA). HEK293 cells were seeded at a density of 200,000 cells/well on collagen/poly-L-lysine (PLL)-coated 24-well plates and incubated for 24 h in growth medium. Next, medium was exchanged with 500  $\mu$ l of fresh medium containing Bepridil (0.1 - 50  $\mu$ M; Sigma-Aldrich) and/or STO-609 (50  $\mu$ M; Calbiochem), or DMSO vehicle. After 16 h medium was removed and wells were washed 3x with ice cold PBS. Next the cells were lysed in 120  $\mu$ l of ice cold lysis buffer and the lysates were used to quantify the AMPK activity level using the method adapted from Moreno-Navarrete *et al.* [303]. The assay was performed according to the manufacturer's instructions. In brief, to each well of the ELISA plate 100  $\mu$ l of the lysates or calibration standards was added and incubated for 2 h at room temperature, followed by 4x washing using assay wash buffer. Next 100  $\mu$ l of detection antibody was added to each well and incubated for 1 h at room temperature, followed by 4x washing using assay wash buffer. Then 100  $\mu$ l of HRP anti-rabbit antibody was added to the wells and incubated for 30 min at room temperature, followed by 4x washing using the assay wash buffer. Finally 100  $\mu$ l of stabilized chromagen was added to the wells and the reaction was stopped after 30 min by adding "stop" solution to the wells. The absorbance was measured at 450 nm using a microtiter-plate reader (FLUOstar Optima, BMG Labtech GmbH). pAMPK levels were calculated based on the absorptions of the standards and their calibration curve. All the measurements were performed in duplicates.

### 6.3.9 Statistical data analysis

GraphPad Prism 5.0b (GraphPad Software, San Diego, CA, USA) was used for statistical analysis of the data. Values represent mean  $\pm$  standard deviation. To test significance, two-tailed student's t-test was performed and differences were considered statistically significant if  $p < 0.05$ . The Z'-factors were computed according to Zhang *et al.* [304], where TP was used as a positive and DMSO as a negative control.

## 6.4 Results

### 6.4.1 *FAD-PS1 mutations enhance the amplitude of CCh-induced calcium release and the number of responsive cells*

Mutations in presenilins (PS1 and PS2) account for the vast majority of early onset familial Alzheimer's disease (FAD) cases. These mutations result in enhancement of inositol 1,4,5-trisphosphate (IP<sub>3</sub>) receptor sensitivity [69, 235]. As expected, the peak size of CCh-evoked calcium release in all FAD-PS1 lines was approximately 3 folds higher than in wild type PS1 line (Figure 6.1a). Moreover, a remarkable increase in the number of CCh-responsive cells was consistently detected in all FAD-PS1 lines. In wild type PS1 line, only 29% of the cell population was CCh-responsive, whereas in all FAD-PS1 mutant lines, over 95% of the cell population responded to CCh (10 μM) (Figure 6.1b). Taken together, FAD-PS1 expression enhances the number of responsive cells to CCh and amplifies the peak size of CCh-evoked calcium response. Likewise, the expression of a  $\gamma$ -secretase-deficient mutant form of PS1 (PS1-D385N) results in increased responsiveness to CCh and augmented calcium release from ER upon CCh stimulation (Figure 6.1a and 6.1b). In the next set of experiments, the augmented CCh-evoked calcium release in FAD-PS1 expressing cells was used as the target to screen for compounds that can restore exaggerated calcium release to physiological levels.

### 6.4.2 *High-throughput compound screening assay enables the discovery novel lead structures*

We addressed intracellular store calcium dyshomeostasis as an innovative target for drug discovery with a novel FRET single-cell-based calcium imaging technique in a fully automated high-throughput kinetic assay on the Opera<sup>®</sup> system (PerkinElmer) for compound screening.

Yellow Cameleon 3.6 (YC3.6), a superior genetically-encoded FRET-based calcium probe with expanded dynamic range and fast kinetics [212], was introduced to HEK293 cells as a tool to monitor both the basal calcium concentrations and the released calcium from ER in real-time by confocal imaging. YC3.6 is composed of CFP and YFP linked

via calmodulin (CaM) and a CaM-binding peptide (M13). Upon calcium binding it undergoes a conformational change and thereby FRET efficiency increases (Figure 6.2a) [212]. The assay readout was the peak size of potentiated inositol-1,4,5-trisphosphate receptor (IP<sub>3</sub>R)-evoked calcium release from ER in HEK293 cells carrying a disease-causing mutated form of PS1 (PS1-M146L). Agonist-induced IP<sub>3</sub> production by CCh results in calcium release from ER (Figure 6.2b). As presented here and reported by others as well [223], FAD-PS mutations mediate exaggerated CCh-induced calcium release compared to wild type PS1 expressing cells (Figures 6.1a and 6.2c). Notably, CCh-evoked calcium responses were evaluated at several different CCh concentrations. However, the most remarkable difference in the peak size of CCh-evoked calcium release in FAD-PS1 versus wild type PS1 lines was detected at 10 μM CCh (data not shown).

As illustrated in figure 6.2d, HEK293 cells stably coexpressing FAD-linked PS1-M146L mutation and YC3.6 were seeded on 384-well optical bottom plates. After 6 h, compounds from the library plates were added to separate wells using a pipetting robot. After 24 h incubation with compounds, DRAQ5 nuclear marker was added to the wells. After 2 h, time-lapse calcium imaging was performed and CCh-induced calcium release was monitored sequentially for each well with the use of YC3.6 calcium indicator. In addition, the signal of DRAQ5 dye was also collected throughout the entire course of time-lapse imaging. Using “Acapella” software (PerkinElmer), an automated image analysis tool was developed to convert fluorescent signals in large number of cell populations to numerical values. To that end, DRAQ5 signal was used to detect all nuclei in each frame and the YC3.6 signal was used to assign the detected single cell boundaries to their corresponding segmented nuclei over the entire course of time-lapse calcium imaging. On average, approximately 150-200 cells were detected for each well. For every detected cell, calcium transients were measured by calculating YFP/CFP over the course of imaging. The peak amplitude size of the calcium rise upon CCh injection was the output of automated analysis at single cell level. The ability to simultaneously monitor calcium transients for all individual cells of a well enabled us to filter out CCh-non-responsive cells from the analysis by setting an arbitrarily defined threshold. The average peak amplitude of all responsive cells in a well was calculated as the final output of the image analysis tool.

The performance of the high-throughput compound screening assay remained very robust throughout screening of 201 plates ( $Z'$ -factor  $> 0.8$ ).  $Z'$ -factors for ten randomly selected screened plates are presented in figure 6.2e. The average  $Z'$ -factor for those ten plates was determined to be  $0.806 \pm 0.029$ , reflecting a robust assay for high-throughput screening (HTS).

After filtering the autofluorescent and highly toxic compounds, 53 active small molecule hits were identified from the primary screen (Figure 6.3). A compound was regarded as active if the peak size of calcium release in cells treated with that compound was 90% or smaller than the peak size of DMSO-treated controls on the same plate. To each library compound a numerical value typically  $< 1.0$  was assigned indicating a measure for its efficacy, calculated by dividing the peak size of calcium release in cells treated with that given compound to the peak size of DMSO-treated controls on the same plate. Hereafter, we refer to this value as “normalized ER calcium response”. In figure 6.3, the list of all hits from the primary screen including their chemical structures and corresponding normalized ER calcium response values is presented.

The activity of the entire set of 53 hits in terms of reducing the peak size of CCh-evoked calcium release was validated and confirmed in PS1-M146L line again (Figure 6.4a). Moreover, all primary hits were capable to attenuate the CCh-evoked calcium release in three other cell lines expressing either different FAD-PS1 mutations (PS1-DeltaE9 and PS1-C92S) or a  $\gamma$ -secretase-deficient PS1 mutant (PS1-D385N) (Figures 6.4e-6.4g). This indicates that the activity of the identified hits in normalizing the exaggerated FAD-PS1-mediated CCh-evoked calcium release is indeed not only specific to the FAD-PS1 mutation used in the primary screen, but present across other examined PS1 mutations as well.

53 structures identified from the primary screen were classified into different categories based on their efficacy in attenuating the peak size of the CCh-evoked calcium release (Figure 6.4c and 6.4d). These categories are separated according to the corresponding value of normalized ER calcium response, presented as percentages relative to the peak size of DMSO-treated control.

Next, we performed an MTT assay in order to assess the cytotoxicity of the entire set of 53 hits generated from the primary screen. Majority of identified active compounds showed no toxicity and HEK293 cells treated with 10  $\mu$ M of the compounds for 24 h remained viable (Figure 6.4h). Treatment with only 5 compounds, 3 of which belonging to Thiazolidine lead structure, resulted in 30-40% reduction in cellular viability.

After performing structure-activity-relationship (SAR) studies with the entire collection of library compounds using “Benchware DataMiner” software (Tripos), 4 different lead structures were identified. Those structures belonged to following compound classes: Thiazolidine, Phenothiazine, Imidazole and Benzhydrylpiperidinamin (Figure 6.4b, 6.S1, 6.S2, 6.S3 and 6.S4). To that end, first the library consisting of 20,000 compounds was imported to the data mining software and active compounds (normalized ER calcium response  $< 0.9$ ) were selected. Using the “OptiSim” algorithm groups of similar compounds, called clusters, were identified. Subsequently inactive compounds were added to the existing clusters. Then the clusters were combined according to their structures in order to reduce their number. Then a SAR map of the clusters was generated and clusters with more than 50% active compounds were represented as stars and clusters with less than 50% active compounds as rectangles. In addition, all clusters that have more than 4 active compounds were colored in blue and otherwise in red. The sizes of the symbols correlate directly with the number of compounds in each cluster (Figure 6.4b).

### 6.4.3 *Effect of Bepridil on CCh-evoked calcium release from ER*

In addition to 4 discovered lead structures, the HTS led to the identification of Bepridil, a calcium antagonist drug which was previously shown to be beneficial against AD through simultaneously targeting  $\beta$ - and  $\gamma$ -secretases [299]. In view of the detected Bepridil activity in dampening the exaggerated FAD-PS1-mediated calcium release and the promising indications linking it to lowered A $\beta$  generation, we synthesized 15 derivative structures in an attempt to generate Bepridil-analogous molecules with improved efficacy (Figure 6.S5). The derivatisation strategy aimed to explore the contribution of different fragments to the potency and efficacy by removal of these moieties (BSc4040 and BSc4209). We varied the lipophilicity (BSc4040 and BSc3946), solubility, basicity (BSc4049) and membrane permeation by introduction of an ammonium salt (BSc3947) or sulfonic acid (BSc3963) and carboxylic acids (BSc3964 and BSc4065). Using the same

HTS assay employed in primary screening, we measured dose-dependent effects for Bepridil and its synthesized derivatives at 30, 10, 3, 1, 0.3 and 0.1  $\mu\text{M}$  (Figure 6.5). The chemical modifications in the structure of Bepridil did not further improve the efficacy in attenuating the CCh-evoked calcium release (Figure 6.5). Therefore in the following experiments the original Bepridil structure identified from the primary screen was further characterized to determine its mode of action. Notably, Bepridil had no effect on the peak size of CCh-evoked calcium release in wildtype PS1 expressing cells (Figure 6.S6).

#### **6.4.4 Effect of Bepridil on APP processing and A $\beta$ generation**

Mitterreiter and colleagues have shown that Bepridil treatment decreases the formation of A $\beta$  by shifting the balance of APP processing from amyloidogenic  $\beta$ -cleavage towards non-amyloidogenic  $\alpha$ -cleavage [299]. In line with their observation, we also detected reductions in the level of secreted A $\beta$ 38, A $\beta$ 40 and A $\beta$ 42 peptides upon 16 h exposure of APPsw/PS1-M146L-overexpressing HEK293 cells with Bepridil at 30  $\mu\text{M}$  (Figure 6.6a). Likewise, in APP-overexpressing HEK293 cells we detected lower A $\beta$ 38, A $\beta$ 40 and A $\beta$ 42 generation after Bepridil treatment (30  $\mu\text{M}$ ) for 16 h (Figure 6.S7a). However, upon Bepridil treatment at lower concentrations (10  $\mu\text{M}$  and 3  $\mu\text{M}$ ), we detected reduced A $\beta$ 38 and A $\beta$ 40, but increased A $\beta$ 42 levels (Figure 6.S7a). Treatment of C99-overexpressing HEK293 cells with Bepridil (30  $\mu\text{M}$ ) also leads to decreased A $\beta$ 38 and A $\beta$ 40 and increased A $\beta$ 42 levels, suggesting an inverse  $\gamma$ -secretase modulator (iGSM), as previously also described [299] (Figure 6.S7b). The reduction in the A $\beta$  amounts was accompanied by an increase in sAPP $\alpha$  and a decrease in sAPP $\beta$  secreted fragments in a dose-dependent manner, indicating that Bepridil treatment indeed enhances the activity of  $\alpha$ -secretase and inhibits the activity of  $\beta$ -secretase in two different cell lines (Figure 6.6b and 6.S7c). Furthermore, we also tested the effect the other active compounds derived from the primary calcium screen on A $\beta$  peptide production. Depending on the compound tested, we detected increased, decreased or unchanged A $\beta$  levels upon 16 h exposure of APPsw/PS1-M146L HEK293 cells with the compounds (Figure 6.S8).

#### **6.4.5 Effect of Bepridil on AMPK activity**

There exists evidence that the activation of AMP-activated protein kinase (AMPK) is partially calcium-dependent and modulating its activity affects APP processing [305]. In

order to assess the effect of Bepridil on AMPK activity, we measured phosphorylated AMPK (pAMPK) levels. pAMPK is the activated form of AMPK and its phosphorylation is directly associated with AMPK activity [305]. We detected increased pAMPK levels upon 16 h treatment of HEK293 cells with Bepridil in a dose-dependent manner (Figure 6.6c). Calcium/calmodulin-dependent protein kinase kinase  $\beta$  (CaMKK $\beta$ ) is an upstream kinase responsible for calcium-dependent activation of AMPK [306, 307]. In order to examine whether AMPK activation by Bepridil is a CaMKK $\beta$ -dependent phenomenon, we used STO-609, a specific CaMKK inhibitor [308]. Indeed, cotreatment of HEK293 cells with STO-609 and Bepridil partially abolished the Bepridil-dependent AMPK activation (Figure 6.6d). Moreover, CaMKK inhibition with STO-609 also reversed the Bepridil-mediated increase in sAPP $\alpha$ , but not the decrease in sAPP $\beta$  (Figure 6.S7d).

## 6.5 Discussion

Here we describe the development and implementation of a high-throughput compound screening assay targeting ER calcium dysregulation as an innovative approach for AD drug discovery. As opposed to the majority of AD drug discovery strategies that target late stage disease hallmarks, this approach targets one of the earliest and most upstream events in AD progression before the appearance of characteristic AD pathological features. Targeting late events in the course of the AD, during which the disease has likely reached an irreversible stage, could be one of the reasons for the consistent recent failure of disease-modifying AD drug candidates targeting A $\beta$  and tangle pathologies in late clinical phases [14]. To our knowledge, the possibility of targeting disrupted ER store calcium homeostasis as an upstream event in disease pathogenesis has never been examined in AD drug discovery in the past.

The HTS assay developed offers several advantages compared to current calcium measurement screening technologies. Firstly, the use of genetically-encoded calcium sensors as opposed to conventional synthetic organic dyes allows monitoring long-term intracellular calcium dynamics without the drawbacks caused by dye toxicity, loading, washing and leakage. In addition to being able to follow long-term calcium concentrations, short-term calcium imaging can be performed at multiple time points, which could even be spread over several days. Since the Opera<sup>®</sup> HTS platform is



equipped with an environmental control chamber, excellent long-term cell viability conditions are ensured by maintaining regulated temperature, humidity and CO<sub>2</sub>. Secondly, the developed HTS assay allows performing rapid automated dispensing of reagent jets to individual wells during calcium measurements with no time lag between dispensing and imaging. The latter is ideal for kinetic measurements that require rapid imaging with no delay post dispensing, e.g. fast agonist-induced calcium release. Thirdly, the single-cell-based nature of this assay in combination with automated image analysis enables the detection of even slight changes in calcium concentration which cannot be achieved with the use of conventional single-well-based calcium measurement screening technologies (e.g. FLIPR) [309]. Moreover, the ability to simultaneously monitor calcium transients for individual cells of a well, allows applying multiple filtering parameters in image analysis software to set apart different cell subpopulations from each other, e.g. “active” from “inactive”, “responsive” from “non-responsive”, “transfected” from “untransfected” cells, etc. The latter is not possible in single-well-based calcium measurement assays. Furthermore, the assay offers superior robustness reflected by Z'-factor > 0.8. Overall, the aforementioned advantages of the developed HTS assay enabled us to identify drugs, which by having even a modest effect on exaggerated IP<sub>3</sub>R-evoked calcium signals may be beneficial for AD therapy.

Calcium alterations associated with FAD-PS expression provide ideal means to investigate the disruption of ER calcium homeostasis. FAD-PS-dependent calcium alterations in intracellular calcium stores have been linked to synaptic dysfunction, the underlying basis of cognitive impairment in AD [310]. Nevertheless, the potential of the developed HTS assay is not only restricted to FAD drug discovery. Early studies indicate that the disrupted ER calcium release correlates with A $\beta$  and tangle pathologies in AD [48]. During physiological aging [52, 311] and in several neurodegenerative diseases [25, 312] the neuronal store calcium homeostasis is also altered. Yet the alterations in ER calcium homeostasis during aging are much more subtle [313]. Notably, age is the main risk factor for developing sporadic AD [314]. Moreover, PS1 mutations are also associated with heart failure and cardiac diseases as a result of similar alterations in ER calcium signaling as in AD [315]. Therefore, targeting intracellular store calcium homeostasis in HTS assays may allow the identification of drugs relevant for treatment of undesired effects associated with physiological aging and a wide range of neurodegenerative and cardiac diseases. As recently reviewed by Chadwick *et al.*, ER is

not a classical AD drug target, however due to its multifactorial involvement in several cellular aspects of AD, even a modest modulation in its function may present tremendous therapeutic efficacy [316].

Screening of over 20,000 small molecules using the HTS assay yielded the discovery of four lead structures and 53 primary hit molecules, one of them being Bepridil, a calcium channel blocker. Bepridil specifically attenuated the FAD-PS1-mediated exaggerated ER calcium release, without affecting the latter in wildtype PS1 expressing cells. Bepridil is reported to modulate APP processing by simultaneously affecting the activity of  $\beta$ - and  $\gamma$ -secretases [299]. Hence, we synthesized 15 Bepridil derivatives in an attempt to identify analogous structures with improved efficacy and potency in restoring the exaggerated IP<sub>3</sub>R-evoked calcium release in cells carrying FAD-linked PS1 mutations. However, the modifications in the chemical structure of Bepridil did not further improve the activity of synthesized derivatives in the ER calcium release assay.

Bepridil treatment increased the activity of AMPK in a dose-dependent manner. We demonstrate that Bepridil-associated AMPK activation is indeed a CaMKK $\beta$ -dependent mechanism, since CaMKK $\beta$  inhibitor STO-609 partially abolishes the Bepridil-mediated activation of AMPK. Such a partial effect may be due to incomplete CaMKK $\beta$  inhibition by STO-609 and the residual activity of calcium-stimulated CaMKK $\beta$ .

Based on our finding that Bepridil dampens the calcium release from ER, at the first sight it may appear that, in contradiction to our hypothesis, Bepridil should lower the AMPK activity. However, the control of AMPK activation is a complex mechanism which is regulated in a context- and tissue-dependent manner [317]. While calcium can activate AMPK, chronic elevated cytosolic calcium concentrations have been shown to lower the AMPK activity [318]. The consequence of the FAD-PS-associated exaggerated calcium release from ER may also be chronically increased cytosolic calcium concentrations. Moreover, both in AD and aging, where long-term disturbed calcium homeostasis is present, declined AMPK activity has been described [305, 319].

Alterations in intracellular calcium homeostasis can directly affect A $\beta$  production [49]. Indeed, many of the active compounds identified from the primary calcium screen either increased or decreased the production of A $\beta$  peptides. Such a wide range of effects on A $\beta$

generation is rather predictable, since most likely those compounds target different components of intracellular calcium homeostasis, thus, also differently affecting APP processing. In accordance with the findings of Mitterreiter *et al.* [299], we also detected less A $\beta$  generation upon Bepridil treatment. Here we propose an alternative calcium-dependent mechanism for the described Bepridil-mediated decrease in  $\beta$ -secretase cleavage and the consequent lowered A $\beta$  production [299]. Several publications have previously demonstrated that AMPK is implicated in APP metabolism and its pharmacological activation is associated with reduced A $\beta$  generation [320, 321]. Interestingly the activity of SIRT1, a downstream protein target of AMPK activation, leads to lowered A $\beta$  production through ADAM10 activation [322], the major physiologically relevant form of APP  $\alpha$ -secretase [323]. Moreover, AMPK activation has been shown to be associated with reduced expression of BACE1 [324]. Taken together, the observed simultaneous Bepridil-dependent increase in sAPP $\alpha$  and decrease in sAPP $\beta$  cleavage products may respectively be attributed to ADAM10 activation and BACE1 downregulation, mediated by increased AMPK activity. Indeed, CaMKK $\beta$  inhibition with STO-609 reversed the Bepridil-dependent increase in secreted sAPP $\alpha$ , however did not rescue the decreased sAPP $\beta$  levels. This might be due to the fact that BACE1 activity itself is calcium-dependent [39], thus interfering with calcium homeostasis and CaMKK $\beta$  activity may also additionally affect APP processing through calcium-dependent, but AMPK-independent mechanisms.

In cells overexpressing C99, which is the  $\beta$ -cleaved product of APP and the substrate for  $\gamma$ -secretase, treatment with Bepridil decreased A $\beta$ 38 and A $\beta$ 40 levels, but on the other hand increased A $\beta$ 42 amounts. Mitterreiter *et al.* have also described such a concurrent iGSM feature for Bepridil. This might also explain our observation that in APP-overexpressing cells, Bepridil treatment at lower concentrations (10  $\mu$ M and 3  $\mu$ M) increases, but at higher concentration (30  $\mu$ M) decreases A $\beta$ 42 levels. However, A $\beta$ 38 and A $\beta$ 40 levels were decreased at all Bepridil concentrations in all cell types tested. In other words, it appears that at low Bepridil concentrations, the iGSM effect of Bepridil (increase in A $\beta$ 42 levels) overbalances the reduced BACE1 activity (decrease in A $\beta$ 42 levels), whereas at higher Bepridil concentrations this effect is *visa versa*.

There exists evidence that calcium ions can directly regulate the activity of  $\gamma$ -secretase [325] and BACE1 [39]. Therefore we cannot exclude the possibility that stabilization of

ER calcium by treatment with Bepridil may also reduce the activity of  $\gamma$ -secretase and BACE1 and thus lead to lowered A $\beta$  production. Mitterreiter *et al.* report that APP protein expression level is indeed unaffected by Bepridil treatment [299]. Therefore the possibility that reduced APP protein levels may account for Bepridil-dependent A $\beta$  reduction can be excluded.

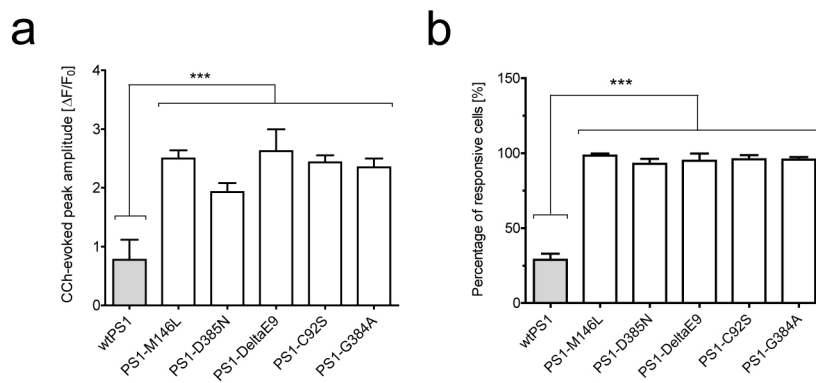
Mitterreiter *et al.* have already described that Bepridil can inhibit  $\beta$ -secretase cleavage by mildly raising the membrane-proximal endosomal pH, while independently modulating  $\gamma$ -secretase activity as well [299]. Here we describe an additional mode of action for Bepridil which involves AMPK activation, a mechanism modulating APP processing. AMPK activity is implicated in several aspects involved in AD pathogenesis [305]. For example, AMPK activation has been shown to promote autophagy and A $\beta$  clearance [326, 327] and also regulate tau phosphorylation through direct and indirect mechanisms [328, 329]. In view of such promising indications, the potential protective role of Bepridil associated with improved A $\beta$  clearance or tau pathology should be examined in more complex models.

Novel molecular target(s) of Bepridil are yet to be determined. However, based on the known function of Bepridil as a calcium channel blocker, one may speculate that by dampening the hyperactivated calcium channels located on the ER [69, 230], Bepridil could stabilize the disturbed ER calcium homeostasis. Indeed, treatment with ryanodine receptor (RyR) blocker dantrolene was shown to reduce A $\beta$  burden, increase PSD-95 expression and improve learning and memory in a APP<sup>sw</sup>-expressing mouse model of AD [204]. Moreover, PS holoprotein has been shown to form passive leak calcium channel on the ER membrane [228]. Therefore future studies are necessary to closely examine whether Bepridil exerts any modulatory effect on the activity of ER calcium receptor channels or the passive calcium leakage through PS holoprotein.

In this report, we focused on characterization of Bepridil, a hit identified from the HTS. However other lead structures and hits identified from the primary screen may also provide therapeutic potential for AD treatment which shall be investigated in future.

**Acknowledgements**

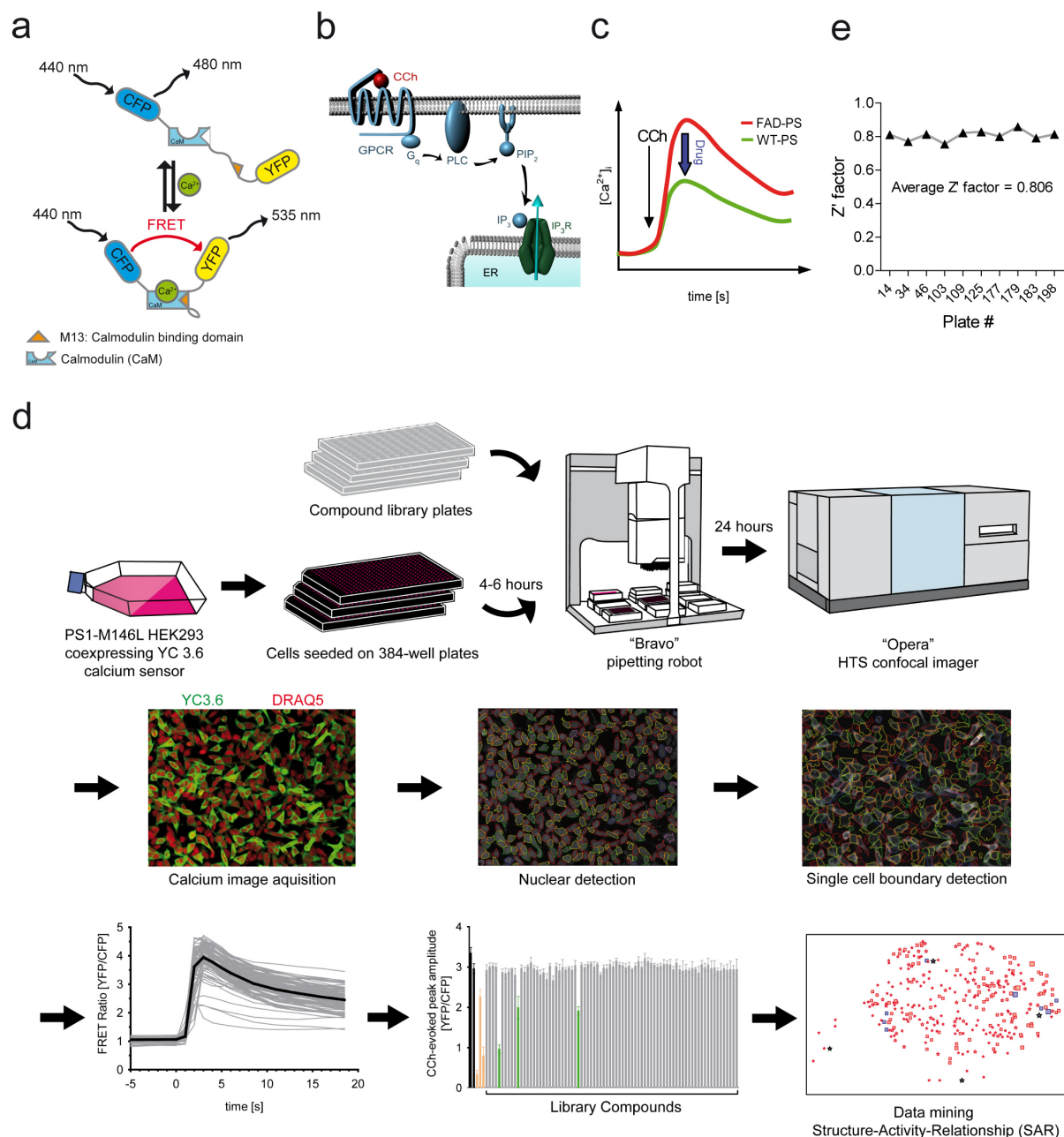
The authors are grateful to Dr. A. Miyawaki for YC3.6 construct, to Dr. A. Kirsch for the support in developing image analysis tool, to Dr. T. Hirschberger for his help in data mining and SAR studies, to P. Schmitz and F. Wachter for data management, to M. Taverna, Drs. S. Lichtenthaler, S. Lammich, H. Steiner and C. Haass for kindly providing the stable PS1 and APP lines and the support in the A $\beta$  and sAPP $\alpha/\beta$  measurements. We also would like to thank T. Kares, J. Knörndel and O. Stelmakh for their excellent technical assistance.



**Figure 6.1. CCh-induced calcium release in HEK293 carrying PS1 mutations**

(a) The average peak amplitude of CCh-induced calcium release is significantly potentiated in FAD and inactive PS1 mutants compared to wild type PS1 cells (\*\* $P < 0.001$ ).

(b) The average number of responsive cells to CCh is remarkably increased in cells expressing FAD and inactive PS1 mutants compared to wild type PS1 cells (\*\* $P < 0.001$ ).



**Figure 6.2. Work flow of the high-throughput FRET calcium imaging based compound screening assay and data analysis**

**(a)** Structure of the calcium sensor YC3.6 which is a fusion protein composed of CFP and YFP attached via calmodulin (CaM) and a CaM-binding peptide (M13). Calcium binding brings CFP and YFP together, shifting the emission of 480 nm to 535 nm upon excitation at 440 nm.

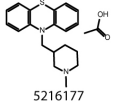
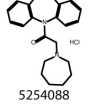
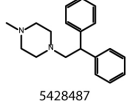
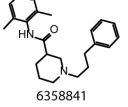
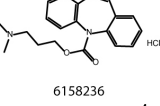
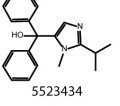
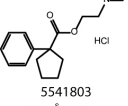
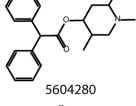
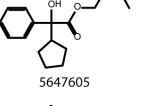
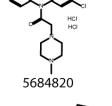
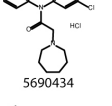
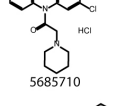
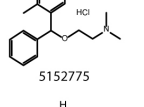
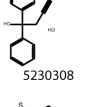
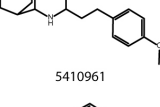
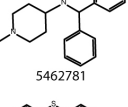

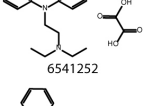
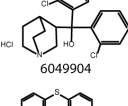
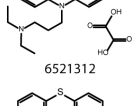
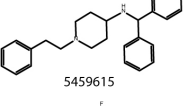
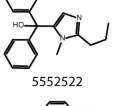
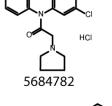
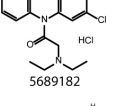
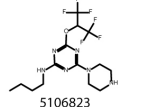
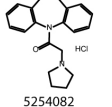
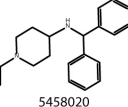
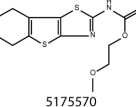
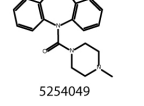
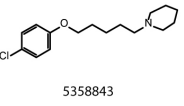
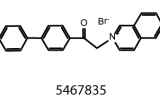
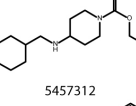
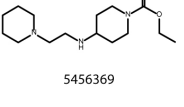
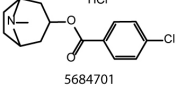
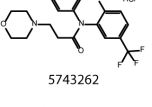
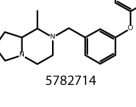
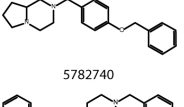
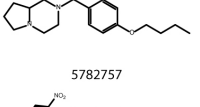
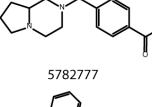
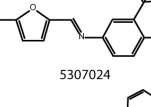
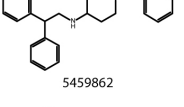
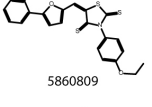
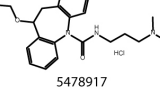
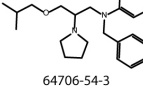
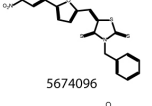
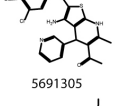
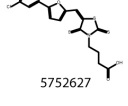
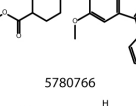
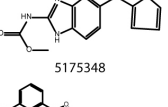
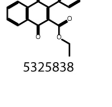
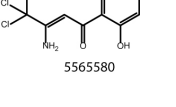
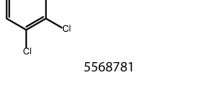
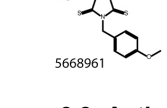
**(b)** CCh application initiates a pathway which results in calcium release from ER. CCh exposure leads to G-coupled activation of PLC catalyzing the hydrolysis of the membrane-associated PIP<sub>2</sub> molecule to IP<sub>3</sub>. Binding of IP<sub>3</sub> molecule to IP<sub>3</sub> receptor channels (IP<sub>3</sub>R) on the ER membrane in turn leads to opening of IP<sub>3</sub>R channels and calcium release from ER to cytosol.

**(c)** Representative calcium transients of CCh-evoked calcium release in cells expressing FAD-linked PS mutant versus wildtype PS. FAD-PS expressing cells show an exaggerated calcium release upon CCh exposure. The arrow shows the time point at which CCh is applied. The HTS screening rationale was to identify drugs that can restore the FAD-PS-associated potentiation of CCh-evoked calcium release to the level of wildtype PS.

**(d)** HEK293 cells stably expressing PS1-M146L and YC3.6 calcium indicator are seeded in 384-well format plates. 6-8 h post seeding, using a pipetting robot, library compounds are added to separate wells. After 24 h, to stain nuclei, DRAQ5 is added to each well using the pipetting robot. After 2 h plates are confocally imaged by Opera<sup>®</sup> system which is equipped with a fast dispensing unit applying CCh to each well during time-lapse imaging. An image analysis tool within the Acapella<sup>®</sup> software is developed to automatically analyze single cell calcium transients. Using DRAQ5 nuclear segmentation, image analysis tool detects the boundaries of individual cells in the first time point and measures then the intensities of in FRET–acceptor and –donor over the course of imaging. The FRET efficiency of individual cells are then calculated and normalized. For each cell the signal maximum (peak) is determined. The compounds which attenuated the peak amplitude of CCh-induced calcium release to <90% of the DMSO controls were regarded as hit. Finally by data mining and determining the structure-activity-relationships (SAR) of the entire library consisting of over 20,000 compounds, active lead structures were identified.

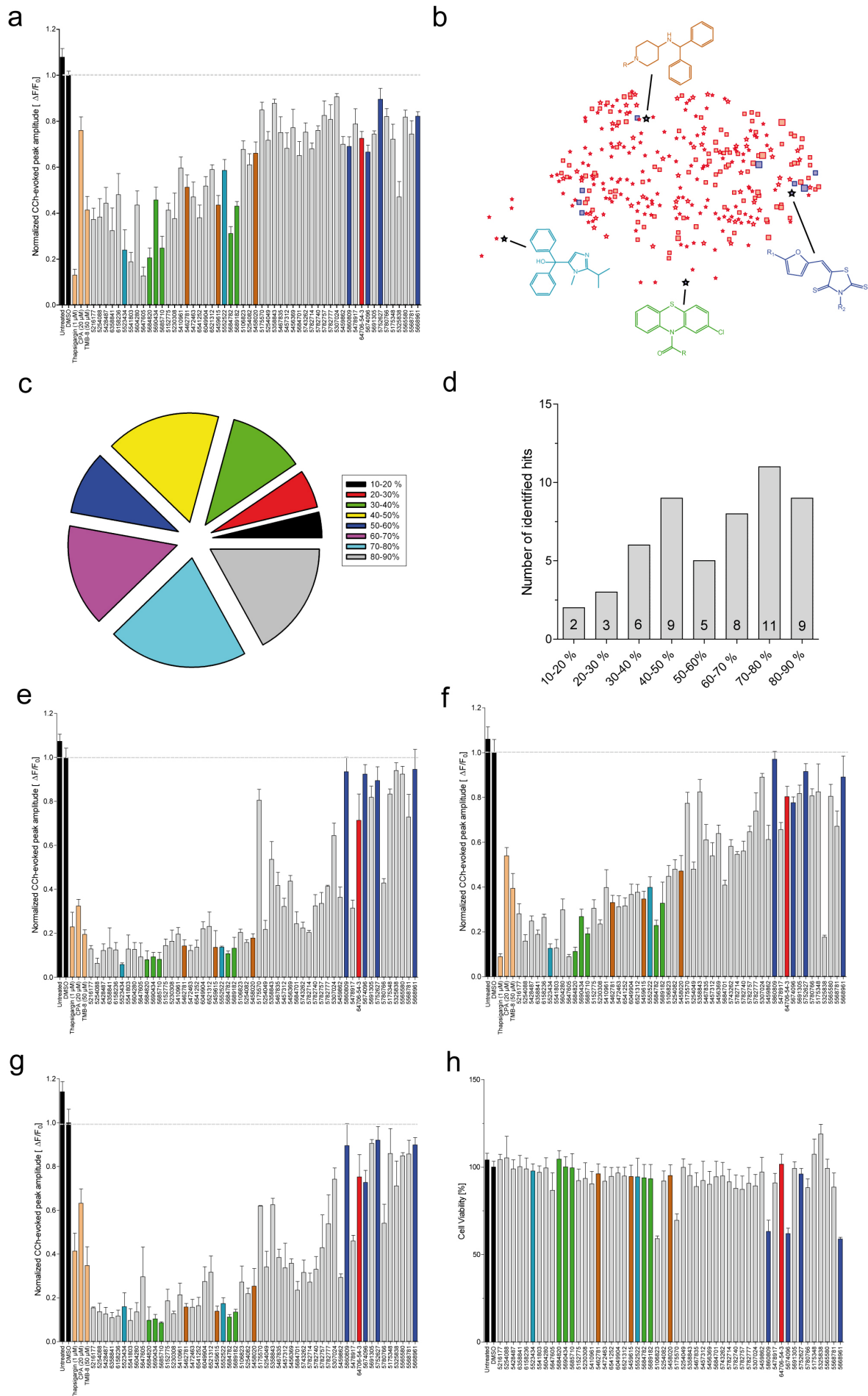
**(e)** Z'-factor as a measure for the robustness of the screening assay is evaluated for ten randomly selected imaged plates. The average Z'-factor for the screened plates exceeded 0.8.



Compound Structure and ID	normalized ER-Calcium response	Compound Structure and ID	normalized ER-Calcium response	Compound Structure and ID	normalized ER-Calcium response	Compound Structure and ID	normalized ER-Calcium response
	0.31		0.19		0.34		0.15
	0.24		0.28		0.15		0.26
	0.14		0.16		0.34		0.17
	0.45		0.53		0.54		0.50
	0.54		0.46		0.56		0.59
	0.52		0.48		0.38		0.51
	0.57		0.61		0.64		0.72
	0.77		0.78		0.78		0.73
	0.76		0.77		0.75		0.69
	0.77		0.85		0.84		0.85
	0.79		0.80		0.83		0.81
	0.82		0.84		0.83		0.86
	0.82		0.58		0.76		0.78
	0.72						

**Figure 6.3. Active structures identified from primary HTS screen**

Shown are 53 small molecules identified from the primary screen with their chemical structure and the corresponding normalized ER calcium response values generated at 10  $\mu$ M, as a measure for their activity.



**Figure 6.4. Validation of primary hits, structure-activity-relationship (SAR) analysis and their in vitro cytotoxicity**

**(a)** The activity of all 53 primary hits was validated in PS1-M146L/YC3.6 line. All the hits were capable of reducing the peak size of CCh-induced calcium release to <90% of DMSO-treated controls.

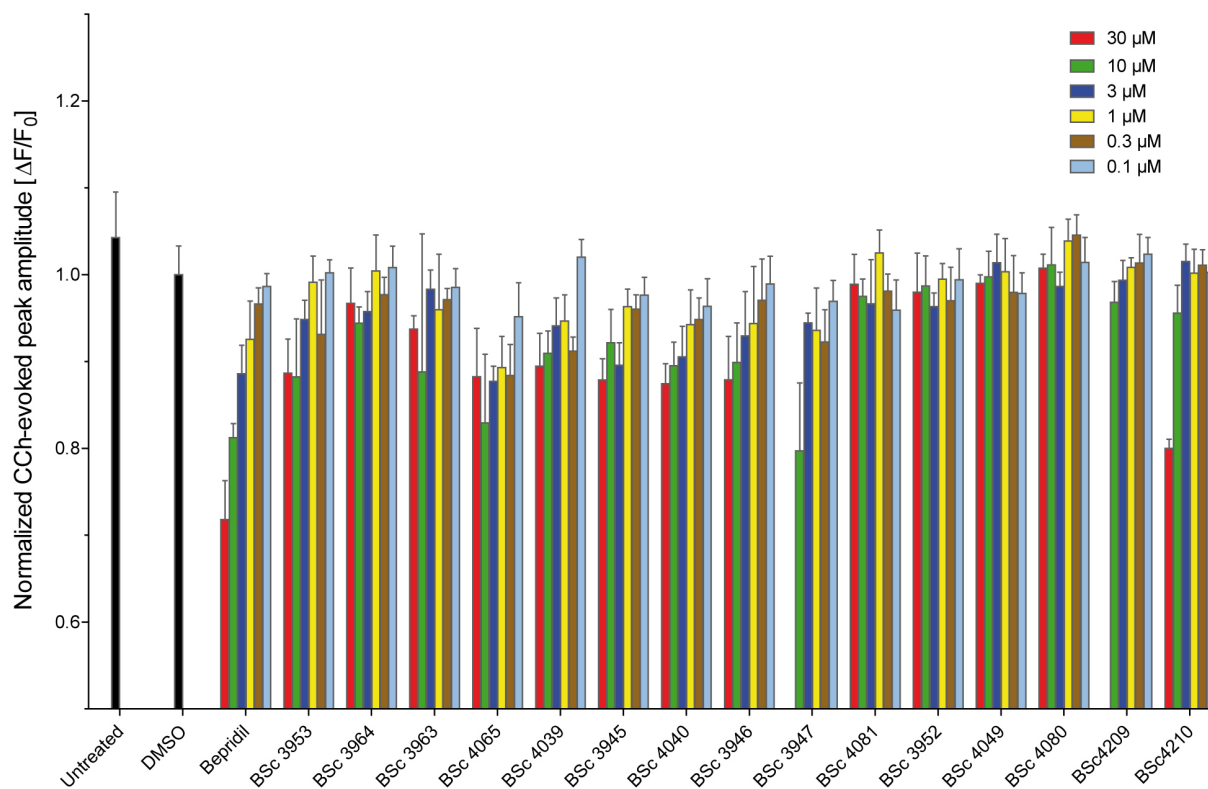
**(b)** The structure-activity-relationship (SAR) map of the screened compounds. The symbols represent compound clusters generated by Benchware DataMiner software. The distance between the clusters correlates with the similarity between their chemical structures. The number of compounds within a cluster is illustrated by the size of the symbol. A cluster with more than 50% active compounds is represented by a star, and marked in blue if the actual number of active compounds is greater than 4. The highlighted identified lead structures belong to compound classes Thiazolidine (blue), Phenothiazine (green), Imidazole (turquoise) and Benzhydrylpiperidinamin (brown).

Primary hits were also active in HEK293 cells expressing **(e)** PS1-DeltaE9/YC3.6, **(f)** PS1-C92S/YC3.6, and **(g)** PS1-D385N/YC3.6, by attenuating the mutant PS1-induced amplified calcium release.

**(c)** and **(d)** The hits from the primary screen were classified into 8 categories based on their efficacy in lowering the CCh-evoked calcium release. These categories are separated according to the value of normalized ER calcium response. The noted numbers in each category indicates the number of compounds belonging to that category.

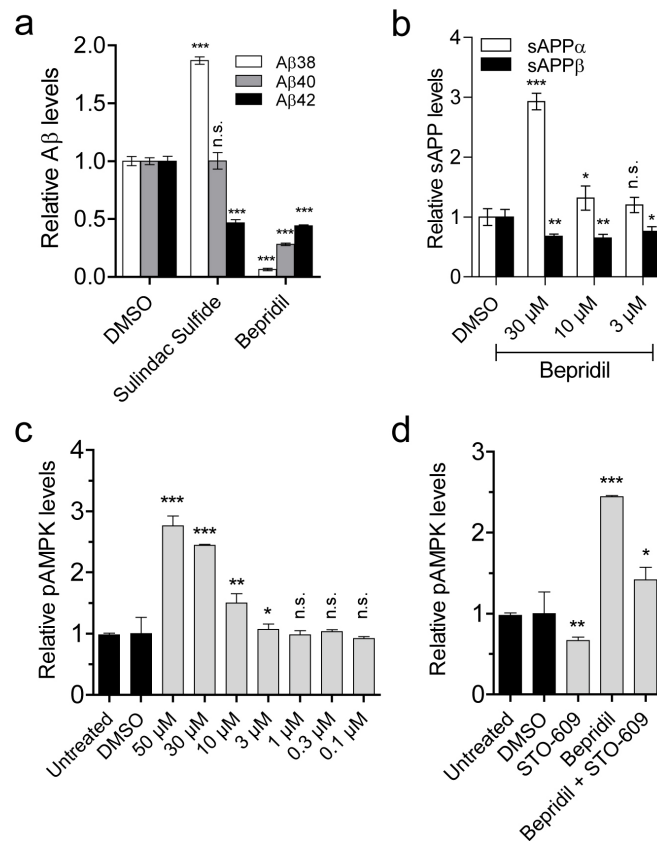
**(h)** Viability of HEK293 cells treated with the primary screen hits was assessed by means of MTT assay after 24 h compound treatment. Values are presented as percentage of viable cells.

In (a), (e), (f) and (g), the peak size of DMSO-treated control is set to 1. Each color denotes a different lead structure in (a), (b), (e), (f), (g) and (h). The data for analogous molecules belonging to the same lead structure are marked with the same color.



**Figure 6.5. Dose-dependent effect of Bepridil and its derivative structures on the amplitude of CCh-evoked ER calcium release in PS1-M146L cells**

The effect of Bepridil and its 15 synthesized derivative structures were tested at 30, 10, 3, 1, 0.3 and 0.1  $\mu\text{M}$ . The peak size of DMSO-treated control is set to 1. The relative peak amplitude of CCh-evoked calcium release is plotted for each treatment condition. Compounds BSc3947 and BSc4209 were toxic at 30  $\mu\text{M}$  concentration.



**Figure 6.6. Effect of on Bepridil on APP processing and AMPK activity**

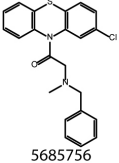
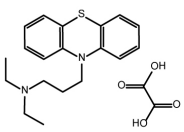
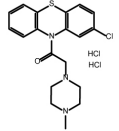
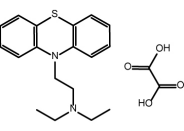
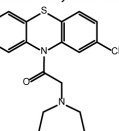
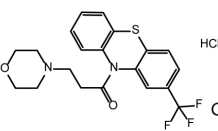
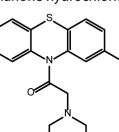
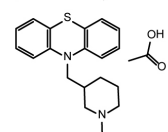
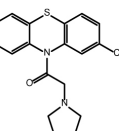
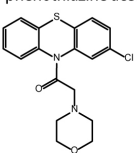
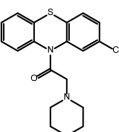
**(a)** Reduced production of Aβ38, Aβ40 and Aβ42 after 16 h Bepridil (30 μM) treatment in HEK293 cells coexpressing APPsw and PS1-M146L. Sulindac sulfide (50 μM) was used as a γ-secretase modulator control.

**(b)** Increased levels of sAPPα and decreased sAPPβ secreted fragments after 16 h treatment with Bepridil in HEK293 cells coexpressing APPsw and PS1-M146L.

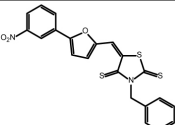
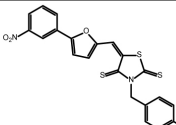
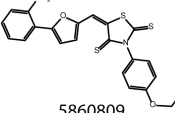
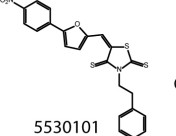
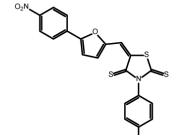
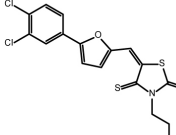
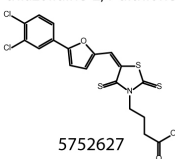
**(c)** Dose-dependent activation of AMPK upon 16 h treatment of HEK293 cells with Bepridil.

**(d)** Cotreatment with STO-609 (50 μM) partially abolishes the Bepridil-dependent activation of AMPK in HEK293 cells.

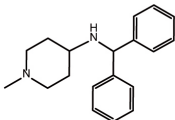
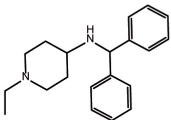
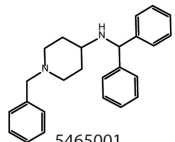
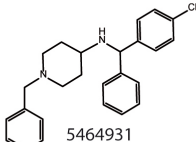
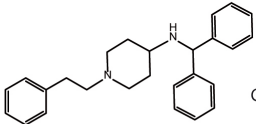
(n.s.: non-significant; \* P<0.05, \*\* P<0.01 and \*\*\* P<0.001).

Compound Structure, ID and name	Molecular formula	MW	clogP	normalized ER-Calcium response	Compound Structure, ID and name	Molecular formula	MW	clogP	normalized ER-Calcium response
 5685756 2-(benzyl(methyl)amino)-1-(2-chloro-10H-phenothiazin-10-yl)ethanone	C <sub>22</sub> H <sub>19</sub> ClN <sub>2</sub> OS	394.92	5.03	1.03	 6521312 N,N-diethyl-3-(10H-phenothiazin-10-yl)propan-1-amine oxalate	C <sub>21</sub> H <sub>26</sub> N <sub>2</sub> O <sub>4</sub> S	402.51	1.52	0.59
 5684820 1-(2-chloro-10H-phenothiazin-10-yl)-2-(4-methylpiperazin-1-yl)ethanone dihydrochloride	C <sub>19</sub> H <sub>22</sub> Cl <sub>3</sub> N <sub>3</sub> OS	446.82	1	0.16	 6541252 N,N-diethyl-2-(10H-phenothiazin-10-yl)ethanamine oxalate	C <sub>20</sub> H <sub>24</sub> N <sub>2</sub> O <sub>4</sub> S	388.48	1.40	0.46
 5690434 2-(azepan-1-yl)-1-(2-chloro-10H-phenothiazin-10-yl)ethanone hydrochloride	C <sub>20</sub> H <sub>22</sub> Cl <sub>2</sub> N <sub>2</sub> OS	409.37	5.07	0.33	 5743262 3-morpholino-1-(2-(trifluoromethyl)-10H-phenothiazin-10-yl)propan-1-one hydrochloride	C <sub>20</sub> H <sub>20</sub> ClFN <sub>2</sub> O <sub>2</sub> S	444.90	2.55	0.75
 5689182 1-(2-chloro-10H-phenothiazin-10-yl)-2-(diethylamino)ethanone	C <sub>18</sub> H <sub>19</sub> ClN <sub>2</sub> OS	346.87	4.26	0.51	 5216177 10-((1-methylpiperidin-3-yl)methyl)-10H-phenothiazine acetate	C <sub>21</sub> H <sub>26</sub> N <sub>2</sub> O <sub>2</sub> S	370.51	2.95	0.30
 5684782 1-(2-chloro-10H-phenothiazin-10-yl)-2-(pyrrolidin-1-yl)ethanone	C <sub>18</sub> H <sub>17</sub> ClN <sub>2</sub> OS	344.86	3.95	0.38	 5690013 1-(2-chloro-10H-phenothiazin-10-yl)-2-morpholinoethanone	C <sub>18</sub> H <sub>17</sub> ClN <sub>2</sub> O <sub>2</sub> S	360.86	3.29	0.96
 5685710 1-(2-chloro-10H-phenothiazin-10-yl)-2-(piperidin-1-yl)ethanone	C <sub>19</sub> H <sub>19</sub> ClN <sub>2</sub> OS	358.88	4.51	0.17					

**Figure 6.S1.** Shown are the 11 compounds belonging to the lead structure Phenothiazine. Their chemical structure, physical properties and normalized CCh-evoked calcium release peak size are presented at 10  $\mu$ M as a measure for their activity in the ER calcium release assay.

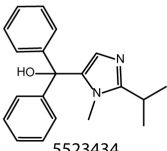
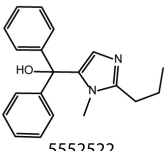
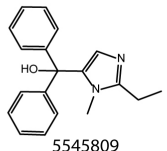
Compound Structure, ID and name	Molecular formula	MW	clogP	normalized ER-Calcium response	Compound Structure, ID and name	Molecular formula	MW	clogP	normalized ER-Calcium response
 <p>5674096 (E)-3-benzyl-5-((5-(3-nitrophenyl)furan-2-yl)methylene)thiazolidine-2,4-dithione</p>	$C_{21}H_{14}N_2O_2S_3$	438.54	5.98	0.82	 <p>5668961 (E)-3-(4-methoxybenzyl)-5-((5-(3-nitrophenyl)furan-2-yl)methylene)thiazolidine-2,4-dithione</p>	$C_{22}H_{16}N_2O_4S_3$	468.57	5.89	0.72
 <p>5860809 (E)-3-(4-ethoxyphenyl)-5-((5-(2-nitrophenyl)furan-2-yl)methylene)thiazolidine-2,4-dithione</p>	$C_{22}H_{16}N_2O_4S_3$	468.57	6.09	0.80	 <p>5530101 (E)-5-((5-(4-nitrophenyl)furan-2-yl)methylene)-3-phenethylthiazolidine-2,4-dithione</p>	$C_{22}H_{16}N_2O_2S_3$	452.57	6.30	0.70
 <p>5678418 (E)-3-(4-methoxyphenyl)-5-((5-(4-nitrophenyl)furan-2-yl)methylene)thiazolidine-2,4-dithione</p>	$C_{21}H_{14}N_2O_2S_3$	454.54	5.56	0.79	 <p>5759369 (E)-3-(5-((5-(3,4-dichlorophenyl)furan-2-yl)methylene)-2,4-dithioxothiazolidin-3-yl)propanoic acid</p>	$C_{17}H_{11}Cl_2NO_2S_3$	444.38	5.28	0.81
 <p>5752627 (E)-4-(5-((5-(3,4-dichlorophenyl)furan-2-yl)methylene)-2,4-dithioxothiazolidin-3-yl)butanoic acid</p>	$C_{18}H_{13}Cl_2NO_3S_3$	458.40	5.54	0.82					

**Figure 6.S2.** Shown are the 7 compounds belonging to the lead structure Thiazolidine. Their chemical structure, physical properties and normalized CCh-evoked calcium release peak size are presented at 10  $\mu$ M as a measure for their activity in the ER calcium release assay.

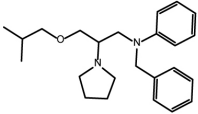
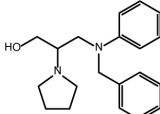
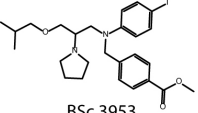
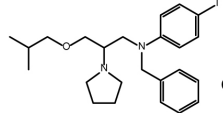
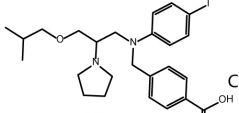
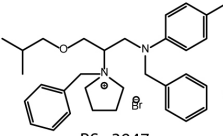
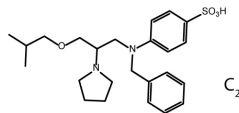
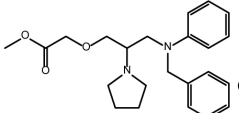
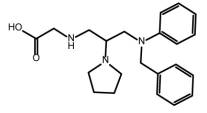
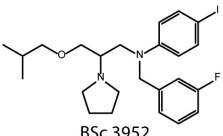
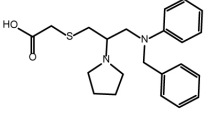
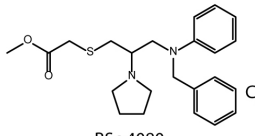
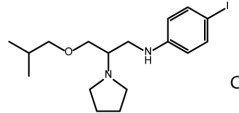
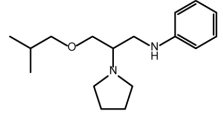
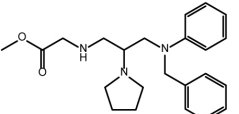
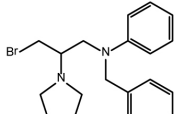
Compound Structure, ID and name	Molecular formula	MW	clogP	normalized ER-Calcium response	Compound Structure, ID and name	Molecular formula	MW	clogP	normalized ER-Calcium response
 5462781 N-benzhydryl-1-methylpiperidin-4-amine	$C_{19}H_{24}N_2$	280.41	2.93	0.49	 5458020 N-benzhydryl-1-ethylpiperidin-4-amine	$C_{20}H_{26}N_2$	294.43	3.46	0.64
 5465001 N-benzhydryl-1-benzylpiperidin-4-amine	$C_{25}H_{28}N_2$	356.50	4.70	0.87	 5464931 1-benzyl-N-(4-chlorophenyl)(phenyl)methylpiperidin-4-amine	$C_{25}H_{27}ClN_2$	390.95	5.42	0.98
 5459615 N-benzhydryl-1-phenethylpiperidin-4-amine	$C_{26}H_{30}N_2$	370.51	4.84	0.52					

**Figure 6.S3.** Shown are the 5 compounds belonging to the lead structure Benzhydrylpiperidinamin. Their chemical structure, physical properties and normalized CCh-evoked calcium release peak size are presented at 10  $\mu$ M as a measure for their activity in the ER calcium release assay.

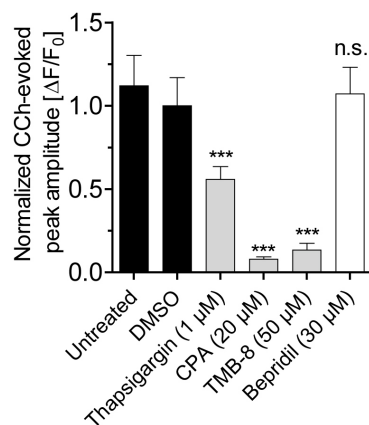


Compound Structure, ID and name	Molecular formula	MW	clogP	normalized ER-Calcium response	Compound Structure, ID and name	Molecular formula	MW	clogP	normalized ER-Calcium response
 5523434 (2-isopropyl-1-methyl-1H-imidazol-5-yl) diphenylmethanol	$C_{20}H_{22}N_2O$	306.4	2.93	0.28	 5552522 (1-methyl-2-propyl-1H-imidazol-5-yl) diphenylmethanol	$C_{20}H_{22}N_2O$	306.4	3.06	0.48
 5545809 (2-ethyl-1-methyl-1H-imidazol-5-yl) diphenylmethanol	$C_{19}H_{20}N_2O$	292.37	2.53	0.92					

**Figure 6.S4.** Shown are the 3 compounds belonging to the lead structure Imidazole. Their chemical structure, physical properties and normalized CCh-evoked calcium release peak size are presented at 10  $\mu$ M as a measure for their activity in the ER calcium release assay.

Compound Structure, ID and name	Molecular formula	MW	clogP	normalized ER-Calcium response	Compound Structure, ID and name	Molecular formula	MW	clogP	normalized ER-Calcium response
 Bepridil N-benzyl-N-(3-isobutoxy-2-pyrrolidin-1-yl-propyl)aniline	$C_{24}H_{34}IN_2O$	366.54	6.20	0.81	 BSc 4040 3-(Benzyl(phenyl)amino)-2-(pyrrolidin-1-yl)propan-1-ol	$C_{24}H_{34}IN_2O$	310.43	4.64	0.89
 BSc 3953 Methyl 4-(((4-iodophenyl)(3-isobutoxy-2-(pyrrolidin-1-yl)propyl)amino)methyl)benzoate	$C_{26}H_{35}IN_2O_3$	550.47	7.46	0.88	 BSc 3946 N-Benzyl-4-iodo-N-(3-isobutoxy-2-(pyrrolidin-1-yl)propyl)aniline	$C_{24}H_{32}FIN_2O$	492.44	7.49	0.90
 BSc 3964 4-(((4-iodophenyl)(3-isobutoxy-2-(pyrrolidin-1-yl)propyl)amino)methyl)benzoic acid	$C_{25}H_{33}IN_2O_3$	536.45	4.97	0.94	 BSc 3947 1-Benzyl-1-(1-(benzyl(4-iodophenyl)amino)-3-isobutoxypropan-2-yl)pyrrolidinium bromide	$C_{31}H_{40}BrIN_2$	663.47	7.70	0.80
 BSc 3963 4-(Benzyl(3-isobutoxy-2-(pyrrolidin-1-yl)propyl)amino)benzenesulfonic acid	$C_{24}H_{34}N_2O_4S$	446.60	1.14	0.89	 BSc 4081 Methyl 2-(3-(benzyl(phenyl)amino)-2-(pyrrolidin-1-yl)propoxy)acetate	$C_{23}H_{30}N_2O_3$	382.50	4.75	0.98
 BSc 4065 2-(3-(Benzyl(phenyl)amino)-2-(pyrrolidin-1-yl)propylamino)acetic acid	$C_{22}H_{29}N_3O_2$	367.48	2.31	0.83	 BSc 3952 N-(3-Fluorobenzyl)-4-iodo-N-(3-isobutoxy-2-(pyrrolidin-1-yl)propyl)aniline	$C_{24}H_{32}FIN_2O$	510.43	7.64	0.99
 BSc 4039 2-(3-(Benzyl(phenyl)amino)-2-(pyrrolidin-1-yl)propylthio)acetic acid	$C_{22}H_{28}N_2O_2S$	384.53	2.63	0.91	 BSc 4080 Methyl 2-(3-(benzyl(phenyl)amino)-2-(pyrrolidin-1-yl)propylthio)acetate	$C_{23}H_{30}N_2O_2S$	398.56	5.21	1.01
 BSc 3945 4-iodo-N-(3-isobutoxy-2-(pyrrolidin-1-yl)propyl)aniline	$C_{17}H_{27}IN_2O$	402.31	5.22	0.92	 BSc 4209 N-(3-Isobutoxy-2-(pyrrolidin-1-yl)propyl)aniline	$C_{17}H_{28}N_2O$	276.42	3.79	0.97
 BSc 4049 Methyl 2-(3-(benzyl(phenyl)amino)-2-(pyrrolidin-1-yl)propylamino)acetate	$C_{17}H_{27}IN_2O$	381.51	4.60	0.99	 BSc 4210 N-Benzyl-N-(3-bromo-2-(pyrrolidin-1-yl)propyl)aniline	$C_{20}H_{25}BrN_2$	373.33	5.58	0.96

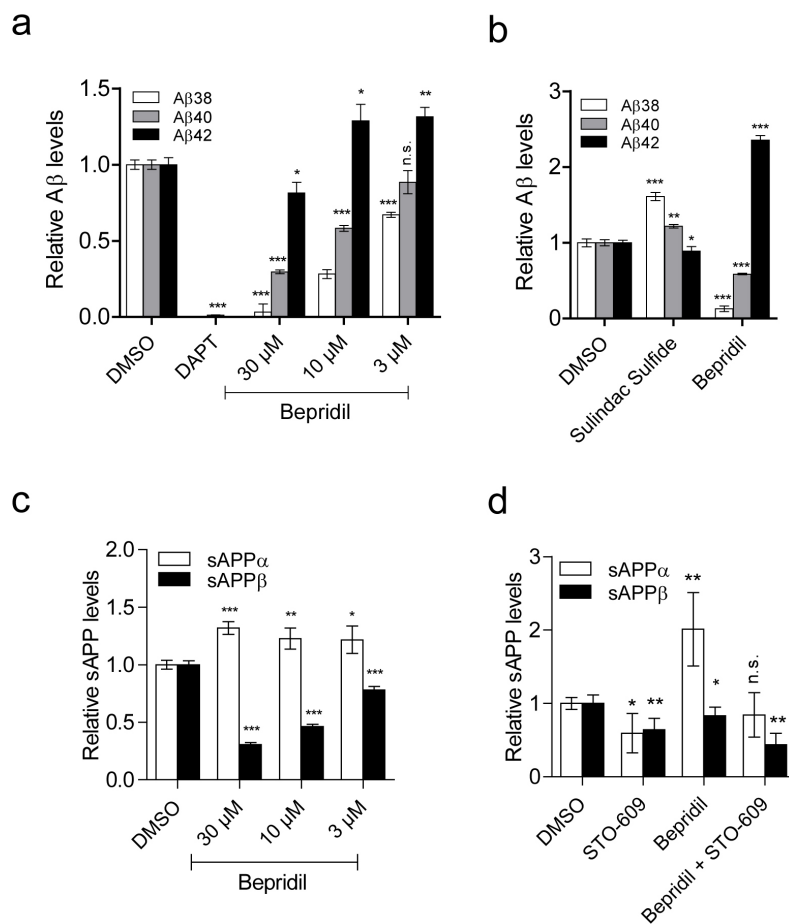
**Figure 6.S5.** Shown are Bepridil and 15 synthesized derivatives, their chemical structure, physical properties and the normalized CCh-evoked calcium release peak size at 10  $\mu$ M as a measure for their activity in the ER calcium release assay.



**Figure 6.S6. The effect of Bepridil on the amplitude of CCh-evoked ER calcium release in wildtype PS1-expressing HEK293 cells**

Bepridil (30 μM) does not alter the amplitude of CCh-evoked ER calcium release in wildtype PS1-expressing HEK293 cells. The peak size of DMSO-treated control is set to 1. Thapsigargin (1 μM), CPA (20 μM) and TMB-8 (50 μM) were used as positive controls.

(n.s.: non-significant and \*\*\* P<0.001).



**Figure 6.S7. Effect of on Bepridil on APP processing**

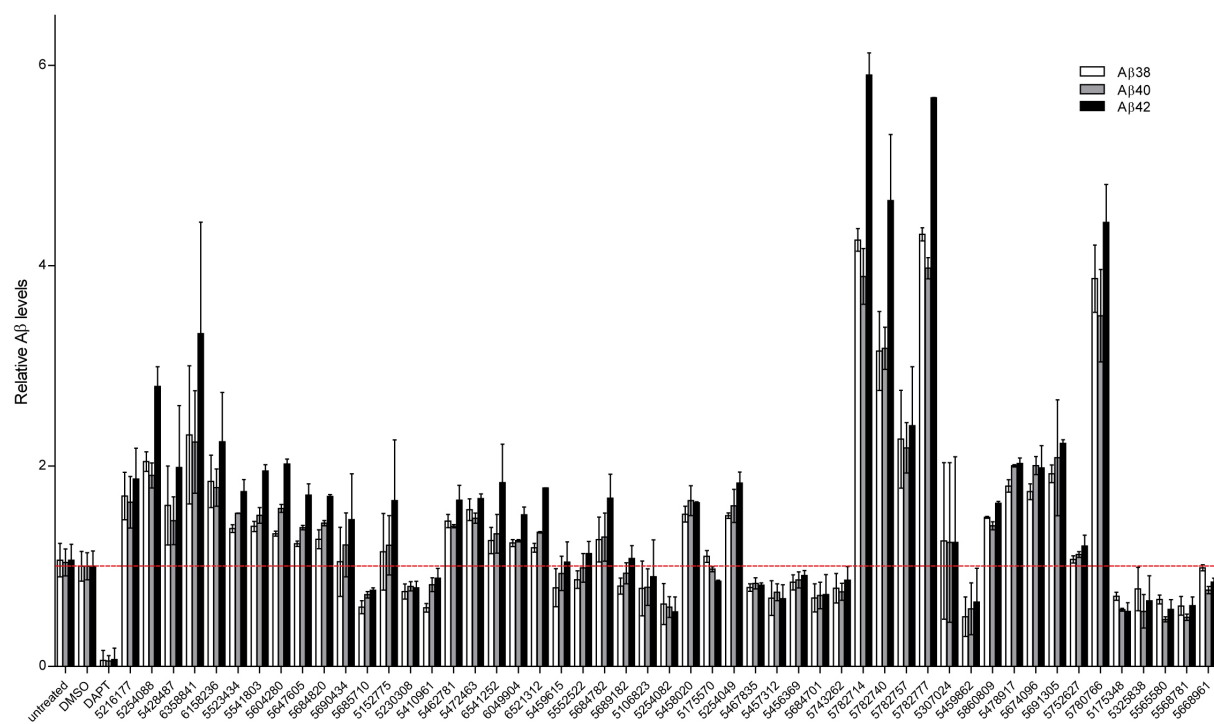
(a) Altered production of Aβ38, Aβ40 and Aβ42 after 16 h treatment of APP-overexpressing HEK293 cells with Bepridil. DAPT (10 μM), a γ-secretase inhibitor, was used as a positive control.

(b) Altered production of Aβ38, Aβ40 and Aβ42 after 16 h treatment of C99-overexpressing HEK293 cells with Bepridil (30 μM). Sulindac sulfide (50 μM), a γ-secretase modulator, was used as a positive control.

(c) Increased levels of sAPPα and decreased sAPPβ secreted fragments after 16 h treatment with Bepridil in APP-overexpressing HEK293 cells.

(d) Cotreatment with STO-609 (50 μM) reverses the Bepridil-dependent (30 μM) increase in sAPPα (but not the decrease in sAPPβ) in HEK293 cells coexpressing APPsw and PS1-M146L.

(n.s.: non-significant; \* P<0.05, \*\* P<0.01 and \*\*\* P<0.001).



**Figure 6.S8. Effects of the active compounds from the calcium HTS on Aβ production**

Altered production of Aβ38, Aβ40 and Aβ42 after 16 h treatment of HEK293 cells coexpressing APPsw and PS1-M146L with the active structures identified from the calcium HTS. DAPT (10 μM) was used as a γ-secretase inhibitor control.



CUMULATIVE THESIS: PAPER IV**7 Identification of tetrahydrocarbazoles as novel multifactorial drug candidates in the treatment of Alzheimer's disease**

Kamran Honarnejad <sup>1,2,3</sup>, Alexander Daschner <sup>1,2</sup>, André P. Gehring <sup>4</sup>, Aleksandra Szybinska <sup>5</sup>, Armin Giese <sup>2</sup>, Jacek Kuznicki <sup>5,6</sup>, Franz Bracher <sup>4</sup>, Jochen Herms <sup>1,2,7</sup>

<sup>1</sup> Department of Translational Brain Research, DZNE – German Center for Neurodegenerative Diseases, Munich, Germany

<sup>2</sup> Center for Neuropathology and Prion Research, Ludwig Maximilian University, Munich, Germany

<sup>3</sup> Graduate School of Systemic Neurosciences, Ludwig Maximilian University, Munich, Germany

<sup>4</sup> Department of Pharmacy, Center for Drug Research, Ludwig Maximilian University, Munich, Germany

<sup>5</sup> Laboratory of Neurodegeneration, International Institute of Molecular and Cell Biology, Warsaw, Poland

<sup>6</sup> Nencki Institute of Experimental Biology, Warsaw, Poland

<sup>7</sup> Munich Cluster for Systems Neurology (SyNergy), Munich, Germany

*Alternative title: “Identification of tetrahydrocarbazoles as novel multifactorial drug candidates for treatment of Alzheimer's disease from a high-throughput screen”*

*This manuscript is under peer-review in Translational Psychiatry journal and published in its essence under the patent publication number WO/2013/139929 (PCT/EP2013/055969).*

*The author of this doctoral thesis has majorly contributed to this work by conceiving, designing and performing the experiments, analyzing the data, preparing the figures and entirely writing the manuscript.*

## 7.1 Abstract

Alzheimer's disease (AD) is a progressive neurodegenerative brain disorder and the most frequent cause of dementia. To date, there are few approved drugs for AD, which show little or no effect on disease progression. Impaired intracellular calcium homeostasis is believed to occur early in the cascade of events leading to AD. Here we examined the possibility of normalizing the disrupted calcium homeostasis in the endoplasmic reticulum (ER) store as an innovative approach for AD drug discovery. High-throughput screening of a small-molecule compound library led to the identification of tetrahydrocarbazoles, a novel multifactorial class of compounds that can normalize the impaired ER calcium homeostasis. We found that the tetrahydrocarbazole lead structure, firstly, dampens the enhanced calcium release from ER in HEK293 cells expressing familial Alzheimer's disease (FAD)-linked presenilin 1 mutations. Secondly, the lead structure also improves mitochondrial function, measured by increased mitochondrial membrane potential. Thirdly, the same lead structure also attenuates the production of amyloid-beta ( $A\beta$ ) peptides by decreasing the cleavage of Amyloid Precursor Protein (APP) by  $\beta$ -secretase, without notably affecting  $\alpha$ - and  $\gamma$ -secretase cleavage activities. Considering the multiple modes of action of tetrahydrocarbazoles in addressing three key pathological aspects of AD, these compounds hold promise for development of a potentially effective AD drug candidate.



## 7.2 Introduction

Alzheimer's disease (AD) is the most common cause of dementia in the elderly [293]. Currently, there is no effective therapeutic modality for prevention, halting or reversal of AD [330]. The two principal neuropathological hallmarks of AD are the accumulation of extracellular plaques of  $\beta$ -amyloid ( $A\beta$ ) peptides and intracellular neurofibrillary tangles of hyperphosphorylated tau protein in the brain.  $A\beta$  and tau are thus the prime drug targets for development of disease-modifying therapy in AD [293]. Nevertheless, the lack of breakthrough in effective therapy, along with the consistent failure of drug candidates targeting late-stage  $A\beta$  and tau pathologies in clinical trials, have recently led to a major shift in the search for alternative AD drug targets [14]. Importantly, dysregulated calcium signaling plays a central role in AD pathogenesis [22, 29], for example by triggering both  $A\beta$  and tau pathology [48, 50]. Indeed, calcium imaging with cells derived from mild-cognitive-impairment (MCI) subjects, familial and sporadic AD patients [46, 229], and neurons from transgenic AD mouse models [331] indicate that disturbances in endoplasmic reticulum (ER) calcium homeostasis are early events in AD pathogenesis, most likely preceding the clinical manifestation of the disease [41]. Practically, every gene that is known to directly cause AD or increase susceptibility to it, somehow also affects calcium homeostasis [22]. Hence, therapeutic interventions aiming at preventing such early calcium dyshomeostasis have been proposed to present a promising opportunity for disease-modifying therapy of AD [6]. Furthermore, due to the multifactorial involvement of ER in the pathogenesis of AD, even minimal levels of therapeutic modulation in the ER may yield tremendous therapeutic efficacy [316]. In light of such indications and the novelty of this approach, we developed and performed a high-throughput screen for small-molecule compounds that can normalize the enhanced agonist-evoked ER calcium release phenotype in HEK293 cells expressing FAD-linked Presenilin-1 (PS1) mutations. Various mechanisms have been proposed to underlie the FAD-PS1-mediated enhancement of the ER calcium release, e.g. enhanced inositol 1,4,5-trisphosphate ( $IP_3$ ) and ryanodine receptor (RyR) channel activities, altered sarcoendoplasmic reticulum calcium transport ATPase (SERCA) pump function, decreased capacitative calcium entry and loss of ER passive calcium leakage [255]. Irrespective of the controversies in the field as to which of these are the primary causative and which the secondary phenomena, we performed a large-scale phenotypic compound

screening [332]. This resulted in identification of a novel class of chemical structures that normalize the exaggerated calcium release from ER in cells expressing a FAD-PS1 mutation. Stabilization of calcium signaling by the identified lead structure was accompanied by improved mitochondrial function and decreased A $\beta$  peptide production.

### 7.3 Material and Methods

#### 7.3.1 Cell culture and cell lines

Human embryonic kidney 293 (HEK293) cells were cultured in Dulbecco's modified eagle medium (DMEM) supplemented with 10% fetal bovine serum and 1% penicillin/streptomycin while being incubated at 37°C, 5% CO<sub>2</sub> and 90% humidity. The stable PS1 lines (generously provided by Dr. S. Lammich) were carrying PS1 variants that were cloned into pcDNA3.1/Zeo(+) and single cells were selected via Zeocin antibiotic resistance [333, 334]. The PS1 lines were then stably transfected with YC3.6/pcDNA3 construct (kindly provided by Dr. A. Miyawaki) and single cells were respectively isolated by G418 antibiotic resistance leading to generation of double stable lines. The APP- , C99- and APPsw/PS1-M146L-overexpressing HEK293 lines were kindly provided by Dr. S. Lichtenthaler and Dr. H. Steiner and cultured as previously described [299, 300].

#### 7.3.2 Automated high-throughput FRET-based calcium imaging and image analysis

HEK293 cells stably expressing PS1-M146L and Yellow Cameleon 3.6. (YC3.6) [212], were seeded at 13,000 cells/well in 40  $\mu$ l of growth medium on collagen-coated 384-well CellCarrier plates (PerkinElmer, Rodgau, Germany). After 6 h, using an automated pipetting robot (Bravo, Agilent Technologies, Santa Clara, CA, USA), library compounds were added to each well at the final concentration of 10  $\mu$ M in 1% DMSO, each in 4 replicates. All plates contained Thapsigargin (TP; 1  $\mu$ M; Calbiochem, Darmstadt, Germany), Cyclopiazonic acid (CPA; 20  $\mu$ M; Calbiochem), 3,4,5-trimethoxybenzoic acid 8-(diethylamino)octyl ester (TMB-8; 50  $\mu$ M; Sigma-Aldrich, Taufkirchen, Germany) and Bepridil (20  $\mu$ M; Sigma-Aldrich) as positive controls reducing the amount of calcium release from ER, as well as untreated and DMSO vehicle-treated wells. After 24 h using

the pipetting robot, DRAQ5 (Biostatus Ltd, Leicestershire, UK), a far-red fluorescent nuclear dye, was added to each well at the final concentration of 500 nM. After 2 h, plates were measured for CCh-induced calcium release using Opera<sup>®</sup> high-throughput confocal imaging platform (PerkinElmer Cellular Technologies GmbH, Hamburg, Germany). Throughout imaging of the entire plate, 37°C temperature, 5% CO<sub>2</sub> and 90% humidity was maintained in the plate chamber. Using a 442 nm laser, YC3.6 was excited and its CFP and YFP emissions were separated respectively using 483/35 nm and 540/75 nm filters. Additionally, using a 640 nm laser DRAQ5 dye was excited and its emission was collected by 690/50 nm filter in order to locate the nuclei. Imaging was performed with a 20x water immersion autofocus objective. The duration of the entire time-lapse calcium imaging for each well was 23.5 s. This was achieved by imaging at 2.5 s interval resolution prior to dispensing CCh (for 5 s) to monitor the basal calcium levels. Next, the CCh-induced calcium rise and decay were monitored for 18.5 s post dispensing. Imaging was performed first at 1 s interval resolution immediately after dispensing (for 5 s) and subsequently at 2.5 s interval resolution (for 12.5 s). During dispensing, 10 µl of CCh (Calbiochem) diluted in HBSS (10 µM) was injected to each well concurrent with calcium imaging by an automated dispensing unit which is part of the Opera<sup>®</sup> platform. Imaging was performed sequentially for all 384 wells. Using Acapella<sup>®</sup> software (PerkinElmer Cellular Technologies GmbH), an automated image analysis tool was developed to translate fluorescent signals to numerical values. Here, DRAQ5 and YC3.6 signals were used respectively to detect single cell nuclei and single cell boundaries over the entire course of time-lapse calcium imaging. After assigning each cell to its segmented nuclei and excluding the cells positioned at the edges of the imaging frames, calcium transients for every cell were monitored by plotting the kinetics of YFP/CFP versus time and normalizing the signals using the equation,  $\Delta F/F_0 = (F - F_0)/F_0$ , where F is the measured fluorescence signal at any given time and F<sub>0</sub> is the average fluorescence signal of the time points preceding CCh application. The peak amplitude of calcium rise upon CCh injection was the output of automated image analysis at single cell level. Non-responsive cells to CCh were excluded from analysis by setting an arbitrarily defined threshold. The average peak amplitude of all responsive cells in each well was calculated as the final readout in this assay.

### 7.3.3 Mitochondrial membrane potential TMRM assay

The measurement method for mitochondrial membrane potential with TMRM dye was adapted from Scaduto *et al.* [335]. HEK293 cells were seeded at the density of 50,000 cells/well on collagen/poly-L-lysine (PLL)-coated 96-well plates (Advanced-TC plates, Greiner Bio-One GmbH, Frickenhausen, Germany) and incubated for 24 h. Next, the cells were loaded with 50 nM tetramethylrhodamine methyl ester (TMRM; Invitrogen, Carlsbad, CA, USA) dye in the presence of either tetrahydrocarbazoles analogues (10  $\mu$ M), positive control Dimebon (10  $\mu$ M; Sigma-Aldrich), or DMSO vehicle which were pre-incubated on the cells 1 h prior to adding of TMRM dye. After 30 min each well was washed 3 times using PBS. Fresh medium containing each of the corresponding tested compounds (10  $\mu$ M) was added into the wells. Live cell image acquisition was performed using inverted confocal microscope LSM510 with 25x magnification (Carl Zeiss MicroImaging GmbH, Jena, Germany) and the images were analyzed using ImageJ (NIH, USA) software to quantify the intensity of TMRM fluorescence signal. All measurements were performed with at least eight replicates.

### 7.3.4 A $\beta$ measurements

The levels of three different A $\beta$  species (A $\beta$ 38, A $\beta$ 40 and A $\beta$ 42) were measured using sandwich ELISA. Pools of HEK293 cells stably transfected with either APP<sub>sw</sub>/PS1-M146L or APP were used to study the effect of compounds on A $\beta$  generation. According to Page *et al.* [300], cells were seeded at a density of 200,000 cells/well in collagen/poly-L-lysine (PLL)-coated 24-well plates and incubated for 24 h in growth medium. Next, the medium was exchanged with 500  $\mu$ l of fresh medium containing either the tested compounds, or the positive controls DAPT (10  $\mu$ M, Calbiochem), Sulindac sulfide (50  $\mu$ M, Sigma-Aldrich), Bepridil (30  $\mu$ M, Sigma-Aldrich) [299], or DMSO vehicle. After 16 h conditioned medium was collected and the levels of secreted A $\beta$ 38, A $\beta$ 40 and A $\beta$ 42 fragments were quantified using “Human (6E10) Abeta 3-Plex” sandwich ELISA immunoassay kit (Meso Scale Discovery, Rockville, MD, USA) according to the instructions of the manufacturer. In brief, 150  $\mu$ l of blocker reagent was added to each well and incubated for 1 h at room temperature, followed by 3x washing using TRIS wash buffer. Next, 25  $\mu$ l of detection antibody was added to each well. At appropriate dilution, each of the samples or calibration standards were added to separate wells of ELISA plate

and incubated for 2 h at room temperature, followed by 3x washing using TRIS wash buffer. Finally, 150  $\mu$ l of read buffer was added to the wells. The light emission after electrochemical stimulation was measured using Sector Imager 2400 reader (Meso Scale Discovery). Based on the values generated with calibration standards, corresponding concentrations of A $\beta$  species were calculated using the Meso Scale Discovery Workbench software. All measurements were performed with at least two replicates.

### 7.3.5 *sAPP $\alpha$ and sAPP $\beta$ measurements*

Levels of sAPP $\alpha$  and sAPP $\beta$  fragments were measured using sandwich ELISA adapted from Colombo *et al.* [336]. Wild type HEK293 cells were seeded at a density of 200,000 cells/well in collagen/poly-L-lysine (PLL)-coated 24-well plates and incubated for 24 h in growth medium. Next, the medium was exchanged with 500  $\mu$ l of fresh medium containing either compounds or vehicle. After 16 h conditioned medium was collected and the levels of secreted sAPP $\alpha$  and sAPP $\beta$  fragments were quantified using sAPP $\alpha$ /sAPP $\beta$  sandwich ELISA immunoassay kit (Meso Scale Discovery) according to the instructions of the manufacturer. Briefly, 150  $\mu$ l of blocker reagent was added to each well of the ELISA plate and incubated for 1 h at room temperature, followed by 3x washing using TRIS wash buffer. Next, 25  $\mu$ l of samples or calibration standards were added to separate wells of ELISA plate and incubated for 1 h at room temperature, followed by 3x washing using TRIS wash buffer. Then 25  $\mu$ l of detection antibody was added to each well and incubated for 1 h at room temperature, followed by 3x washing using TRIS wash buffer. Finally, 150  $\mu$ l of read buffer was added to the wells. The light emission after electrochemical stimulation was measured using Sector Imager 2400 reader (Meso Scale Discovery). Based on the values generated with calibration standards, corresponding concentrations of sAPP $\alpha$  and sAPP $\beta$  were calculated using the Meso Scale Discovery Workbench software. All measurements were performed in four replicates.

### 7.3.6 *Statistical data analysis*

GraphPad Prism 5.0b (GraphPad Software, San Diego, CA, USA) was used for statistical analysis of the data. For comparison and p-value determination, we used one-way analysis of variance (ANOVA) method, followed by Dunnett's multiple comparison test.

All data are represented as means  $\pm$  standard deviation. Differences were considered statistically significant if  $p < 0.05$ .

## 7.4 Results

### *7.4.1 Discovery of a novel lead structure from a high-throughput compound screen targeting disrupted ER calcium homeostasis*

In light of growing evidence towards the role of impaired intracellular store calcium homeostasis in the pathogenesis of Alzheimer's disease [271], here we screened for low-molecular-weight compounds that can normalize the disrupted ER calcium homeostasis. We chose the potentiated agonist-evoked ER calcium release in FAD-PS1-expressing cells as a robust phenotypic model to target ER calcium dyshomeostasis for AD drug discovery [332, 337].

All mutant PS1 lines tested revealed remarkably enhanced calcium release when compared to wild type PS1-expressing cells (Figure 7.1a). A phenotypic screening for compounds that are capable of dampening the potentiated Carbachol (CCh)-evoked ER calcium release in PS1-M146L HEK293 cells was subsequently performed. Screening a diverse compound library consisting of 20,000 small molecules led to the discovery of a novel lead structure. Six recognized analogues of the lead structure in the library, which showed activity in the screen (Figure 7.1b), remained active across several other mutant PS1-expressing lines (Figure 7.1c, d, e). Importantly, the amplitude of CCh-evoked calcium release in wild type PS1 expressing cells was not significantly altered (Figure 7.1f). For the primary screen, a compound was regarded as active if it reduced the peak amplitude of CCh-induced calcium release to  $<90\%$  of DMSO-treated controls (normalized ER calcium  $< 0.9$ ).

The discovered lead structure, identified as and hereafter called tetrahydrocarbazoles, consists of a core moiety having two variable R groups, shown as  $R^1$  and  $R^2$  (Figure 7.1g). Comprehensive data mining revealed that the entire compound library contained 10

analogues of the lead structure, 8 of which were found to be active in the screen (Figure 7.1g).

#### ***7.4.2 Tetrahydrocarbazoles attenuate the FAD-PS1 mediated exaggerated ER calcium release***

In order to explore the contribution of different R<sup>1</sup> and R<sup>2</sup> groups to the activity of the lead structure, we further tested 28 commercially available tetrahydrocarbazole analogues and related structures. We also validated the activity of the 10 structures previously identified from the primary screen (Figure 7.2a and 7.S1). Based on the structure-activity-relationship (SAR) knowledge gained, we synthesized 23 further derivative structures with the aim of reaching an improved efficacy (Figure 7.2b and 7.S2). Replacement of nitro group at R<sup>1</sup> position with other electron-withdrawing substituents, e.g. halogens, trifluoromethyl, and cyano groups, maintains the activity of the lead structure, while other small substituents, e.g. hydrogen, lead to the loss of activity. Aliphatic residues at R<sup>2</sup> position (e.g. 5781439, 5781448, 5781457, gea\_87) diminish that effect, while additional attachment of an aromatic motif (e.g. phenyl group) is beneficial to the activity (e.g. 5781464, 5781441).

#### ***7.4.3 Tetrahydrocarbazoles increase the mitochondrial membrane potential***

It has been demonstrated that ER and mitochondria are physically and functionally interdependent [338]. Constitutive calcium release from IP<sub>3</sub>R to mitochondria is a crucial mechanism involved in mitochondrial function [126]. Indications suggest that FAD-PS mutations affect the physical interaction between ER and mitochondria [339], leading to altered shuttling of calcium between the two organelles and modulating the mitochondrial calcium uptake [127]. Thus, in the next set of experiments we explored whether the modulation of ER calcium homeostasis by the lead structure also affects mitochondrial function. To that end, we analyzed mitochondrial membrane potential as an important parameter for addressing mitochondrial activity. We used TMRM dye, a fluorescent rhodamine derivative, to monitor mitochondrial membrane potential [335]. Indeed, pretreatment of HEK293 cells for 1 h with several lead structure analogues led to a remarkable increase in the mitochondrial membrane potential, measured by the TMRM

fluorescence signal (Figure 7.3a and 7.3b). At 10  $\mu$ M, the increases in mitochondrial membrane potential after treatment with many of the analogues were comparable or even superior to that for Dimebon, a known enhancer of mitochondrial activity [152] (Figure 7.3a and 7.3b). We particularly found that compounds 5781464 and 5781441, respectively possessing *N*-(1-benzylpiperidin-4-yl) and *N*-(1-phenethylpiperidin-4-yl) groups at their R<sup>2</sup> position, were among the most active compounds both in terms of efficacy and potency (Figure 7.3b and 7.3d). Therefore, in several lead structure derivatives that we synthesized, the R<sup>2</sup> position remained incorporating *N*-(1-benzylpiperidin-4-yl) or *N*-(1-phenethylpiperidin-4-yl) groups, while we varied the groups at R<sup>1</sup> position to explore their influence on the activity of the lead structure (Figure 7.S2). Indeed the latter analogues were also among the most active synthesized compounds in enhancing mitochondrial function (Figure 7.3c). Therefore, we concluded that the highest activity in terms of improving mitochondrial membrane potential is achieved if the lead structure possesses *N*-(1-benzylpiperidin-4-yl) or *N*-(1-phenethylpiperidin-4-yl) groups at R<sup>2</sup> position, given that R<sup>1</sup> position incorporates electron-withdrawing residues. Exemplarily, the EC<sub>50</sub> for one of the most promising synthesized derivatives of the lead structure (gea\_133; R<sup>1</sup> : cyano) was determined to be at the therapeutically relevant value of 4.84  $\mu$ M (Figure 7.3d). Moreover, the efficacy of compound gea\_133 was remarkably higher than the one of Dimebon, especially at concentrations beyond 1  $\mu$ M (Figure 7.3d).

#### 7.4.4 Tetrahydrocarbazoles lower A $\beta$ peptide production

Next, we studied the impact of tetrahydrocarbazoles on the production of A $\beta$  peptides. Modulation of intracellular calcium homeostasis directly affects A $\beta$  production [49]. Thus, we hypothesized that normalizing the disrupted ER calcium homeostasis may additionally result in lowered A $\beta$  production. Indeed we detected remarkably decreased levels of secreted A $\beta$ <sub>38</sub>, A $\beta$ <sub>40</sub> and A $\beta$ <sub>42</sub> peptides upon 16 h treatment of HEK293 cells expressing either APP<sub>sw</sub>/PS1-M146L or wildtype APP with the lead structure analogues at 10  $\mu$ M (Figure 7.4a, 7.4c and 7.S3). The IC<sub>50</sub> of the select analogues in terms of decreasing levels of all three A $\beta$  species lies in the low micromolar range (Figure 7.5a, b, c). However, compound treatment in both cell lines did not affect the A $\beta$ <sub>42</sub>/A $\beta$ <sub>40</sub> ratio for most analogues, suggesting that the identified lead structure is not a  $\gamma$ -secretase



modulator (Figures 7.4b, 7.4d and 7.S4). In order to investigate the  $\gamma$ -cleavage of APP independently from its  $\beta$ -cleavage, we used HEK293 cells expressing C99, the  $\beta$ -cleaved C-terminal fragment of APP and the substrate for  $\gamma$ -secretase. Here we observed that treatment of HEK293-C99 cells with the majority of the lead structure derivatives tested, did not (or only marginally) affect the production of A $\beta$ 38, A $\beta$ 40 and A $\beta$ 42 (Figure 7.6a). Moreover, A $\beta$ 42/A $\beta$ 40 ratios remained unaffected upon exposure of HEK293-C99 cells with the lead structure analogues (Figure 7.6b). Taken together, these results support the conclusion that the detected decrease in A $\beta$  peptide levels is not a  $\gamma$ -secretase-dependent phenomenon. In accordance, we postulated that reduced  $\beta$ -cleavage of APP may contribute to lowered A $\beta$  generation. Hence, we measured the levels of sAPP $\alpha$  and sAPP $\beta$ , the first cleavage products of APP, generated by  $\alpha$ -secretase and  $\beta$ -secretase, respectively. Indeed, we detected significantly decreased levels of secreted sAPP $\beta$ , while sAPP $\alpha$  levels were unaffected (or only mildly reduced) upon treatment of wildtype HEK293 cells with most lead structure derivatives (Figure 7.4e). These results imply that the attenuated A $\beta$  production caused by the lead structure is mediated through decreased cleavage of APP by  $\beta$ -secretase. The SAR analysis among the lead structure analogues in terms of lowering A $\beta$  production was comparable to their determined SAR for increasing mitochondrial membrane potential. We found that analogues incorporating electron-withdrawing residues at R<sup>1</sup> position, in combination with *N*-(1-benzypiperidin-4-yl) or *N*-(1-phenethylpiperidin-4-yl) at R<sup>2</sup> show the most robust reduction in A $\beta$  production (Figure 7.4a).

## 7.5 Discussion

Dysfunction and loss of neurons and synapses are by far the best available correlates of cognitive deficits in AD patients [53, 297]. Regulation of calcium homeostasis is essential for neuronal function and synaptic activity [27]. Early-stage aberrant calcium signaling in AD is proposed to underlie the late-stage synaptic dysfunction and memory deficits [98]. Notably, alterations in ER calcium channels were found to correlate with neurofibrillary and A $\beta$  pathologies of AD brain [48]. Moreover, altered calcium homeostasis in peripheral tissues was proposed as diagnostic biomarkers of mild AD [46, 47]. Furthermore, the beneficial effects of Memantine, an NMDA receptor antagonist, for

treatment of moderate-to-severe AD patients reinforce the relevance of calcium-signaling-targeted AD therapy [37]. Indeed, pharmacological normalization of disrupted ER calcium signaling by blocking hyperactivated RyR channels with dantrolene was demonstrated to restore synaptic transmission and plasticity, decrease A $\beta$  burden, increase PSD-95 expression, and improve learning and memory in different AD mouse models [203, 204]. Altogether, given the central role of calcium both in triggering the early disease-initiating pathomechanisms as well as accelerating the AD pathology at later stages [294], targeting altered calcium signaling presents an attractive target for both AD prevention and treatment. Accordingly, we developed and performed a high-throughput screen for compounds that can normalize the aberrant ER calcium homeostasis phenotype caused by FAD-linked PS1 mutations [255]. This approach led to the discovery of tetrahydrocarbazoles, a novel lead structure capable of lowering the exaggerated CCh-evoked ER calcium release in FAD-PS1 cells.

In addition to the stabilization of ER calcium homeostasis, we observed that tetrahydrocarbazoles can improve mitochondrial function, measured by increased mitochondrial membrane potential. Mitochondrial dysfunction is proposed to act as a trigger in AD pathogenesis and a contributing factor to both onset and progression of the disease [134]. In addition to aberrant calcium homeostasis, mitochondrial dysfunction is an additional early event in the course of AD, thus presenting an attractive target for preventative therapy [340]. Growing body of evidence indicates that the ER–mitochondria physical interfaces and calcium shuttling between the two organelles through IP<sub>3</sub> receptors play a crucial role in the regulation of mitochondrial function [126], which appears to be affected in AD [127, 339]. Treatment with many of the lead structure derivatives resulted in a larger increase in the mitochondrial membrane potential than treatment with Dimebon. The latter suggests higher efficacy for tetrahydrocarbazoles compared to Dimebon. Despite not having reached the efficacy endpoints in clinical phase III, Dimebon is a drug which is thought to be beneficial in particular stages of the disease [341]. It was demonstrated that Dimebon can improve cognitive functions in mild-to-moderate Alzheimer’s disease patients [342, 343], presumably by enhancing the mitochondrial activity [152, 344].

We also found that treatment with many tetrahydrocarbazole analogues results in notably less A $\beta$ 38, A $\beta$ 40 and A $\beta$ 42 production in two different cell lines. Yet, A $\beta$ 42/A $\beta$ 40 ratios

remained largely unchanged. The latter indicates that the identified lead structure does not possess the properties of a  $\gamma$ -secretase modulator (GSM). GSMs are characterized by decreased production of longer A $\beta$  species (e.g. A $\beta$ 42) accompanied by increased generation of shorter A $\beta$  species (e.g. A $\beta$ 38 and A $\beta$ 40), resulting in lowering of A $\beta$ 42/A $\beta$ 40 ratio [161]. Although there is evidence that  $\gamma$ -secretase activity may be affected by calcium ions [325], the detected decreases in A $\beta$  levels were not predominantly caused by  $\gamma$ -secretase inhibition. The evidence for the latter comes from the experiments with HEK293-C99 cells, suitable for exclusively addressing the  $\gamma$ -secretase cleavage of APP (independently from  $\beta$ -secretase activity). In HEK293-C99 cells, we detected unchanged or only slightly decreased A $\beta$  levels upon treatment with the derivative structures tested. These minor reductions in A $\beta$  levels caused by some lead structure derivatives can be due to the fact that calcium ions can modulate the  $\gamma$ -secretase activity to some extent [325]. However, such minor effects cannot account for the remarkable decrease in A $\beta$  levels observed after treatment of APPsw/PS1-M146L and APP-expressing cells with tetrahydrocarbazole analogues. Our findings rather suggest that lowered A $\beta$  production is mainly attributed to decreased  $\beta$ -cleavage of APP. We detected remarkably decreased sAPP $\beta$  levels upon exposure of HEK293 cells with the lead structure derivatives. Indeed, it has been demonstrated that calcium directly enhances the proteolytic activity of  $\beta$ -secretase (BACE1) [39]. Therefore, it is plausible that stabilization of ER calcium homeostasis by the lead structure results in lowered BACE1 activity and consequently decreased A $\beta$  production. The decrease in sAPP $\beta$  was not accompanied by an increase sAPP $\alpha$ , indicating that the lead structure does not alter the  $\alpha$ -secretase cleavage activity. The lack of inverse coupling between  $\alpha$ - and  $\beta$ -secretase activities in frequently used cell lines, e.g. HEK293 cells, may explain our finding that the lead structure lowers sAPP $\beta$  generation without changing sAPP $\alpha$  levels [336]. The observation that most lead structure analogues do not affect A $\beta$  and sAPP $\alpha$  levels, respectively in HEK293-C99 and wildtype HEK293 cells (e.g. *gea\_133*), indicates that the decreased A $\beta$  production through lowering  $\beta$ -cleavage of APP is indeed a specific effect which is not caused by reduced protein production.

The structure-activity-relationship analysis revealed that the effect of lead structure analogues is most prominent with specific residues at C-6 (R<sup>1</sup>) and the exocyclic amino group (R<sup>2</sup>). We found that when R<sup>1</sup> represents halogens and other electron-withdrawing substituents, e.g. nitro, trifluoromethyl, and cyano, this leads to a strong increase in

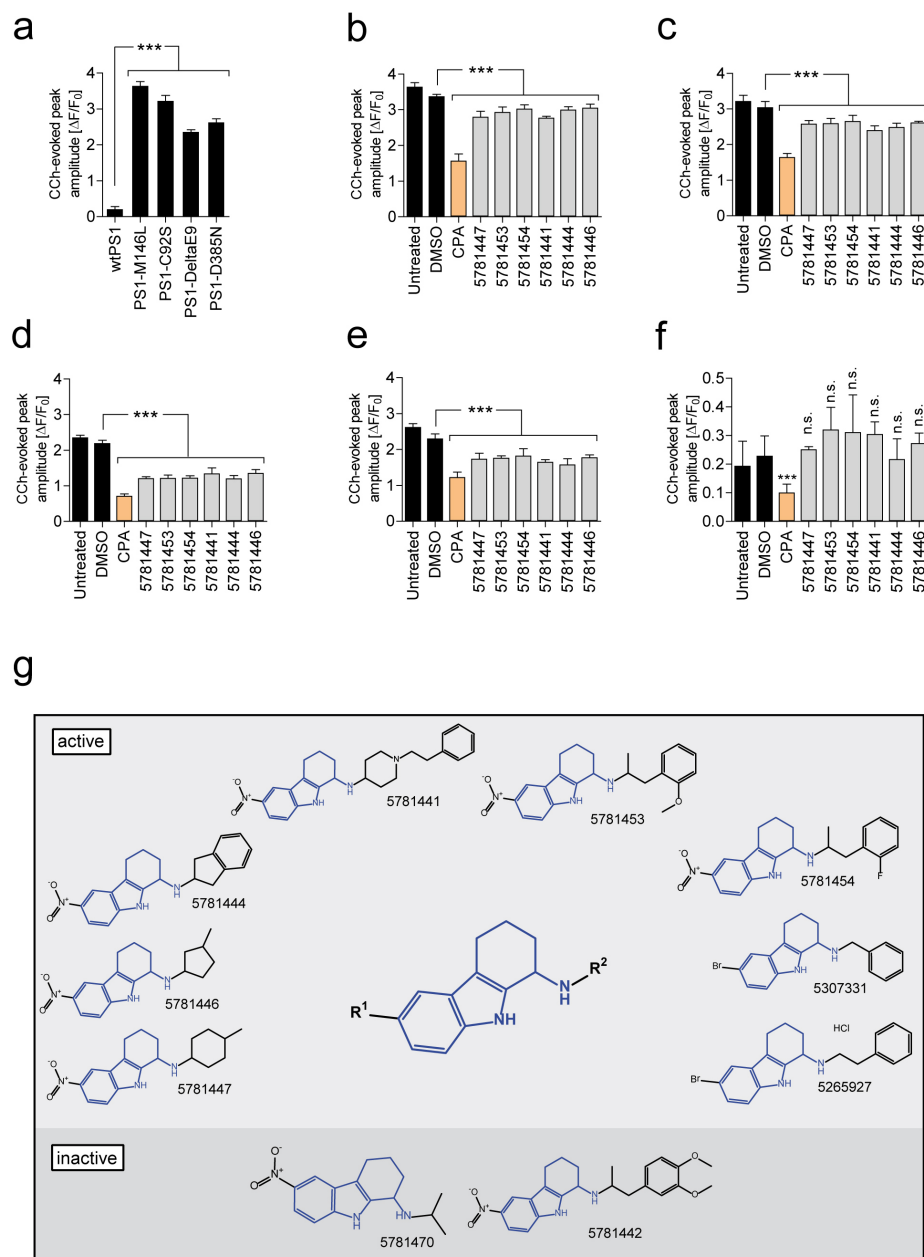
mitochondrial membrane potential, while also strongly attenuating A $\beta$  peptide production and ER calcium release. On the other hand, substitution at C-7 and C-8 (gea\_84) was found to be detrimental to the activity. Furthermore, *N*-methylation at either the pyrrole nitrogen (gea\_90) or the side chain secondary amino group (gea\_92) led to the complete loss of the activity. Merely aliphatic residues at the exocyclic nitrogen (R<sup>2</sup>; i.e. 5781439, 5781448, 5781457, gea\_87) result in lowering or loss of the activity, while additional attachment of an aromatic motif (phenyl group) shows benefit in all three assays (i.e. 5781464, 5781441). The best effect in all of the three assays was detectable for tetrahydrocarbazoles containing a diamino side chain R<sup>2</sup> (aminopiperidine) with an attached *N*-benzyl or *N*-phenethyl residue (i.e. 5781441, 5781464, gea\_96, gea\_97, gea\_101, gea\_102, gea\_130, gea\_133). Therefore, by a systematic optimization of lead structure analogues, we generated a subclass of compounds that are highly active in all three assays.

The vast majority of AD patients are sporadic late-onset cases and age remains the main risk factor for developing sporadic AD [345]. Importantly, aging process involves disturbances in the intracellular calcium homeostasis, particularly in ER and mitochondria [346, 347]. Lymphocytes derived from sporadic AD patients show elevated cytosolic basal calcium concentrations and disturbed ER calcium homeostasis [46, 348]. Every gene that is known to increase susceptibility to AD also modulates some aspect of calcium signaling [22]. In particular, a polymorphism in the CALHM1 gene encoding an ion channel's pore-forming subunit that affects intracellular calcium homeostasis has been linked to susceptibility to sporadic AD [71, 349]. Along with the ER stress, mitochondrial damage also contributes to aging process [350]. Moreover, sporadic AD is associated with reduced mitochondrial membrane potential [351] as well as elevated BACE1 activity [352] which in turn leads to increased A $\beta$  production and plaque deposition [353]. Therefore we predict that the benefits of tetrahydrocarbazoles, will not be limited to familial AD cases, but also may present a high potential for sporadic AD cases as well (patent pending; PCT/EP2013/055969).

It is established that modulation of ER calcium homeostasis can affect mitochondrial function [126] and APP metabolism [49]. However, since the direct molecular target(s) of tetrahydrocarbazoles remain unknown, this study is limited by the fact that we cannot firmly conclude that the improved mitochondrial activity and decreased A $\beta$  production

are downstream effects of normalizing calcium homeostasis. Therefore, future studies addressing the exact molecular target(s) of tetrahydrocarbazole lead structure and their detailed therapeutic mode of action are of utmost importance. Whether or not the beneficial effects of tetrahydrocarbazoles on calcium homeostasis, mitochondrial function and APP processing follow a dependency, should not, however jeopardize the therapeutic relevance of this discovery. Another important open question which remains to be elucidated is whether tetrahydrocarbazoles also reverse the late-stage A $\beta$ -plaque-dependent calcium disturbances in the brain [89, 90], which may be caused by A $\beta$ -induced calcium release from ER [354]. Apart from IP<sub>3</sub> receptor channel gating itself [69], multiple upstream elements of IP<sub>3</sub>R-mediated calcium release are affected in AD, e.g. GPCR in general [355], and muscarinic receptors in particular [356], G-proteins [357], as well as PLC [358]. Given that the screening hits may potentially target any of those upstream elements, such a phenotypic multi-targeted drug screening assay provides the important advantage of collectively addressing several aspects of AD.

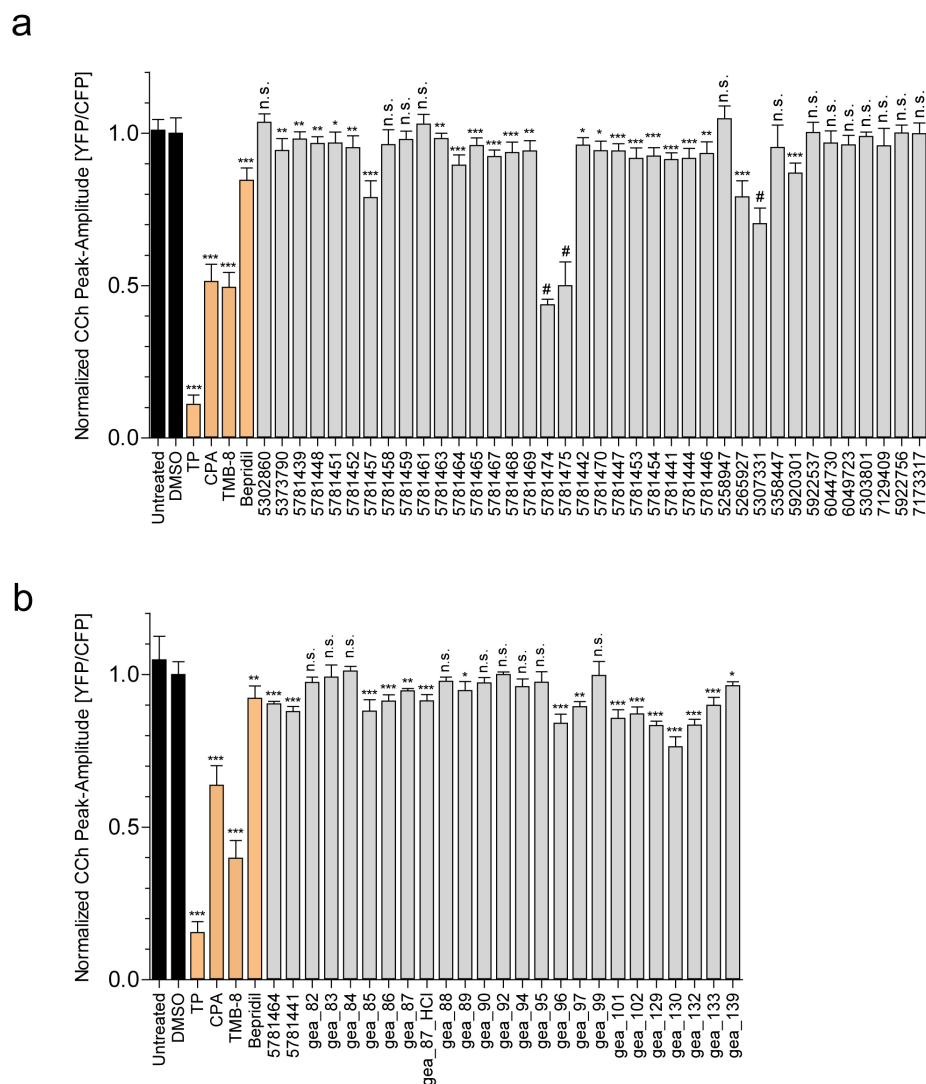
AD is believed to be a multifactorial disease, caused by complex interactions among several contributing pathomechanisms [330, 359]. Nevertheless, the majority of current disease-modifying drug development strategies address only single aspects of the disease. Therefore, similar to combinational therapy [330], drugs such as tetrahydrocarbazoles which simultaneously address several central pathophysiological aspects of AD are clearly of advantage.



**Figure 7.1. Tetrahydrocarbazole analogue screening hits/lead structure and their effects on FAD-PS1-mediated disrupted ER calcium release**

(a) The peak amplitude of CCh-evoked calcium release in HEK293 cells expressing wild type PS1, FAD-linked (PS1-M146L, PS1-C92S and PS1-DeltaE9) or a  $\gamma$ -secretase deficient (PS1-D385N) PS1 mutations. The effect of six tetrahydrocarbazole hits identified from the primary screen at 10  $\mu$ M in (b) PS1-M146L, (c) PS1-C92S, (d) PS1-DeltaE9, (e) PS1-D385 and (f) wild type PS1 expressing HEK293 cells on the peak amplitude of CCh-evoked calcium release. CPA, an inhibitor of calcium-dependent ATPases, was used as a positive control. (g) The tetrahydrocarbazole lead structure, identified from a high-throughput compound screen for substances stabilizing the exaggerated CCh-evoked calcium release in PS1-M146L HEK293 cells. Illustrated are chemical structures of the ten tetrahydrocarbazole analogues present in the entire screened compound library. The upper and lower panels indicate, respectively, eight active and two inactive analogues of the lead structure. Compounds capable of reducing the peak amplitude of CCh-induced calcium release to <90% of DMSO-treated controls (normalized ER calcium < 0.9) were regarded as active hits.

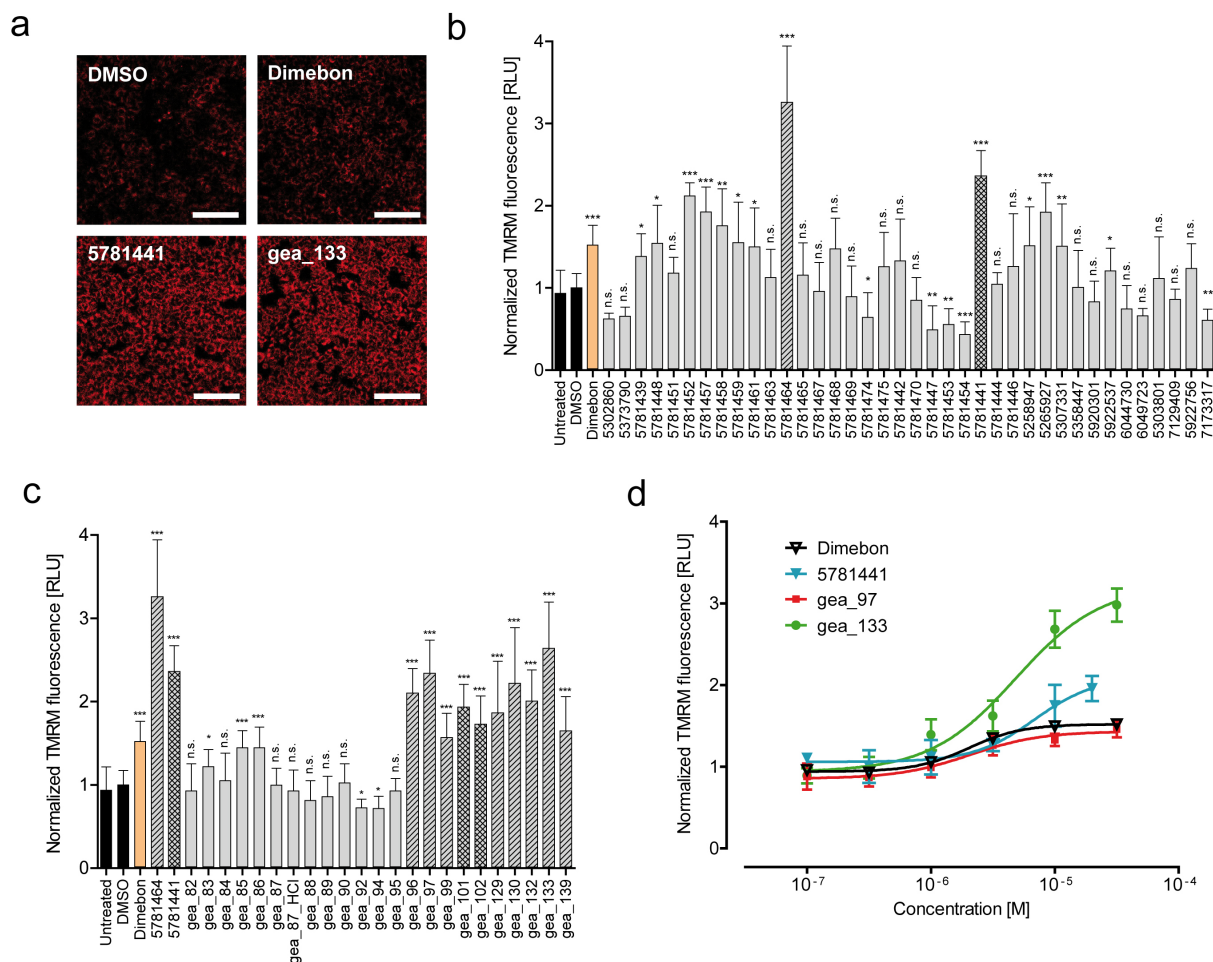
(n.s.: non-significant; \*  $P < 0.05$ , \*\*  $P < 0.01$  and \*\*\*  $P < 0.001$ ;  $n = 4$ ).



**Figure 7.2. The effects of tetrahydrocarbazole analogues on the FAD-PS1-mediated disrupted ER calcium release**

(a) The activity of commercially available and (b) synthesized tetrahydrocarbazole analogues tested at 10  $\mu$ M in PS1-M146L HEK293 cells. The presented values indicate the normalized peak amplitude of CCh-evoked calcium release for cells treated with each compound for 24 h relative to the peak amplitude of DMSO-treated control (normalized ER calcium). Compounds marked with # symbol possess a certain level of toxicity which interferes with calcium release measurement in this assay. TP (1  $\mu$ M), CPA (20  $\mu$ M), TMB-8 (50  $\mu$ M) and Bepridil (20  $\mu$ M), all lowering the amount of calcium release from ER, were used as positive controls.

(n.s.: non-significant; \*  $P < 0.05$ , \*\*  $P < 0.01$  and \*\*\*  $P < 0.001$ ;  $n = 4$ ).



**Figure 7.3. The effect of tetrahydrocarbazole analogues on mitochondrial membrane potential**

**(a)** Representative TMRM staining images of HEK293 cells pretreated for 1 h with the indicated tetrahydrocarbazole analogues (10  $\mu$ M) or Dimebon (10  $\mu$ M) as a positive control, relative to DMSO-treated control (scale bars: 100  $\mu$ m).

**(b)** Quantification of the average TMRM staining signals showing relative intensity for commercially available analogues of the tetrahydrocarbazole lead structure upon 1 h pretreatment of HEK293 cells (10  $\mu$ M). The bars highlighted with single- and double-stripes represent the most active compounds 5781464 and 5781441, which respectively possess N-(1-benzylpiperidin-4-yl) and N-(1-phenethylpiperidin-4-yl) groups at their R<sup>2</sup> position.

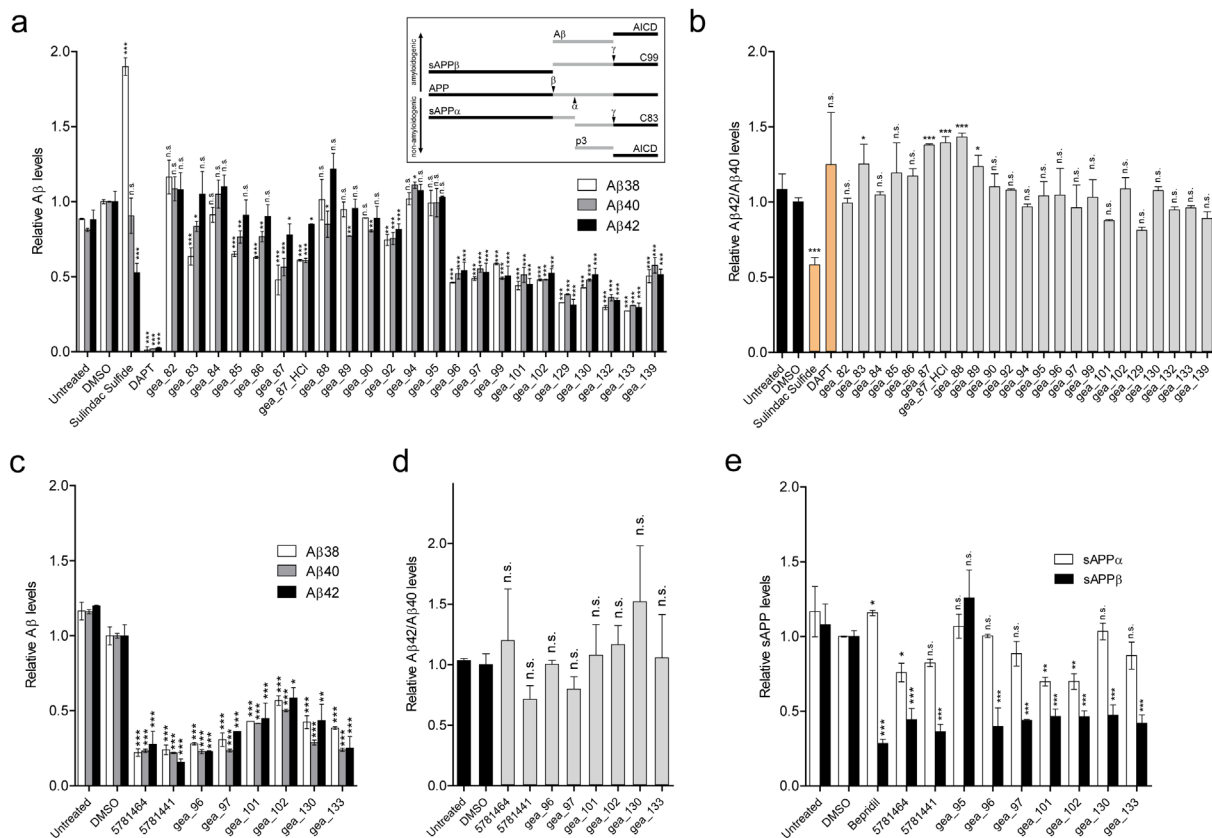
**(c)** Quantification of average TMRM intensity for synthesized tetrahydrocarbazole derivatives tested at 10  $\mu$ M. The marked single-striped bars represent the analogous structures similar to 5781464, possessing N-(1-benzylpiperidin-4-yl) at their R<sup>2</sup> position, and double-striped bars represent derivative compounds similar to 5781441, which contain N-(1-phenethylpiperidin-4-yl) group at R<sup>2</sup> position.

**(d)** Quantification of average dose-dependent TMRM relative intensities for 3 select analogues of the lead structure tested at 6 different concentrations relative to Dimebon. The EC<sub>50</sub> of all analogues tested lies at low micromolar range.

All values are normalized to DMSO value, which is set to 1.

(n.s.: non-significant; \* P<0.05, \*\* P<0.01 and \*\*\* P<0.001; n=8).





**Figure 7.4. The effect of tetrahydrocarbazoles on APP processing**

(a) Relative Aβ38, Aβ40 and Aβ42 levels, decreased after 16 h treatment with synthesized tetrahydrocarbazole derivatives at 10 μM in HEK293 cells coexpressing APP<sup>sw</sup> and PS1-M146L. Sulindac sulfide (50 μM) a γ-secretase modulator, and DAPT (10 μM) a γ-secretase inhibitor, were used as positive controls. Inside of the box, a schematic illustration of APP processing by α-, β- and γ-secretase is presented.

(b) Relative Aβ42/Aβ40 ratios calculated from (a). Treatment with the majority of the lead structure derivatives does not alter Aβ42/Aβ40 ratio, whereas positive control Sulindac sulfide significantly lowers Aβ42/Aβ40 ratio.

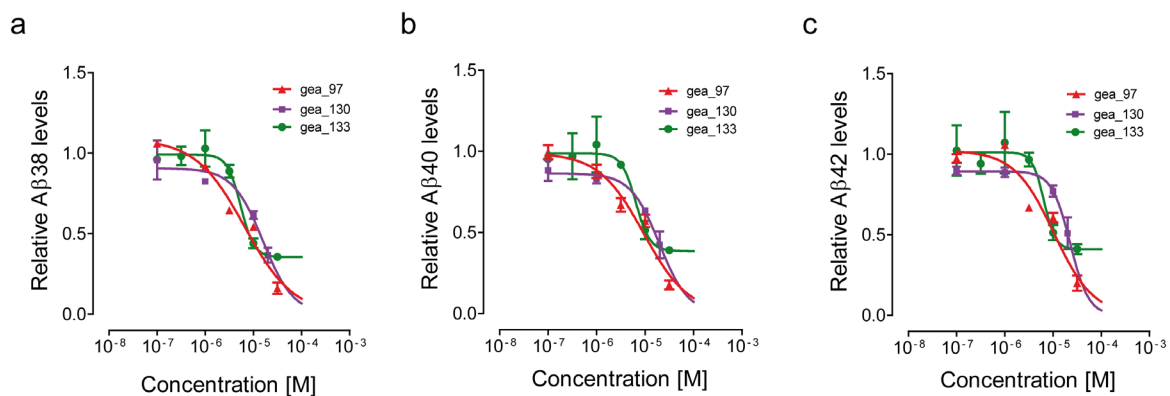
(c) Relative Aβ38, Aβ40 and Aβ42 levels are decreased after 16 h treatment with select tetrahydrocarbazole derivatives at 10 μM in HEK293 cells overexpressing wild type APP.

(d) Relative Aβ42/Aβ40 ratios calculated from (c). Treatment with select lead structure derivatives tested does not alter Aβ42/Aβ40 ratio.

(e) Relative sAPPα and sAPPβ levels after 16 h compound treatment in wild type HEK293 cells. Treatment with select tetrahydrocarbazole derivatives does not (or only marginally) affect secreted sAPPα levels, whereas secreted sAPPβ fragment levels are remarkably decreased.

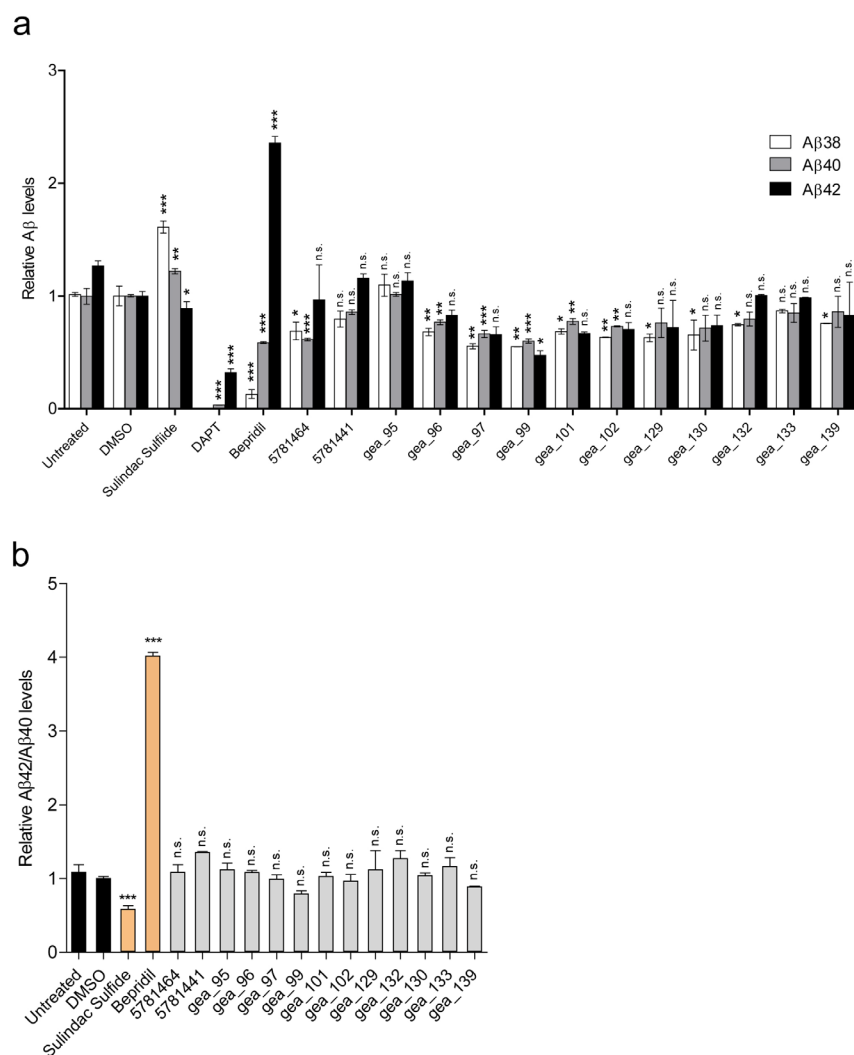
All values are normalized to the value of DMSO, which is set to 1.

(n.s.: non-significant; \* P<0.05, \*\* P<0.01 and \*\*\* P<0.001; n=2).



**Figure 7.5. Dose-dependent effects of tetrahydrocarbazole derivatives on Aβ production**

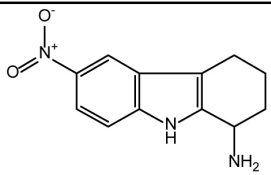
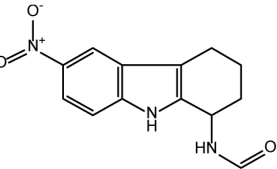
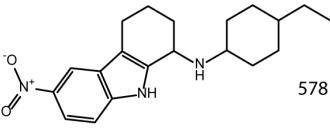
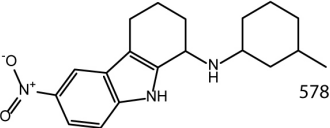
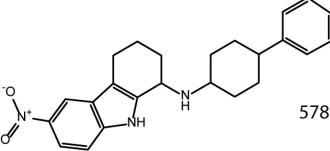
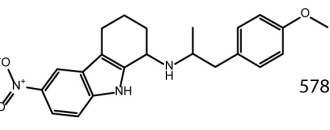
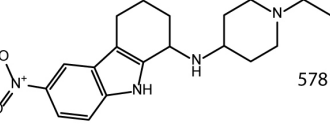
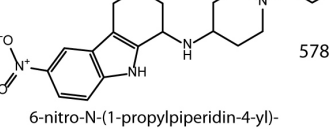
The effect of three select synthesized derivatives of tetrahydrocarbazole lead structure on the production of (a) Aβ38, (b) Aβ40 and (c) Aβ42 peptides tested at 6 different concentrations in APPsw/PS1-M146L-expressing HEK293 cells. The IC<sub>50</sub> of all Aβ species for all derivative structures tested lies at low micromolar range. All values are normalized to the value of DMSO, which is set to 1. (n.s.: non-significant; \* P<0.05, \*\* P<0.01 and \*\*\* P<0.001; n=4).



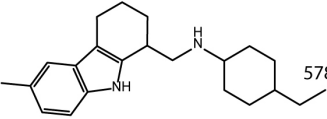
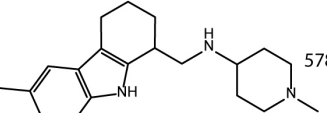
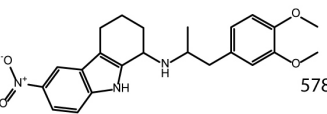
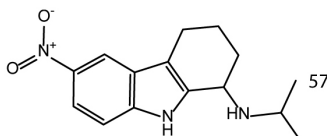
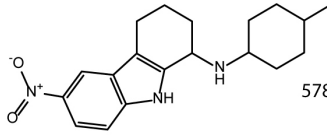
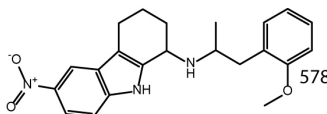
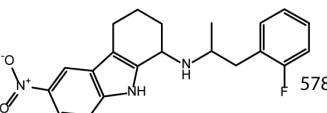
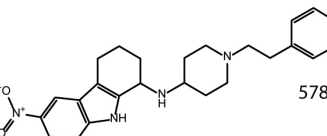
**Figure 7.6. The effect of synthesized tetrahydrocarbazole analogues on  $\gamma$ -secretase cleavage activity in HEK293-C99 cells**

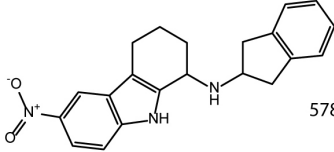
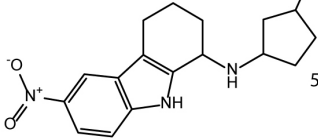
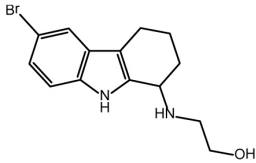
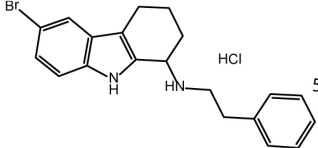
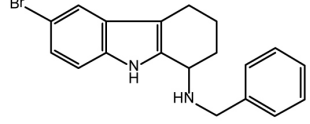
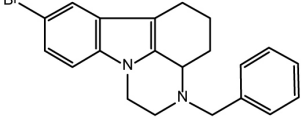
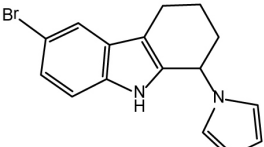
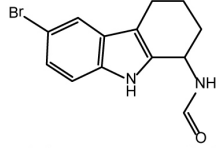
**(a)** Relative A $\beta$ 38, A $\beta$ 40 and A $\beta$ 42 levels after 16 h treatment with select tetrahydrocarbazole derivatives at 10  $\mu$ M in HEK293-C99 cells. Sulindac sulfide (50  $\mu$ M), Bepridil (30  $\mu$ M) and DAPT (10  $\mu$ M), respectively, a  $\gamma$ -secretase modulator, an iGSM, and a  $\gamma$ -secretase inhibitor, were used as positive controls. All values are normalized to the value of DMSO, which is set to 1. (n.s.: non-significant; \*  $P < 0.05$ , \*\*  $P < 0.01$  and \*\*\*  $P < 0.001$ ;  $n = 2$ ).

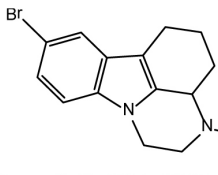
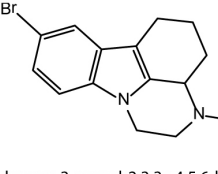
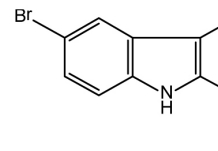
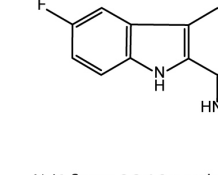
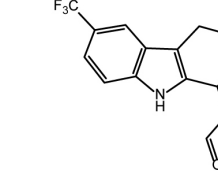
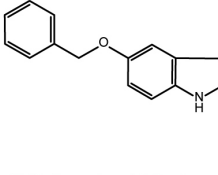
**(b)** Relative A $\beta$ 42/A $\beta$ 40 ratios calculated from (a). Treatment with tested analogues does not alter A $\beta$ 42/A $\beta$ 40 ratios, whereas positive controls Sulindac sulfide and Bepridil, respectively lead to a significant decrease and increase in A $\beta$ 42/A $\beta$ 40 ratios. All values are normalized to the value of DMSO, which is set to 1. (n.s.: non-significant; \*  $P < 0.05$ , \*\*  $P < 0.01$  and \*\*\*  $P < 0.001$ ;  $n = 2$ ).

Compound Structure and name	ID	Molecular formula	MW	clogP	Calcium	TMRM	A $\beta$ 42	A $\beta$ 40	A $\beta$ 38
 6-nitro-2,3,4,9-tetrahydro-1H-carbazol-1-amine	5302860	C <sub>12</sub> H <sub>13</sub> N <sub>3</sub> O <sub>2</sub>	231.25	2.16	1.038	0.622	0.473	0.494	0.421
 N-(6-nitro-2,3,4,9-tetrahydro-1H-carbazol-1-yl)formamide	5373790	C <sub>13</sub> H <sub>13</sub> N <sub>3</sub> O <sub>3</sub>	259.26	1.86	0.944	0.656	0.988	0.875	0.981
 N-(4-ethylcyclohexyl)-6-nitro-2,3,4,9-tetrahydro-1H-carbazol-1-amine	5781439	C <sub>20</sub> H <sub>27</sub> N <sub>3</sub> O <sub>2</sub>	341.45	5.65	0.981	1.384	1.058	0.733	0.584
 N-(3-methylcyclohexyl)-6-nitro-2,3,4,9-tetrahydro-1H-carbazol-1-amine	5781448	C <sub>19</sub> H <sub>25</sub> N <sub>3</sub> O <sub>2</sub>	327.42	5.13	0.966	1.545	0.593	0.726	0.593
 6-nitro-N-(4-phenylcyclohexyl)-2,3,4,9-tetrahydro-1H-carbazol-1-amine	5781451	C <sub>24</sub> H <sub>27</sub> N <sub>3</sub> O <sub>2</sub>	389.49	6.01	0.967	1.180	1.093	0.777	0.648
 N-(1-(4-methoxyphenyl)propan-2-yl)-6-nitro-2,3,4,9-tetrahydro-1H-carbazol-1-amine	5781452	C <sub>22</sub> H <sub>25</sub> N <sub>3</sub> O <sub>3</sub>	379.45	4.90	0.952	2.118	0.961	0.564	0.609
 N-(1-ethylpiperidin-4-yl)-6-nitro-2,3,4,9-tetrahydro-1H-carbazol-1-amine	5781457	C <sub>19</sub> H <sub>26</sub> N <sub>4</sub> O <sub>2</sub>	342.44	3.16	0.789	1.926	0.702	0.503	0.623
 6-nitro-N-(1-propylpiperidin-4-yl)-2,3,4,9-tetrahydro-1H-carbazol-1-amine	5781458	C <sub>20</sub> H <sub>28</sub> N <sub>4</sub> O <sub>2</sub>	356.46	3.69	0.962	1.756	0.683	0.503	0.618



Compound Structure and name	ID	Molecular formula	MW	clogP	Calcium	TMRM	A $\beta$ 42	A $\beta$ 40	A $\beta$ 38
 4-ethyl-N-((6-methyl-2,3,4,9-tetrahydro-1H-carbazol-1-yl)methyl)cyclohexanamine	5781474	C <sub>22</sub> H <sub>32</sub> N <sub>2</sub>	324.50	6.21	0.437	0.641	1.471	0.769	0.815
 1-methyl-N-((6-methyl-2,3,4,9-tetrahydro-1H-carbazol-1-yl)methyl)piperidin-4-amine	5781475	C <sub>20</sub> H <sub>29</sub> N <sub>3</sub>	311.46	3.19	0.499	1.259	1.068	0.753	0.916
 N-(1-(3,4-dimethoxyphenyl)propan-2-yl)-6-nitro-2,3,4,9-tetrahydro-1H-carbazol-1-amine	5781442	C <sub>23</sub> H <sub>27</sub> N <sub>3</sub> O <sub>4</sub>	409.48	4.64	0.961	1.329	1.053	0.692	0.772
 N-isopropyl-6-nitro-2,3,4,9-tetrahydro-1H-carbazol-1-amine	5781470	C <sub>15</sub> H <sub>19</sub> N <sub>3</sub> O <sub>2</sub>	273.33	3.41	0.942	0.850	0.760	0.545	0.582
 N-(4-methylcyclohexyl)-6-nitro-2,3,4,9-tetrahydro-1H-carbazol-1-amine	5781447	C <sub>19</sub> H <sub>25</sub> N <sub>3</sub> O <sub>2</sub>	327.42	5.13	0.942	0.491	0.983	0.827	0.735
 N-(1-(2-methoxyphenyl)propan-2-yl)-6-nitro-2,3,4,9-tetrahydro-1H-carbazol-1-amine	5781453	C <sub>22</sub> H <sub>25</sub> N <sub>3</sub> O <sub>3</sub>	379.45	4.90	0.917	0.554	0.896	0.779	0.850
 N-(1-(2-fluorophenyl)propan-2-yl)-6-nitro-2,3,4,9-tetrahydro-1H-carbazol-1-amine	5781454	C <sub>21</sub> H <sub>22</sub> FN <sub>3</sub> O <sub>2</sub>	367.42	5.12	0.925	0.433	0.846	0.706	0.692
 6-nitro-N-(1-phenethylpiperidin-4-yl)-2,3,4,9-tetrahydro-1H-carbazol-1-amine	5781441	C <sub>25</sub> H <sub>30</sub> N <sub>4</sub> O <sub>2</sub>	418.53	4.56	0.914	2.357	0.566	0.531	0.523

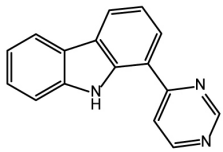
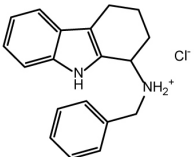
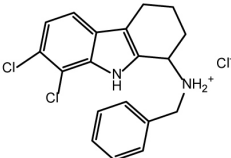
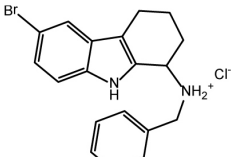
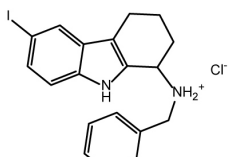
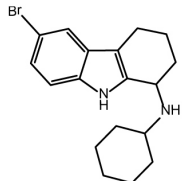
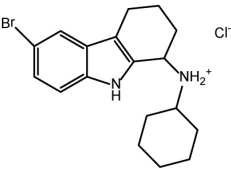
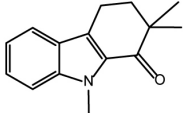
Compound Structure and name	ID	Molecular formula	MW	clogP	Calcium	TMRM	A $\beta$ 42	A $\beta$ 40	A $\beta$ 38
 <p>N-(2,3-dihydro-1H-inden-2-yl)-6-nitro-2,3,4,9-tetrahydro-1H-carbazol-1-amine</p>	5781444	C <sub>21</sub> H <sub>21</sub> N <sub>3</sub> O <sub>2</sub>	347.41	4.56	0.917	1.046	0.785	0.769	0.857
 <p>1-methyl-N-((6-methyl-2,3,4,9-tetrahydro-1H-carbazol-1-yl)methyl)piperidin-4-amine</p>	5781446	C <sub>18</sub> H <sub>23</sub> N <sub>3</sub> O <sub>2</sub>	313.39	4.57	0.933	1.259	1.038	0.593	0.594
 <p>2-((6-bromo-2,3,4,9-tetrahydro-1H-carbazol-1-yl)amino)ethanol</p>	5258947	C <sub>14</sub> H <sub>17</sub> BrN <sub>2</sub> O	309.20	2.91	1.047	1.514	0.335	0.355	0.317
 <p>6-bromo-N-phenethyl-2,3,4,9-tetrahydro-1H-carbazol-1-amine hydrochloride</p>	5265927	C <sub>20</sub> H <sub>22</sub> BrClN <sub>2</sub>	405.76	5.60	0.791	1.922	0.292	0.278	0.176
 <p>N-benzyl-6-bromo-2,3,4,9-tetrahydro-1H-carbazol-1-amine</p>	5307331	C <sub>19</sub> H <sub>19</sub> BrN <sub>2</sub>	355.27	4.66	0.703	1.508	0.683	0.503	0.357
 <p>3-benzyl-8-bromo-2,3,3a,4,5,6-hexahydro-1H-pyrazino[3,2,1-jk]carbazole</p>	5358447	C <sub>21</sub> H <sub>21</sub> BrN <sub>2</sub>	381.31	6.11	0.953	1.008	0.332	0.397	0.421
 <p>6-bromo-1-(1H-pyrrol-1-yl)-2,3,4,9-tetrahydro-1H-carbazole</p>	5920301	C <sub>16</sub> H <sub>15</sub> BrN <sub>2</sub>	315.21	4.98	0.869	0.831	0.492	0.481	0.449
 <p>N-(6-bromo-2,3,4,9-tetrahydro-1H-carbazol-1-yl)formamide</p>	5922537	C <sub>13</sub> H <sub>13</sub> BrN <sub>2</sub> O	293.16	2.79	1.002	1.207	1.056	0.712	0.874

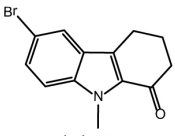
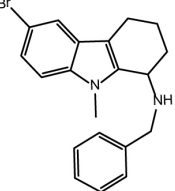
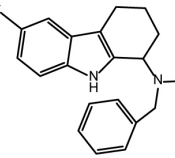
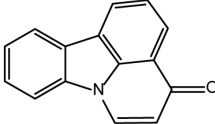
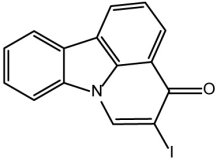
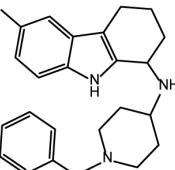
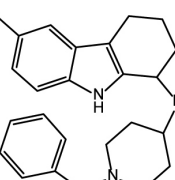
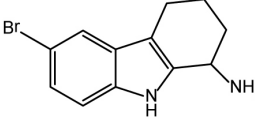
Compound Structure and name	ID	Molecular formula	MW	clogP	Calcium	TMRM	A $\beta$ 42	A $\beta$ 40	A $\beta$ 38
 8-bromo-3-ethyl-2,3,3a,4,5,6-hexahydro-1H-pyrazino[3,2,1-jk]carbazole hydrochloride	6044730	C <sub>16</sub> H <sub>20</sub> BrClN <sub>2</sub>	355.70	4.72	0.968	0.745	1.180	0.745	1.003
 8-bromo-3-propyl-2,3,3a,4,5,6-hexahydro-1H-pyrazino[3,2,1-jk]carbazole	6049723	C <sub>17</sub> H <sub>21</sub> BrN <sub>2</sub>	333.27	5.25	0.961	0.663	0.840	0.642	0.817
 6-bromo-2,3,4,9-tetrahydro-1H-carbazol-1-amine	5303801	C <sub>12</sub> H <sub>13</sub> BrN <sub>2</sub>	265.15	3.09	0.989	1.116	0.269	0.271	0.309
 N-(6-fluoro-2,3,4,9-tetrahydro-1H-carbazol-1-yl)formamide	7129409	C <sub>13</sub> H <sub>13</sub> FN <sub>2</sub> O	232.25	2.07	0.958	0.860	0.592	0.470	0.589
 N-(6-(trifluoromethyl)-2,3,4,9-tetrahydro-1H-carbazol-1-yl)formamide	5922756	C <sub>14</sub> H <sub>13</sub> F <sub>3</sub> N <sub>2</sub> O	282.26	2.93	1.001	1.236	0.999	1.033	1.057
 N-(6-(benzyloxy)-2,3,4,9-tetrahydro-1H-carbazol-1-yl)formamide	7173317	C <sub>20</sub> H <sub>20</sub> N <sub>2</sub> O <sub>2</sub>	320.38	3.55	0.998	0.606	1.012	0.997	1.104

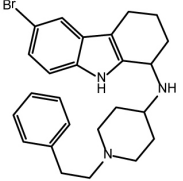
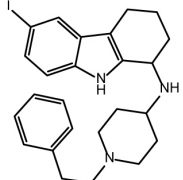
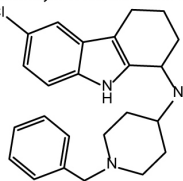
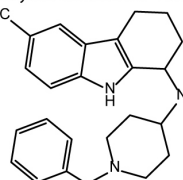
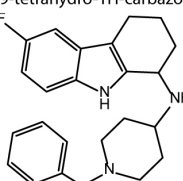
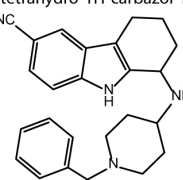
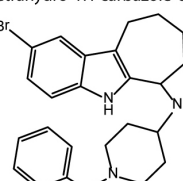
**Figure 7.S1. The list of commercially available tetrahydrocarbazole analogues**

Shown are 38 tested commercially available tetrahydrocarbazole analogues. Next to their chemical structure and physical properties, the measures for their activity in different assays are presented with their corresponding normalized values for: CCh-evoked calcium release peak; mitochondrial membrane potential (TMRM); and the levels of three different secreted A $\beta$  peptides (measured at 10  $\mu$ M).



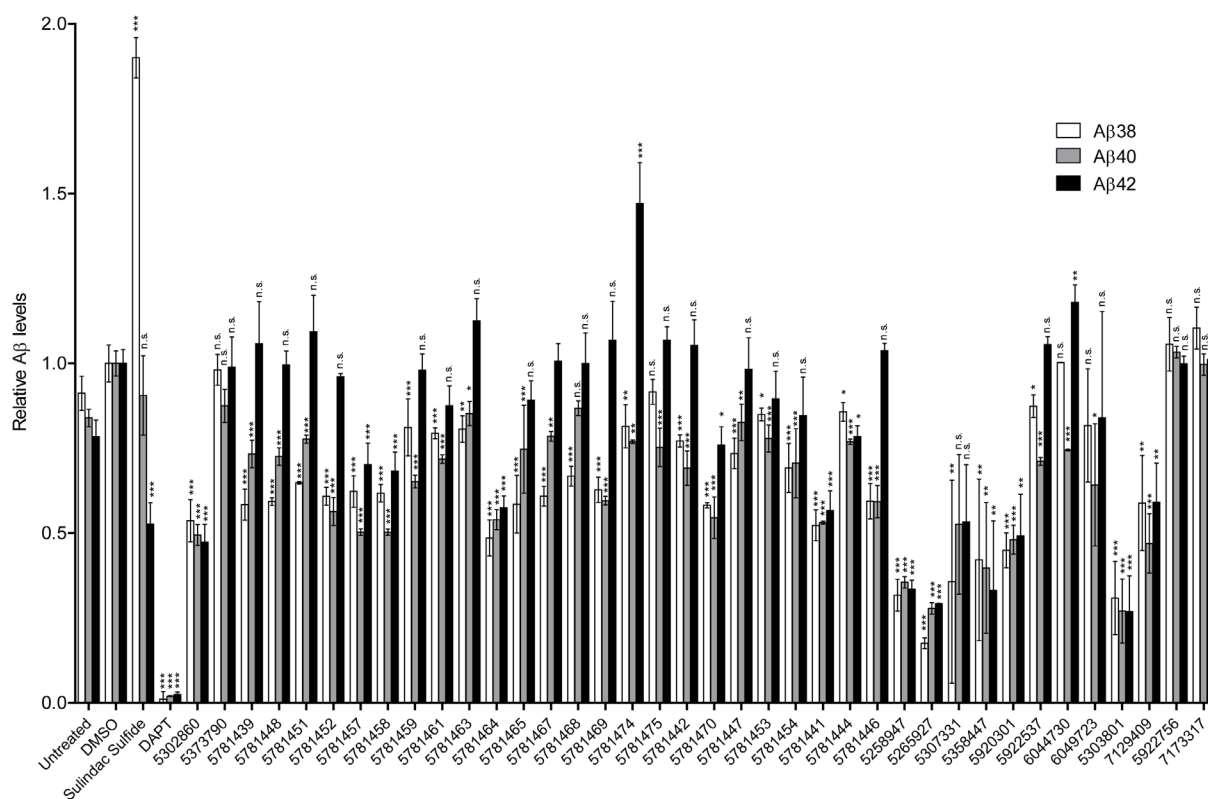
Compound Structure and name	ID	Molecular formula	MW	clogP	Calcium	TMRM	A $\beta$ 42	A $\beta$ 40	A $\beta$ 38
 1-(pyrimidin-4-yl)-9H-carbazole	gea_82	C <sub>16</sub> H <sub>11</sub> N <sub>3</sub>	245.28	3.16	0.974	0.926	1.080	1.086	1.164
 N-benzyl-2,3,4,9-tetrahydro-1H-carbazol-1-aminium chloride	gea_83	C <sub>19</sub> H <sub>28</sub> ClN <sub>2</sub>	312.84	4.63	0.991	1.219	1.050	0.835	0.635
 N-benzyl-7,8-dichloro-2,3,4,9-tetrahydro-1H-carbazol-1-aminium chloride	gea_84	C <sub>19</sub> H <sub>19</sub> Cl <sub>3</sub> N <sub>2</sub>	381.73	6.16	1.011	1.049	1.100	1.050	0.913
 N-benzyl-6-bromo-2,3,4,9-tetrahydro-1H-carbazol-1-aminium chloride	gea_85	C <sub>19</sub> H <sub>20</sub> BrClN <sub>2</sub>	391.73	5.66	0.879	1.444	0.910	0.765	0.651
 N-benzyl-6-iodo-2,3,4,9-tetrahydro-1H-carbazol-1-aminium chloride	gea_86	C <sub>19</sub> H <sub>20</sub> ClIN <sub>2</sub>	438.73	5.92	0.913	1.444	0.901	0.767	0.629
 6-bromo-N-cyclohexyl-2,3,4,9-tetrahydro-1H-carbazol-1-amine	gea_87	C <sub>18</sub> H <sub>23</sub> BrN <sub>2</sub>	347.29	5.53	0.946	0.998	0.779	0.564	0.479
 6-bromo-N-cyclohexyl-2,3,4,9-tetrahydro-1H-carbazol-1-aminium chloride	gea_87_HCl	C <sub>18</sub> H <sub>24</sub> BrClN <sub>2</sub>	383.75	6.01	0.914	0.926	0.848	0.608	0.610
 2,2,9-trimethyl-2,3,4,9-tetrahydro-1H-carbazol-1-one	gea_88	C <sub>15</sub> H <sub>17</sub> NO	227.30	3.80	0.977	0.814	1.218	0.850	1.013

Compound Structure and name	ID	Molecular formula	MW	clogP	Calcium	TMRM	A $\beta$ 42	A $\beta$ 40	A $\beta$ 38
 6-bromo-9-methyl-2,3,4,9-tetrahydro-1H-carbazol-1-one	gea_89	C <sub>13</sub> H <sub>12</sub> BrNO	278.14	3.65	0.947	0.858	0.956	0.772	0.948
 N-benzyl-6-bromo-9-methyl-2,3,4,9-tetrahydro-1H-carbazol-1-amine	gea_90	C <sub>20</sub> H <sub>21</sub> BrN <sub>2</sub>	369.30	5.00	0.972	1.024	0.891	0.806	0.892
 N-benzyl-6-bromo-N-methyl-2,3,4,9-tetrahydro-1H-carbazol-1-amine	gea_92	C <sub>20</sub> H <sub>21</sub> BrN <sub>2</sub>	369.30	5.74	1.000	0.724	0.815	0.754	0.745
 4H-pyrido[3,2,1-jk]carbazol-4-one	gea_94	C <sub>15</sub> H <sub>9</sub> NO	219.24	1.96	0.960	0.716	1.075	1.110	1.019
 5-iodo-4H-pyrido[3,2,1-jk]carbazol-4-one	gea_95	C <sub>15</sub> H <sub>8</sub> INO	345.13	3.09	0.974	0.926	1.031	0.993	0.991
 N-(1-benzylpiperidin-4-yl)-6-iodo-2,3,4,9-tetrahydro-1H-carbazol-1-amine	gea_96	C <sub>24</sub> H <sub>28</sub> IN <sub>3</sub>	485.40	5.61	0.840	2.100	0.542	0.520	0.461
 N-(1-benzylpiperidin-4-yl)-6-bromo-2,3,4,9-tetrahydro-1H-carbazol-1-amine	gea_97	C <sub>24</sub> H <sub>28</sub> BrN <sub>3</sub>	438.40	5.35	0.894	2.335	0.530	0.552	0.487
 6-bromo-2,3,4,9-tetrahydro-1H-carbazol-1-aminium	gea_99	C <sub>12</sub> H <sub>14</sub> BrClN <sub>2</sub>	301.61	3.14	0.997	1.563	0.506	0.489	0.586

Compound Structure and name	ID	Molecular formula	MW	clogP	Calcium	TMRM	A $\beta$ 42	A $\beta$ 40	A $\beta$ 38
 6-bromo-N-(1-phenethylpiperidin-4-yl)-2,3,4,9-tetrahydro-1H-carbazol-1-amine	gea_101	C <sub>25</sub> H <sub>30</sub> BrN <sub>3</sub>	452.43	5.49	0.856	1.929	0.449	0.513	0.441
 6-iodo-N-(1-phenethylpiperidin-4-yl)-2,3,4,9-tetrahydro-1H-carbazol-1-amine	gea_102	C <sub>25</sub> H <sub>30</sub> IN <sub>3</sub>	499.43	5.74	0.871	1.726	0.523	0.480	0.479
 N-(1-benzylpiperidin-4-yl)-6-chloro-2,3,4,9-tetrahydro-1H-carbazol-1-amine	gea_129	C <sub>24</sub> H <sub>28</sub> ClN <sub>3</sub>	393.95	5.2	0.832	1.862	0.327	0.383	0.311
 N-(1-benzylpiperidin-4-yl)-6-(trifluoromethyl)-2,3,4,9-tetrahydro-1H-carbazol-1-amine	gea_130	C <sub>25</sub> H <sub>26</sub> F <sub>3</sub> N <sub>3</sub>	427.51	5.50	0.763	2.214	0.426	0.478	0.514
 N-(1-benzylpiperidin-4-yl)-6-fluoro-2,3,4,9-tetrahydro-1H-carbazol-1-amine	gea_132	C <sub>24</sub> H <sub>28</sub> FN <sub>3</sub>	377.50	4.63	0.834	2.004	0.295	0.361	0.342
 1-((1-benzylpiperidin-4-yl)amino)-2,3,4,9-tetrahydro-1H-carbazole-6-carbonitrile	gea_133	C <sub>25</sub> H <sub>28</sub> N <sub>4</sub>	384.52	4.14	0.899	2.636	0.273	0.308	0.296
 N-(1-benzylpiperidin-4-yl)-2-bromo-5,6,7,8,9,10-hexahydrocyclohepta[b]indol-6-amine	gea_139	C <sub>25</sub> H <sub>30</sub> BrN <sub>3</sub>	452.43	5.91	0.963	1.646	0.504	0.576	0.514

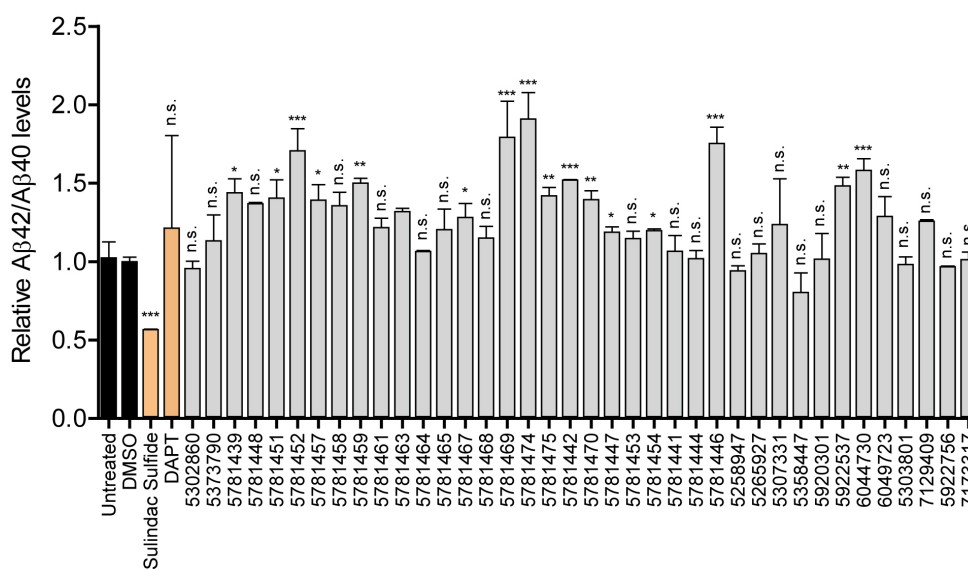
**Figure 7.S2. The list of synthesized tetrahydrocarbazole analogues**

Shown are 23 strategically synthesized tetrahydrocarbazole analogues. Next to their chemical structure and physical properties, the measures for their activity in different assays are presented with their corresponding normalized values for: CCh-evoked calcium release peak; mitochondrial membrane potential (TMRM); and the levels of three different secreted A $\beta$  peptides (measured at 10  $\mu$ M).



**Figure 7.S3. The effect of commercially available tetrahydrocarbazole analogues on Aβ production**

Relative Aβ38, Aβ40 and Aβ42 levels are decreased after 16 h treatment with commercially available tetrahydrocarbazole analogues at 10 μM in HEK293 cells coexpressing APPsw and PS1-M146L. Sulindac sulfide (50 μM) and DAPT (10 μM), respectively, a γ-secretase modulator and a γ-secretase inhibitor, were used as positive controls. All the values are normalized to the value of DMSO, which is set to 1. (n.s.: non-significant; \* P<0.05, \*\* P<0.01 and \*\*\* P<0.001; n=2).



**Figure 7.S4. The effect of commercially available tetrahydrocarbazole analogues on Aβ42/Aβ40 ratio**  
 Relative Aβ42/Aβ40 ratios calculated from figure 7.S2. Treatment with the majority of the lead structure derivatives does not alter the Aβ42/Aβ40 ratio, whereas the positive control Sulindac sulfide (but not DAPT), significantly lowers the Aβ42/Aβ40 ratio. All values are normalized to the value of DMSO, which is set to 1. (n.s.: non-significant; \* P<0.05, \*\* P<0.01 and \*\*\* P<0.001; n=2).

## 7.6 Supplementary Material

*Commercially available compound library and derivatives:* The DIVERSet<sup>®</sup> compound library and further commercially available tetrahydrocarbazole analogues and related structures were obtained from ChemBridge (ChemBridge Corp., San Diego, CA). The database for the library compounds and the tested analogues are available at <http://www.chembridge.com> and <https://www.hit2lead.com>

*Acknowledgements* — This work was supported the German-Polish grants from the German Federal Ministry for Education and Research Council (BMBF — 01GZ0713) to JH and from the Polish Ministry of Science and Higher Education to JK (#S001/P-N/2007/01). The authors are grateful to Dr. A. Miyawaki for YC3.6 construct, to M. Taverna, Drs. S. Lichtenthaler, S. Lammich, H. Steiner and C. Haass for kindly providing the stable PS1 and APP lines and the support in the A $\beta$  and sAPP $\alpha/\beta$  measurements. We also would like to thank T. Kares, J. Knörndel, O. Stelmakh and E. Griebinger for their excellent technical assistance and Dr. N. Vassallo for carefully reading this manuscript and giving constructive comments. The authors declare that there are no conflicts of interest.

*Abbreviations used:* A $\beta$ , Beta-Amyloid; AD, Alzheimer's disease; APP, Amyloid Precursor Protein; BACE1,  $\beta$ -amyloid converting enzyme 1; CALHM1, Calcium Homeostasis Modulator 1; CFP, Cyan Fluorescent Protein; CCh, Carbachol; CPA, Cyclopiazonic acid; DAPT, *N*-[(3,5-Difluorophenyl)acetyl]-L-alanyl-2-phenylglycine-1,1-dimethylethyl ester; DMSO, Dimethyl Sulfoxide; ER, Endoplasmic Reticulum; FAD-PS1, Familial Alzheimer's disease linked mutant Presenilin 1; GSM,  $\gamma$ -secretase modulator; IP<sub>3</sub>, Inositol-1,4,5-trisphosphate; IP<sub>3</sub>R, Inositol-1,4,5-trisphosphate Receptor; NMDA, N-Methyl-D-aspartate; PLC, Phospholipase C; PS, Presenilin; PSD-95, Postsynaptic Density Protein 95; RyR, Ryanodine Receptor; SAR, Structure-Activity-Relationship; SERCA, Sarcoendoplasmic Reticulum Calcium Transport ATPase; TMB-8, 3,4,5-trimethoxybenzoic acid 8-(diethylamino)octyl ester; TMRM, Tetramethylrhodamine Methyl Ester; TP, Thapsigargin; wtPS1, Wild Type Presenilin 1; YC3.6, Yellow Cameleon 3.6; YFP, Yellow Fluorescent Protein

## 8 General Discussion

### 8.1 The role of presenilin holoprotein upregulation in AD-associated calcium dyshomeostasis

In the first part of this work, we could shed light on some of the controversies regarding the role of presenilins in the ER calcium homeostasis. Our results suggest that conditions enhancing the amount of PS1 holoprotein result in reduced ER calcium content. Therefore, in view of the impaired PS autoendoproteolysis caused by FAD-PS mutations and the leak channel property of PS holoprotein, we propose that the consequent increased stability and/or accumulation of PS holoprotein may directly contribute to AD pathogenesis by affecting the ER calcium homeostasis. Considering the strong concentration gradient of calcium ions between ER and cytosol, in addition to very low PS holoprotein expression levels under physiological circumstances, even minor upregulation in the PS holoprotein level may alter intracellular calcium signaling remarkably.

Particularly, in HEK293 cells carrying FAD-PS1 mutations, we detected lowered ER calcium release in response to stimulation with TP and BK. However, amplified CCh-induced ER calcium response was detected in the FAD-PS1 cells. Here we argue that in the case of stimulation with TP and BK, lowered ER calcium content is the cause for the attenuated calcium release from ER. However, in the event of stimulation with CCh, compensatory mechanisms seem to be in action that can mask the lowered ER calcium content of FAD-PS1 cells. Stimulation with CCh typically generates higher levels of IP<sub>3</sub> molecule compared to stimulation with BK [279]. The latter in combination with FAD-PS1-mediated oversensitized IP<sub>3</sub>Rs [69, 235], result in amplified calcium release from ER upon CCh stimulation. Despite the contradicting data around this topic, evidence in support of our hypothesis comes from the studies that detected decreased ER calcium load by directly measuring the absolute amount of ER calcium in cells harboring FAD-PS mutations [233, 234].

We also observed that treatment of HEK293 cells with three different  $\gamma$ -secretase inhibitors result in lowered calcium release from ER, accompanied by elevated levels of PS1 holoprotein, presumably due to inhibition of PS autoendoproteolysis. This indicates a potentially neglected side effect for this class of drugs, which may unexpectedly even accelerate the disease progression. Thus, in view of these findings we suggest that the development of medicines targeting PS molecules and/or  $\gamma$ -secretase complex (e.g.  $\gamma$ -secretase inhibitors and modulators), should carefully address their impact on intracellular calcium homeostasis as well.

Within this study, we could detect elevated levels of PS1 holoprotein in the postmortem brain samples of AD patients carrying FAD-PS1 mutations. On the basis this finding, one could argue that in the AD population carrying FAD-PS mutations, increased PS holoprotein levels may underlie the AD-associated impairments of ER calcium homeostasis. On other hand, regarding sporadic AD and FAD-APP cases, other pathological mechanisms can potentially exist which may eventually give rise to such impairments in the intracellular calcium homeostasis [291]. However, in the case of sporadic AD, as the disease follows a slower progression, those underlying mechanisms responsible for calcium dyshomeostasis are likely to have more subtle effects.

Overall, with respect to the passive calcium leak channel activity of PS holoprotein on the ER membrane [228], we demonstrated that conditions decreasing the autocatalytic function of PS holoprotein result in accumulation of its holoprotein form, which in turn affects the ER calcium homeostasis. Within this study, a number of different approaches were used to mimic the accumulation of PS holoprotein (overexpression of wild type and mutant PS1 variants, treatment with  $\gamma$ -secretase inhibitors, and the knockdown of PEN-2). These approaches resulted in attenuated ER calcium response, likely because of enhanced continuous calcium leakage from ER into cytosol and the subsequent decrease in the ER calcium load.

Given that numerous mechanisms have been associated with the expression of FAD-PS1 mutants (e.g. modulated IP<sub>3</sub>R, RyR, SERCA, PS holoprotein leak channel activity and CCE) [255], one may argue that such mechanisms are downstream effects of PS1 holoprotein accumulation, developed to compensate the decrease in the ER calcium load.



## **8.2 Development of a high-throughput FRET-based calcium imaging assay for drug screening in AD**

Based on our findings regarding the role of presenilins in calcium signaling and the growing evidence towards the involvement of impaired intracellular store calcium homeostasis in the pathogenesis of AD, we took a calcium-signaling-targeted approach for AD drug discovery [332, 337].

To that end, we combined intracellular calcium dyshomeostasis as a novel target for drug screening with an innovative FRET-based confocal calcium imaging technique in a fully automated high-throughput manner using Opera<sup>®</sup> system. This assay targets calcium dysregulation in the ER as a unique approach for AD drug discovery. In contrast to the mainstream AD drug development paradigms, our approach targets one of the earliest (if not the most upstream) events in the AD progression, long before the appearance of characteristic disease hallmarks and cognitive deficits. The latter promises a huge clinical potential for prevention, halting, or reversal of AD. To the best of our knowledge, the possibility of normalizing the impaired ER store calcium homeostasis has never been examined in high-throughput drug discovery of neurodegenerative diseases [332, 337].

Using the developed assay, we can measure the basal cytosolic calcium concentrations and follow the rises in calcium levels (e.g. ER calcium release), simultaneously in hundreds of single cells expressing a genetically-encoded calcium indicator. For the purpose of this assay, it was essential that the Opera<sup>®</sup> system is equipped with a dispenser unit, which allowed performing rapid automated dispensing of reagent jets to individual wells during calcium measurements with no time lag between dispensing and imaging. This was necessary for kinetic measurements that require rapid imaging with no delay post dispensing, e.g. fast agonist-induced calcium release [332, 337].

The single-cell-based feature in this assay is particularly advantageous, as it enables the detection of minimal changes in calcium dynamics that may not be detectable in

conventional single-well-based calcium measurement screening technologies. Moreover, the ability to follow calcium transients in individual cells allows distinguishing distinct cell subpopulations by applying different filtering parameters in image analysis, which is another limiting factor in the single-well-based calcium imaging assays [332, 337].

Traditionally, small calcium dyes are used for conventional calcium imaging. However, their use in high-throughput fashion is prone to a number of disadvantages associated with long-term dye toxicity, loading, washing and leakage. Importantly, the use of genetically-encoded calcium sensors solves the cytotoxicity issue and enables monitoring calcium transients over extended periods and following both slow and fast kinetic events.

Here, the developed assay was validated for CCh-induced calcium release in double-stable HEK293 line transfected with a FAD-PS1 variant and YC3.6. The assay proved to be optimal for high-throughput screening, as it provided a reliable window of separation between positive and negative controls, reflected by the robust  $Z'$ -factor  $> 0.8$ .

While the HTS assay was primarily developed for large-scale compound screening purposes, potentially it can be applied to other applications as well. For example, the assay in its current form can be easily adapted to high-throughput RNAi screens. Performing siRNA screens on the basis of the established HTS assay would identify potential novel genes and pathways that are involved in the FAD-PS1 associated ER calcium dyshomeostasis. Such genes and pathways may even serve as future novel AD drug targets. Furthermore, the established assay has the potential of being employed in the early diagnostics of AD. A recent study shows that intracellular calcium homeostasis is impaired in the peripheral cells (e.g. lymphocytes) derived from patients with mild cognitive impairment and sporadic AD [46]. According to this finding, it is feasible to utilize the established automated calcium imaging assay for monitoring such calcium disturbances at early stages of the disease. However, due to issues associated with the lack of adhesion in lymphocytes and the difficulties in introducing YC3.6 calcium indicator into primary cells, further adjustments are necessary to optimize the assay for automated diagnostic purposes.

Although for the purpose of this project we particularly focused on the use of FAD-PS expressing HEK293 cells in the assay, nevertheless, the developed HTS system provides a broad potential to be applied to sporadic AD and many other disease conditions associated with impaired calcium homeostasis. Amongst them are many neurodegenerative and cardiac disorders and aging.

As opposed to the bulk of current AD drug discovery approaches that largely rely on “target-based” assays, here we developed a “phenotypic” screening approach. Various mechanisms have been proposed to underlie the FAD-PS1-mediated enhancement of the ER calcium release, e.g. enhanced IP<sub>3</sub> and ryanodine receptor (RyR) channel activities, altered SERCA function, decreased store-operated calcium entry (SOCE), and loss of PS holoprotein passive calcium leakage activity [255]. Irrespective as to whether those are the primary causative factors or only downstream secondary phenomena, the present phenotypic assay enables identification of all compounds that can reverse the exaggerated agonist-evoked ER calcium release phenotype in HEK293 cells expressing FAD-PS, independent of their mechanism of action. [332, 337].

Apart from the oversensitivity of IP<sub>3</sub>R itself [69, 235], several upstream components of IP<sub>3</sub>R-mediated calcium response are also affected in AD, e.g. G-protein coupled receptors (GPCR) generally [355], and muscarinic receptors particularly [356], G-proteins [357], and PLC [200]. The combination of those effects in cells expressing FAD-PS1-linked mutations result in an exaggerated IP<sub>3</sub>R-mediated calcium response compared to wild type PS1 expressing cells [223]. Since the hits from the screen may potentially target any of those upstream components, a phenotypic “multi-targeted” compound screening approach as such, provides the advantage of jointly addressing several AD aspects. Considering the recent failure of AD drug candidates identified from target-based approaches, such a multi-targeted phenotypic drug discovery assay may present a promising alternative for identification of novel drugs for AD [332].

### 8.3 High-throughput screening of compound libraries, discovery and characterization of novel drugs for treatment of AD

The developed assay was initially employed in a medium-size pilot screen with a library of ion channel ligands, from which Bepridil was identified as an active hit. The ion channel ligand library was chosen based on the interdependence of ER calcium with basal cytosolic calcium levels and calcium influx. Moreover, we postulated that calcium channel blockers might potentially modulate the activity of ER calcium channels or passive calcium leakage through presenilin holoprotein. We found that Bepridil could reverse the FAD-PS1-dependent potentiation of agonist-evoked ER calcium release.

Interestingly, Bepridil was recently proposed as an AD therapeutic drug candidate based on the finding that it lowers A $\beta$  peptide production. We confirmed those findings and demonstrated that Bepridil attenuates A $\beta$  production by shifting the amyloidogenic  $\beta$ -cleavage of APP towards non-amyloidogenic  $\alpha$ -cleavage, while simultaneously possessing an iGSM mode of action. In addition, we revealed that Bepridil treatment also results in AMPK activation. The activation of AMPK is known to increase  $\alpha$ -secretase activity that accompanies decreased  $\beta$ -secretase activity. Therefore, we propose that beneficial effects of Bepridil in lowering A $\beta$  levels could be at least partially related to AMPK activation.

After a successful pilot screen, we subsequently performed a large-scale screen with a diverse compound library comprising 20,000 low-molecular-weight molecules, which resulted in the identification of five lead structures, one of them being tetrahydrocarbazoles. Characterization of this lead structure using additional AD-relevant secondary assays indicated a multifactorial mode of action for tetrahydrocarbazoles. This class of compounds was able to simultaneously normalize the ER calcium homeostasis, enhance mitochondrial function and lower A $\beta$  production through decreasing  $\beta$ -secretase cleavage.

Notably, for two other lead structures identified in the primary screen, Phenothiazines and Thiazolidines, existing evidence supports the beneficial role of those compound classes for AD treatment [360-362]. Such indications validate the relevance our phenotypic screening strategy as well as the lead structures identified from it [332].

AD is a multifactorial disease, which is believed to be caused by complex interactions among several contributing pathomechanisms [330]. Therefore, in view of the multifactoriality of tetrahydrocarbazoles, we propose that this novel class of compounds may present the basis for an effective therapeutic modality by collectively addressing three central AD-associated pathological mechanisms.

Based on the hypothesis that impaired calcium homeostasis is an early event in the AD pathology, it was anticipated that the pharmacological normalization of ER calcium homeostasis may prevent the appearance of late-stage AD pathologies. Indeed, stabilization of calcium signaling interfered with the appearance of characteristic AD features. In the case of Bepridil, normalization of ER calcium homeostasis led to lowered A $\beta$  production by enhancing AMPK activity in a calcium-dependent manner. Similarly, normalization of ER calcium signaling with tetrahydrocarbazoles resulted in improved mitochondrial function, decreased  $\beta$ -secretase activity and lowered A $\beta$  production. However, since the molecular targets of the identified lead structures are not yet determined we cannot firmly conclude whether the detected changes in APP processing and mitochondrial function are indeed downstream effects of the modulation of intracellular calcium homeostasis.

While strong evidence supports the “association” of A $\beta$  pathology with AD, the field has begun to question the “causative” role of A $\beta$  in the pathogenesis of AD [363]. We could show that pharmacological normalization of calcium homeostasis lowers A $\beta$  production. Although the field has recently faced the failure of many A $\beta$ -focused therapeutic modalities, our results indicate that targeting calcium homeostasis as an upstream event affects the downstream A $\beta$  pathology in AD. Even if therapeutic removal of A $\beta$  would not provide the desired clinical efficacy by itself, nevertheless, A $\beta$  pathology is indicative of disease progression and a relevant biomarker for AD. Hence, the identified lead structures ameliorate the disease hallmarks (which may not necessarily be the causes of AD) by targeting and normalizing intracellular calcium homeostasis.

Impaired maintenance of physiological intracellular calcium homeostasis is critically involved in the pathophysiology of many diseases and aging [35, 346, 347]. Thus, compounds that stabilize the intracellular calcium homeostasis may be of potential benefit against aging and different disease conditions such as dementia, neurodegeneration, central nervous system and cardiovascular disorders [315, 364]. For example, FAD-PS mutations are associated with dilated cardiomyopathy and in many pathological conditions, including cardiac hypertrophy, and the IP<sub>3</sub>R activity is altered in a number of neurodegenerative disorders.

Therefore, targeting disrupted calcium homeostasis and pharmacologically restoring the physiological calcium signaling, particularly in ER, opens novel avenues to more efficiently treat AD and several other human diseases and conditions which are associated with impaired intracellular calcium homeostasis. In this work, the beneficial effects of identified compounds were particularly investigated and confirmed in cellular models of FAD.

## 9 References

1. Prince, M., R. Bryce, and C. Ferri, *World Alzheimer Report 2011*, in *Alzheimer's Disease International*. 2011.
2. Tanzi, R.E. and L. Bertram, *Twenty years of the Alzheimer's disease amyloid hypothesis: a genetic perspective*. *Cell*, 2005. **120**(4): p. 545-55.
3. Alzheimer, A., *Über eine eigenartige Erkrankung der Hirnrinde*. *Allg Z für Psychiat und Psych Gerichtl Med*, 1907(64): p. 146-8.
4. Hippius, H. and G. Neundorfer, *The discovery of Alzheimer's disease*. *Dialogues Clin Neurosci*, 2003. **5**(1): p. 101-8.
5. Braak, H., et al., *Age, neurofibrillary changes, A beta-amyloid and the onset of Alzheimer's disease*. *Neurosci Lett*, 1996. **210**(2): p. 87-90.
6. Corona, C., et al., *New therapeutic targets in Alzheimer's disease: brain deregulation of calcium and zinc*. *Cell Death Dis*, 2011. **2**: p. e176.
7. Querfurth, H.W. and F.M. LaFerla, *Alzheimer's disease*. *N Engl J Med*, 2010. **362**(4): p. 329-44.
8. Corrada, M.M., et al., *Dementia incidence continues to increase with age in the oldest old: the 90+ study*. *Ann Neurol*, 2010. **67**(1): p. 114-21.
9. Price, D.L., et al., *Alzheimer's disease: genetic studies and transgenic models*. *Annu Rev Genet*, 1998. **32**: p. 461-93.
10. Lippa, C.F., et al., *Familial and sporadic Alzheimer's disease: neuropathology cannot exclude a final common pathway*. *Neurology*, 1996. **46**(2): p. 406-12.
11. Masters, C.L., *Etiology and pathogenesis of Alzheimer's disease*. *Pathology*, 1984. **16**(3): p. 233-4.
12. Citron, M., *Alzheimer's disease: strategies for disease modification*. *Nat Rev Drug Discov*, 2010. **9**(5): p. 387-98.
13. Mattson, M.P., *Pathways towards and away from Alzheimer's disease*. *Nature*, 2004. **430**(7000): p. 631-9.
14. Mangialasche, F., et al., *Alzheimer's disease: clinical trials and drug development*. *Lancet Neurol*, 2010. **9**(7): p. 702-16.
15. Galimberti, D. and E. Scarpini, *Disease-modifying treatments for Alzheimer's disease*. *Ther Adv Neurol Disord*, 2011. **4**(4): p. 203-16.

16. Raffi, M.S. and P.S. Aisen, *Recent developments in Alzheimer's disease therapeutics*. BMC Med, 2009. **7**: p. 7.
17. Miller, G., *Alzheimer's research. Stopping Alzheimer's before it starts*. Science, 2012. **337**(6096): p. 790-2.
18. Golde, T.E., L.S. Schneider, and E.H. Koo, *Anti-abeta therapeutics in Alzheimer's disease: the need for a paradigm shift*. Neuron, 2011. **69**(2): p. 203-13.
19. Selkoe, D.J., *Resolving controversies on the path to Alzheimer's therapeutics*. Nat Med, 2011. **17**(9): p. 1060-5.
20. Karran, E., M. Mercken, and B. De Strooper, *The amyloid cascade hypothesis for Alzheimer's disease: an appraisal for the development of therapeutics*. Nat Rev Drug Discov, 2011. **10**(9): p. 698-712.
21. Aisen, P.S., et al., *Report of the task force on designing clinical trials in early (predementia) AD*. Neurology, 2011. **76**(3): p. 280-6.
22. LaFerla, F.M., *Calcium dyshomeostasis and intracellular signalling in Alzheimer's disease*. Nat Rev Neurosci, 2002. **3**(11): p. 862-72.
23. Foskett, J.K., *Inositol trisphosphate receptor  $Ca^{2+}$  release channels in neurological diseases*. Pflugers Arch, 2010. **460**(2): p. 481-94.
24. Stutzmann, G.E., *Calcium dysregulation,  $IP_3$  signaling, and Alzheimer's disease*. Neuroscientist, 2005. **11**(2): p. 110-5.
25. Stutzmann, G.E. and M.P. Mattson, *Endoplasmic reticulum  $Ca^{2+}$  handling in excitable cells in health and disease*. Pharmacol Rev, 2011. **63**(3): p. 700-27.
26. Robert, V., et al., *Direct monitoring of the calcium concentration in the sarcoplasmic and endoplasmic reticulum of skeletal muscle myotubes*. J Biol Chem, 1998. **273**(46): p. 30372-8.
27. Berridge, M.J., *Neuronal calcium signaling*. Neuron, 1998. **21**(1): p. 13-26.
28. Finch, E.A., T.J. Turner, and S.M. Goldin, *Calcium as a coagonist of inositol 1,4,5-trisphosphate-induced calcium release*. Science, 1991. **252**(5004): p. 443-6.
29. Bojarski, L., J. Herms, and J. Kuznicki, *Calcium dysregulation in Alzheimer's disease*. Neurochem Int, 2008. **52**(4-5): p. 621-33.
30. Foskett, J.K., et al., *Inositol trisphosphate receptor  $Ca^{2+}$  release channels*. Physiol Rev, 2007. **87**(2): p. 593-658.
31. Verkhratsky, A., *Physiology and pathophysiology of the calcium store in the endoplasmic reticulum of neurons*. Physiol Rev, 2005. **85**(1): p. 201-79.



32. Pimplikar, S.W., et al., *Amyloid-independent mechanisms in Alzheimer's disease pathogenesis*. J Neurosci, 2010. **30**(45): p. 14946-54.
33. Yu, J.T., R.C. Chang, and L. Tan, *Calcium dysregulation in Alzheimer's disease: from mechanisms to therapeutic opportunities*. Prog Neurobiol, 2009. **89**(3): p. 240-55.
34. Khachaturian, Z.S., *Hypothesis on the regulation of cytosol calcium concentration and the aging brain*. Neurobiol Aging, 1987. **8**(4): p. 345-6.
35. Khachaturian, Z.S., *Calcium hypothesis of Alzheimer's disease and brain aging*. Ann N Y Acad Sci, 1994. **747**: p. 1-11.
36. Green, K.N., I.F. Smith, and F.M. Laferla, *Role of calcium in the pathogenesis of Alzheimer's disease and transgenic models*. Subcell Biochem, 2007. **45**: p. 507-21.
37. Bullock, R., *Efficacy and safety of memantine in moderate-to-severe Alzheimer disease: the evidence to date*. Alzheimer Dis Assoc Disord, 2006. **20**(1): p. 23-9.
38. Bezprozvanny, I. and M.P. Mattson, *Neuronal calcium mishandling and the pathogenesis of Alzheimer's disease*. Trends Neurosci, 2008. **31**(9): p. 454-63.
39. Hayley, M., et al., *Calcium enhances the proteolytic activity of BACE1: An in vitro biophysical and biochemical characterization of the BACE1-calcium interaction*. Biochim Biophys Acta, 2009. **1788**(9): p. 1933-8.
40. Nelson, O., et al., *Familial Alzheimer's disease mutations in presenilins: effects on endoplasmic reticulum calcium homeostasis and correlation with clinical phenotypes*. J Alzheimers Dis, 2010. **21**(3): p. 781-93.
41. Stutzmann, G.E., *The pathogenesis of Alzheimers disease is it a lifelong "calciumopathy"?* Neuroscientist, 2007. **13**(5): p. 546-59.
42. Thibault, O., J.C. Gant, and P.W. Landfield, *Expansion of the calcium hypothesis of brain aging and Alzheimer's disease: minding the store*. Aging Cell, 2007. **6**(3): p. 307-17.
43. Disterhoft, J.F. and M.M. Oh, *Alterations in intrinsic neuronal excitability during normal aging*. Aging Cell, 2007. **6**(3): p. 327-36.
44. Foster, T.C., *Calcium homeostasis and modulation of synaptic plasticity in the aged brain*. Aging Cell, 2007. **6**(3): p. 319-25.
45. Gant, J.C., et al., *Early and simultaneous emergence of multiple hippocampal biomarkers of aging is mediated by Ca<sup>2+</sup>-induced Ca<sup>2+</sup> release*. J Neurosci, 2006. **26**(13): p. 3482-90.

46. Jaworska, A., et al., *Analysis of calcium homeostasis in fresh lymphocytes from patients with sporadic Alzheimer's disease or mild cognitive impairment*. *Biochim Biophys Acta*, 2013. **1833**(7): p. 1692-9.
47. Ripova, D., et al., *Alterations in calcium homeostasis as biological marker for mild Alzheimer's disease?* *Physiol Res*, 2004. **53**(4): p. 449-52.
48. Kelliher, M., et al., *Alterations in the ryanodine receptor calcium release channel correlate with Alzheimer's disease neurofibrillary and beta-amyloid pathologies*. *Neuroscience*, 1999. **92**(2): p. 499-513.
49. Green, K.N. and F.M. LaFerla, *Linking calcium to A $\beta$  and Alzheimer's disease*. *Neuron*, 2008. **59**(2): p. 190-4.
50. Pierrot, N., et al., *Calcium-mediated transient phosphorylation of tau and amyloid precursor protein followed by intraneuronal amyloid-beta accumulation*. *J Biol Chem*, 2006. **281**(52): p. 39907-14.
51. Selkoe, D.J., *Alzheimer's disease is a synaptic failure*. *Science*, 2002. **298**(5594): p. 789-91.
52. Camandola, S. and M.P. Mattson, *Aberrant subcellular neuronal calcium regulation in aging and Alzheimer's disease*. *Biochim Biophys Acta*, 2011. **1813**(5): p. 965-73.
53. Gomez-Isla, T., et al., *Profound loss of layer II entorhinal cortex neurons occurs in very mild Alzheimer's disease*. *J Neurosci*, 1996. **16**(14): p. 4491-500.
54. Terry, R.D., et al., *Physical basis of cognitive alterations in Alzheimer's disease: synapse loss is the major correlate of cognitive impairment*. *Ann Neurol*, 1991. **30**(4): p. 572-80.
55. Hardy, J. and D.J. Selkoe, *The amyloid hypothesis of Alzheimer's disease: progress and problems on the road to therapeutics*. *Science*, 2002. **297**(5580): p. 353-6.
56. O'Brien, R.J. and P.C. Wong, *Amyloid precursor protein processing and Alzheimer's disease*. *Annu Rev Neurosci*, 2011. **34**: p. 185-204.
57. Goate, A. and J. Hardy, *Twenty years of Alzheimer's disease-causing mutations*. *J Neurochem*, 2012. **120 Suppl 1**: p. 3-8.
58. Castellani, R.J. and M.A. Smith, *Compounding artefacts with uncertainty, and an amyloid cascade hypothesis that is 'too big to fail'*. *J Pathol*, 2011. **224**(2): p. 147-52.

59. De Strooper, B., *Proteases and proteolysis in Alzheimer disease: a multifactorial view on the disease process*. *Physiol Rev*, 2010. **90**(2): p. 465-94.
60. Zhang, Y.W., et al., *APP processing in Alzheimer's disease*. *Mol Brain*, 2011. **4**: p. 3.
61. Lichtenthaler, S.F., C. Haass, and H. Steiner, *Regulated intramembrane proteolysis - lessons from amyloid precursor protein processing*. *J Neurochem*, 2011. **117**(5): p. 779-96.
62. Thinakaran, G. and E.H. Koo, *Amyloid precursor protein trafficking, processing, and function*. *J Biol Chem*, 2008. **283**(44): p. 29615-9.
63. Bergmans, B.A. and B. De Strooper, *gamma-secretases: from cell biology to therapeutic strategies*. *Lancet Neurol*, 2010. **9**(2): p. 215-26.
64. Chasseigneaux, S. and B. Allinquant, *Functions of Abeta, sAPPalpha and sAPPbeta : similarities and differences*. *J Neurochem*, 2012. **120 Suppl 1**: p. 99-108.
65. Guo, Q., et al., *APP physiological and pathophysiological functions: insights from animal models*. *Cell Res*, 2012. **22**(1): p. 78-89.
66. Benilova, I., E. Karran, and B. De Strooper, *The toxic Abeta oligomer and Alzheimer's disease: an emperor in need of clothes*. *Nat Neurosci*, 2012. **15**(3): p. 349-57.
67. Sperling, R.A., C.R. Jack, Jr., and P.S. Aisen, *Testing the right target and right drug at the right stage*. *Sci Transl Med*, 2011. **3**(111): p. 111cm33.
68. Kann, O. and R. Kovacs, *Mitochondria and neuronal activity*. *Am J Physiol Cell Physiol*, 2007. **292**(2): p. C641-57.
69. Cheung, K.H., et al., *Mechanism of Ca<sup>2+</sup> disruption in Alzheimer's disease by presenilin regulation of InsP<sub>3</sub> receptor channel gating*. *Neuron*, 2008. **58**(6): p. 871-83.
70. Demuro, A., I. Parker, and G.E. Stutzmann, *Calcium signaling and amyloid toxicity in Alzheimer disease*. *J Biol Chem*, 2010. **285**(17): p. 12463-8.
71. Dreses-Werringloer, U., et al., *A polymorphism in CALHM1 influences Ca<sup>2+</sup> homeostasis, Abeta levels, and Alzheimer's disease risk*. *Cell*, 2008. **133**(7): p. 1149-61.
72. Green, K.N., et al., *SERCA pump activity is physiologically regulated by presenilin and regulates amyloid beta production*. *J Cell Biol*, 2008. **181**(7): p. 1107-16.

73. Isaacs, A.M., et al., *Acceleration of amyloid beta-peptide aggregation by physiological concentrations of calcium*. J Biol Chem, 2006. **281**(38): p. 27916-23.
74. Pierrot, N., et al., *Intraneuronal amyloid-beta1-42 production triggered by sustained increase of cytosolic calcium concentration induces neuronal death*. J Neurochem, 2004. **88**(5): p. 1140-50.
75. Querfurth, H.W., et al., *Caffeine stimulates amyloid beta-peptide release from beta-amyloid precursor protein-transfected HEK293 cells*. J Neurochem, 1997. **69**(4): p. 1580-91.
76. Querfurth, H.W. and D.J. Selkoe, *Calcium ionophore increases amyloid beta peptide production by cultured cells*. Biochemistry, 1994. **33**(15): p. 4550-61.
77. Mattson, M.P., et al., *beta-Amyloid peptides destabilize calcium homeostasis and render human cortical neurons vulnerable to excitotoxicity*. J Neurosci, 1992. **12**(2): p. 376-89.
78. Kawahara, M., M. Negishi-Kato, and Y. Sadakane, *Calcium dyshomeostasis and neurotoxicity of Alzheimer's beta-amyloid protein*. Expert Rev Neurother, 2009. **9**(5): p. 681-93.
79. Arispe, N., E. Rojas, and H.B. Pollard, *Alzheimer disease amyloid beta protein forms calcium channels in bilayer membranes: blockade by tromethamine and aluminum*. Proc Natl Acad Sci U S A, 1993. **90**(2): p. 567-71.
80. Lin, H., R. Bhatia, and R. Lal, *Amyloid beta protein forms ion channels: implications for Alzheimer's disease pathophysiology*. FASEB J, 2001. **15**(13): p. 2433-44.
81. Sepulveda, F.J., et al., *Synaptotoxicity of Alzheimer beta amyloid can be explained by its membrane perforating property*. PLoS One, 2010. **5**(7): p. e11820.
82. Kaye, R., et al., *Permeabilization of lipid bilayers is a common conformation-dependent activity of soluble amyloid oligomers in protein misfolding diseases*. J Biol Chem, 2004. **279**(45): p. 46363-6.
83. Sokolov, Y., et al., *Soluble amyloid oligomers increase bilayer conductance by altering dielectric structure*. J Gen Physiol, 2006. **128**(6): p. 637-47.
84. Butterfield, D.A., et al., *beta-Amyloid peptide free radical fragments initiate synaptosomal lipoperoxidation in a sequence-specific fashion: implications to Alzheimer's disease*. Biochem Biophys Res Commun, 1994. **200**(2): p. 710-5.

85. Mark, R.J., et al., *Amyloid beta-peptide impairs ion-motive ATPase activities: evidence for a role in loss of neuronal Ca<sup>2+</sup> homeostasis and cell death*. J Neurosci, 1995. **15**(9): p. 6239-49.
86. Ye, C., et al., *Amyloid beta-protein induced electrophysiological changes are dependent on aggregation state: N-methyl-D-aspartate (NMDA) versus non-NMDA receptor/channel activation*. Neurosci Lett, 2004. **366**(3): p. 320-5.
87. De Felice, F.G., et al., *Abeta oligomers induce neuronal oxidative stress through an N-methyl-D-aspartate receptor-dependent mechanism that is blocked by the Alzheimer drug memantine*. J Biol Chem, 2007. **282**(15): p. 11590-601.
88. Nimmrich, V., et al., *Amyloid beta oligomers (A beta(1-42) globulomer) suppress spontaneous synaptic activity by inhibition of P/Q-type calcium currents*. J Neurosci, 2008. **28**(4): p. 788-97.
89. Busche, M.A., et al., *Clusters of hyperactive neurons near amyloid plaques in a mouse model of Alzheimer's disease*. Science, 2008. **321**(5896): p. 1686-9.
90. Kuchibhotla, K.V., et al., *Abeta plaques lead to aberrant regulation of calcium homeostasis in vivo resulting in structural and functional disruption of neuronal networks*. Neuron, 2008. **59**(2): p. 214-25.
91. Briggs, C.A., et al., *beta amyloid peptide plaques fail to alter evoked neuronal calcium signals in APP/PS1 Alzheimer's disease mice*. Neurobiol Aging, 2013. **34**(6): p. 1632-43.
92. Supnet, C., et al., *Amyloid-beta-(1-42) increases ryanodine receptor-3 expression and function in neurons of TgCRND8 mice*. J Biol Chem, 2006. **281**(50): p. 38440-7.
93. Supnet, C., et al., *Up-regulation of the type 3 ryanodine receptor is neuroprotective in the TgCRND8 mouse model of Alzheimer's disease*. J Neurochem, 2010. **112**(2): p. 356-65.
94. Guo, Q., et al., *Increased vulnerability of hippocampal neurons to excitotoxic necrosis in presenilin-1 mutant knock-in mice*. Nat Med, 1999. **5**(1): p. 101-6.
95. Guo, Q., et al., *Alzheimer's presenilin mutation sensitizes neural cells to apoptosis induced by trophic factor withdrawal and amyloid beta-peptide: involvement of calcium and oxyradicals*. J Neurosci, 1997. **17**(11): p. 4212-22.
96. Hertle, D.N. and M.F. Yeckel, *Distribution of inositol-1,4,5-trisphosphate receptor isotypes and ryanodine receptor isotypes during maturation of the rat hippocampus*. Neuroscience, 2007. **150**(3): p. 625-38.

97. Demuro, A. and I. Parker, *Cytotoxicity of intracellular abeta42 amyloid oligomers involves  $Ca^{2+}$  release from the endoplasmic reticulum by stimulated production of inositol trisphosphate*. J Neurosci, 2013. **33**(9): p. 3824-33.
98. Chakroborty, S., et al., *Deviant ryanodine receptor-mediated calcium release resets synaptic homeostasis in presymptomatic 3xTg-AD mice*. J Neurosci, 2009. **29**(30): p. 9458-70.
99. Oddo, S., et al., *Triple-transgenic model of Alzheimer's disease with plaques and tangles: intracellular Abeta and synaptic dysfunction*. Neuron, 2003. **39**(3): p. 409-21.
100. Bruno, A.M., et al., *Altered ryanodine receptor expression in mild cognitive impairment and Alzheimer's disease*. Neurobiol Aging, 2011. **33**(5): p. 1001 e1-6.
101. Wang, Y., et al., *Presenilin-1 mutation impairs cholinergic modulation of synaptic plasticity and suppresses NMDA currents in hippocampus slices*. Neurobiol Aging, 2009. **30**(7): p. 1061-8.
102. Lee, V.M., M. Goedert, and J.Q. Trojanowski, *Neurodegenerative tauopathies*. Annu Rev Neurosci, 2001. **24**: p. 1121-59.
103. Arriagada, P.V., et al., *Neurofibrillary tangles but not senile plaques parallel duration and severity of Alzheimer's disease*. Neurology, 1992. **42**(3 Pt 1): p. 631-9.
104. Bierer, L.M., et al., *Neocortical neurofibrillary tangles correlate with dementia severity in Alzheimer's disease*. Arch Neurol, 1995. **52**(1): p. 81-8.
105. Grundke-Iqbal, I., et al., *Abnormal phosphorylation of the microtubule-associated protein tau (tau) in Alzheimer cytoskeletal pathology*. Proc Natl Acad Sci U S A, 1986. **83**(13): p. 4913-7.
106. Alonso, A.D., et al., *Abnormal phosphorylation of tau and the mechanism of Alzheimer neurofibrillary degeneration: sequestration of microtubule-associated proteins 1 and 2 and the disassembly of microtubules by the abnormal tau*. Proc Natl Acad Sci U S A, 1997. **94**(1): p. 298-303.
107. Iqbal, K., et al., *Tau pathology in Alzheimer disease and other tauopathies*. Biochim Biophys Acta, 2005. **1739**(2-3): p. 198-210.
108. Mandelkow, E.M. and E. Mandelkow, *Tau in Alzheimer's disease*. Trends Cell Biol, 1998. **8**(11): p. 425-7.
109. Salminen, A., et al., *AMP-activated protein kinase: a potential player in Alzheimer's disease*. J Neurochem, 2011. **118**(4): p. 460-74.

110. Ahlijanian, M.K., et al., *Hyperphosphorylated tau and neurofilament and cytoskeletal disruptions in mice overexpressing human p25, an activator of cdk5*. Proc Natl Acad Sci U S A, 2000. **97**(6): p. 2910-5.
111. Li, L., et al., *Memantine inhibits and reverses the Alzheimer type abnormal hyperphosphorylation of tau and associated neurodegeneration*. FEBS Lett, 2004. **566**(1-3): p. 261-9.
112. Chen, X., et al., *Involvement of calpain and p25 of CDK5 pathway in ginsenoside Rb1's attenuation of beta-amyloid peptide25-35-induced tau hyperphosphorylation in cortical neurons*. Brain Res, 2008. **1200**: p. 99-106.
113. Fleming, L.M. and G.V. Johnson, *Modulation of the phosphorylation state of tau in situ: the roles of calcium and cyclic AMP*. Biochem J, 1995. **309** ( Pt 1): p. 41-7.
114. Miller, M.L. and G.V. Johnson, *Transglutaminase cross-linking of the tau protein*. J Neurochem, 1995. **65**(4): p. 1760-70.
115. Vega, I.E., et al., *A novel calcium-binding protein is associated with tau proteins in tauopathy*. J Neurochem, 2008. **106**(1): p. 96-106.
116. Gomez-Ramos, A., et al., *Extracellular tau is toxic to neuronal cells*. FEBS Lett, 2006. **580**(20): p. 4842-50.
117. Chakroborty, S. and G.E. Stutzmann, *Early calcium dysregulation in Alzheimer's disease: setting the stage for synaptic dysfunction*. Sci China Life Sci, 2011. **54**(8): p. 752-62.
118. Chance, B., H. Sies, and A. Boveris, *Hydroperoxide metabolism in mammalian organs*. Physiol Rev, 1979. **59**(3): p. 527-605.
119. Moreira, P.I., M.S. Santos, and C.R. Oliveira, *Alzheimer's disease: a lesson from mitochondrial dysfunction*. Antioxid Redox Signal, 2007. **9**(10): p. 1621-30.
120. Supnet, C. and I. Bezprozvanny, *Neuronal calcium signaling, mitochondrial dysfunction, and Alzheimer's disease*. J Alzheimers Dis, 2010. **20** Suppl 2: p. S487-98.
121. Giacomello, M., et al., *Mitochondrial Ca<sup>2+</sup> as a key regulator of cell life and death*. Cell Death Differ, 2007. **14**(7): p. 1267-74.
122. Billups, B. and I.D. Forsythe, *Presynaptic mitochondrial calcium sequestration influences transmission at mammalian central synapses*. J Neurosci, 2002. **22**(14): p. 5840-7.

123. Giorgi, C., et al., *Structural and functional link between the mitochondrial network and the endoplasmic reticulum*. Int J Biochem Cell Biol, 2009. **41**(10): p. 1817-27.
124. Csordas, G. and G. Hajnoczky, *SR/ER-mitochondrial local communication: calcium and ROS*. Biochim Biophys Acta, 2009. **1787**(11): p. 1352-62.
125. Kanwar, Y.S. and L. Sun, *Shuttling of calcium between endoplasmic reticulum and mitochondria in the renal vasculature*. Am J Physiol Renal Physiol, 2008. **295**(5): p. F1301-2.
126. Cardenas, C., et al., *Essential regulation of cell bioenergetics by constitutive InsP<sub>3</sub> receptor Ca<sup>2+</sup> transfer to mitochondria*. Cell, 2010. **142**(2): p. 270-83.
127. Zampese, E., et al., *Presenilin 2 modulates endoplasmic reticulum (ER)-mitochondria interactions and Ca<sup>2+</sup> cross-talk*. Proc Natl Acad Sci USA, 2011. **108**(7): p. 2777-82.
128. Sanz-Blasco, S., et al., *Mitochondrial Ca<sup>2+</sup> overload underlies Abeta oligomers neurotoxicity providing an unexpected mechanism of neuroprotection by NSAIDs*. PLoS One, 2008. **3**(7): p. e2718.
129. Collins, S. and T. Meyer, *Cell biology: A sensor for calcium uptake*. Nature, 2010. **467**(7313): p. 283.
130. Beal, M.F., *Mitochondria take center stage in aging and neurodegeneration*. Ann Neurol, 2005. **58**(4): p. 495-505.
131. Celsi, F., et al., *Mitochondria, calcium and cell death: a deadly triad in neurodegeneration*. Biochim Biophys Acta, 2009. **1787**(5): p. 335-44.
132. Mattson, M.P., M. Gleichmann, and A. Cheng, *Mitochondria in neuroplasticity and neurological disorders*. Neuron, 2008. **60**(5): p. 748-66.
133. Reddy, P.H., *Amyloid beta, mitochondrial structural and functional dynamics in Alzheimer's disease*. Exp Neurol, 2009. **218**(2): p. 286-92.
134. Santos, R.X., et al., *Alzheimer's disease: diverse aspects of mitochondrial malfunctioning*. Int J Clin Exp Pathol, 2010. **3**(6): p. 570-81.
135. Swerdlow, R.H. and S.M. Khan, *A "mitochondrial cascade hypothesis" for sporadic Alzheimer's disease*. Med Hypotheses, 2004. **63**(1): p. 8-20.
136. Hirai, K., et al., *Mitochondrial abnormalities in Alzheimer's disease*. J Neurosci, 2001. **21**(9): p. 3017-23.



137. Mosconi, L., *Brain glucose metabolism in the early and specific diagnosis of Alzheimer's disease. FDG-PET studies in MCI and AD.* Eur J Nucl Med Mol Imaging, 2005. **32**(4): p. 486-510.
138. Rhein, V., et al., *Amyloid-beta and tau synergistically impair the oxidative phosphorylation system in triple transgenic Alzheimer's disease mice.* Proc Natl Acad Sci U S A, 2009. **106**(47): p. 20057-62.
139. Rui, Y., et al., *Acute impairment of mitochondrial trafficking by beta-amyloid peptides in hippocampal neurons.* J Neurosci, 2006. **26**(41): p. 10480-7.
140. Wang, X., et al., *Impaired balance of mitochondrial fission and fusion in Alzheimer's disease.* J Neurosci, 2009. **29**(28): p. 9090-103.
141. Hauptmann, S., et al., *Mitochondrial dysfunction in sporadic and genetic Alzheimer's disease.* Exp Gerontol, 2006. **41**(7): p. 668-73.
142. Reddy, P.H. and M.F. Beal, *Amyloid beta, mitochondrial dysfunction and synaptic damage: implications for cognitive decline in aging and Alzheimer's disease.* Trends Mol Med, 2008. **14**(2): p. 45-53.
143. Lee, S.H., et al., *Impaired short-term plasticity in mossy fiber synapses caused by mitochondrial dysfunction of dentate granule cells is the earliest synaptic deficit in a mouse model of Alzheimer's disease.* J Neurosci, 2012. **32**(17): p. 5953-63.
144. Takuma, K., et al., *Mitochondrial dysfunction, endoplasmic reticulum stress, and apoptosis in Alzheimer's disease.* J Pharmacol Sci, 2005. **97**(3): p. 312-6.
145. Mungarro-Menchaca, X., et al., *beta-Amyloid peptide induces ultrastructural changes in synaptosomes and potentiates mitochondrial dysfunction in the presence of ryanodine.* J Neurosci Res, 2002. **68**(1): p. 89-96.
146. Baloyannis, S.J., *Dendritic pathology in Alzheimer's disease.* J Neurol Sci, 2009. **283**(1-2): p. 153-7.
147. Dumont, M., M.T. Lin, and M.F. Beal, *Mitochondria and antioxidant targeted therapeutic strategies for Alzheimer's disease.* J Alzheimers Dis, 2010. **20 Suppl 2**: p. S633-43.
148. Moreira, P.I., et al., *Mitochondria: a therapeutic target in neurodegeneration.* Biochim Biophys Acta, 2009. **1802**(1): p. 212-20.
149. Chaturvedi, R.K. and M.F. Beal, *Mitochondrial approaches for neuroprotection.* Ann N Y Acad Sci, 2008. **1147**: p. 395-412.
150. Bezprozvanny, I., *The rise and fall of Dimebon.* Drug News Perspect, 2010. **23**(8): p. 518-23.

151. Giorgetti, M., et al., *Cognition-enhancing properties of Dimebon in a rat novel object recognition task are unlikely to be associated with acetylcholinesterase inhibition or N-methyl-D-aspartate receptor antagonism*. J Pharmacol Exp Ther, 2010. **333**(3): p. 748-57.
152. Zhang, S., et al., *Dimebon (latrepirdine) enhances mitochondrial function and protects neuronal cells from death*. J Alzheimers Dis, 2010. **21**(2): p. 389-402.
153. Lawrence, A.D. and B.J. Sahakian, *The cognitive psychopharmacology of Alzheimer's disease: focus on cholinergic systems*. Neurochem Res, 1998. **23**(5): p. 787-94.
154. Yiannopoulou, K.G. and S.G. Papageorgiou, *Current and future treatments for Alzheimer's disease*. Ther Adv Neurol Disord, 2013. **6**(1): p. 19-33.
155. Alfirevic, A., et al., *Tacrine-induced liver damage: an analysis of 19 candidate genes*. Pharmacogenet Genomics, 2007. **17**(12): p. 1091-100.
156. Cummings, J., et al., *Effect of donepezil on cognition in severe Alzheimer's disease: a pooled data analysis*. J Alzheimers Dis, 2010. **21**(3): p. 843-51.
157. Ghosh, A.K., M. Brindisi, and J. Tang, *Developing beta-secretase inhibitors for treatment of Alzheimer's disease*. J Neurochem, 2012. **120 Suppl 1**: p. 71-83.
158. Tomita, T., *Secretase inhibitors and modulators for Alzheimer's disease treatment*. Expert Rev Neurother, 2009. **9**(5): p. 661-79.
159. Imbimbo, B.P. and G.A. Giardina, *gamma-secretase inhibitors and modulators for the treatment of Alzheimer's disease: disappointments and hopes*. Curr Top Med Chem, 2011. **11**(12): p. 1555-70.
160. Basi, G.S., et al., *Amyloid precursor protein selective gamma-secretase inhibitors for treatment of Alzheimer's disease*. Alzheimers Res Ther, 2010. **2**(6): p. 36.
161. Weggen, S., et al., *A subset of NSAIDs lower amyloidogenic Abeta42 independently of cyclooxygenase activity*. Nature, 2001. **414**(6860): p. 212-6.
162. Salomone, S., et al., *New pharmacological strategies for treatment of Alzheimer's disease: focus on disease modifying drugs*. Br J Clin Pharmacol, 2011. **73**(4): p. 504-17.
163. Fahrenholz, F. and R. Postina, *Alpha-secretase activation--an approach to Alzheimer's disease therapy*. Neurodegener Dis, 2006. **3**(4-5): p. 255-61.
164. Marcade, M., et al., *Etazolate, a neuroprotective drug linking GABA(A) receptor pharmacology to amyloid precursor protein processing*. J Neurochem, 2008. **106**(1): p. 392-404.

165. Gauthier, S., et al., *Effect of tramiprosate in patients with mild-to-moderate Alzheimer's disease: exploratory analyses of the MRI sub-group of the Alphase study*. J Nutr Health Aging, 2009. **13**(6): p. 550-7.
166. Adlard, P.A., et al., *Rapid restoration of cognition in Alzheimer's transgenic mice with 8-hydroxy quinoline analogs is associated with decreased interstitial Abeta*. Neuron, 2008. **59**(1): p. 43-55.
167. Fenili, D., et al., *Properties of scyllo-inositol as a therapeutic treatment of AD-like pathology*. J Mol Med (Berl), 2007. **85**(6): p. 603-11.
168. Salloway, S., et al., *A phase 2 randomized trial of ELND005, scyllo-inositol, in mild to moderate Alzheimer disease*. Neurology, 2011. **77**(13): p. 1253-62.
169. Town, T., *Alternative Abeta immunotherapy approaches for Alzheimer's disease*. CNS Neurol Disord Drug Targets, 2009. **8**(2): p. 114-27.
170. Check, E., *Nerve inflammation halts trial for Alzheimer's drug*. Nature, 2002. **415**(6871): p. 462.
171. Morgan, D., *Immunotherapy for Alzheimer's disease*. J Intern Med, 2010. **269**(1): p. 54-63.
172. Gilman, S., et al., *Clinical effects of Abeta immunization (AN1792) in patients with AD in an interrupted trial*. Neurology, 2005. **64**(9): p. 1553-62.
173. Brody, D.L. and D.M. Holtzman, *Active and passive immunotherapy for neurodegenerative disorders*. Annu Rev Neurosci, 2008. **31**: p. 175-93.
174. Mudher, A. and S. Lovestone, *Alzheimer's disease-do tauists and baptists finally shake hands?* Trends Neurosci, 2002. **25**(1): p. 22-6.
175. Forlenza, O.V., et al., *Disease-modifying properties of long-term lithium treatment for amnesic mild cognitive impairment: randomised controlled trial*. Br J Psychiatry, 2011. **198**(5): p. 351-6.
176. Wischik, C. and R. Staff, *Challenges in the conduct of disease-modifying trials in AD: practical experience from a phase 2 trial of Tau-aggregation inhibitor therapy*. J Nutr Health Aging, 2009. **13**(4): p. 367-9.
177. Gura, T., *Hope in Alzheimer's fight emerges from unexpected places*. Nat Med, 2008. **14**(9): p. 894.
178. Martinez, A. and D.I. Perez, *GSK-3 inhibitors: a ray of hope for the treatment of Alzheimer's disease?* J Alzheimers Dis, 2008. **15**(2): p. 181-91.

179. Boutajangout, A., D. Quartermain, and E.M. Sigurdsson, *Immunotherapy targeting pathological tau prevents cognitive decline in a new tangle mouse model*. J Neurosci, 2010. **30**(49): p. 16559-66.
180. Chai, X., et al., *Passive immunization with anti-Tau antibodies in two transgenic models: reduction of Tau pathology and delay of disease progression*. J Biol Chem, 2011. **286**(39): p. 34457-67.
181. Troquier, L., et al., *Targeting phospho-Ser422 by active Tau Immunotherapy in the THYTau22 mouse model: a suitable therapeutic approach*. Curr Alzheimer Res, 2012. **9**(4): p. 397-405.
182. Goodison, W.V., V. Frisardi, and P.G. Kehoe, *Calcium channel blockers and Alzheimer's disease: potential relevance in treatment strategies of metabolic syndrome*. J Alzheimers Dis, 2012. **30 Suppl 2**: p. S269-82.
183. Cosman, K.M., L.L. Boyle, and A.P. Porsteinsson, *Memantine in the treatment of mild-to-moderate Alzheimer's disease*. Expert Opin Pharmacother, 2007. **8**(2): p. 203-14.
184. Raina, P., et al., *Effectiveness of cholinesterase inhibitors and memantine for treating dementia: evidence review for a clinical practice guideline*. Ann Intern Med, 2008. **148**(5): p. 379-97.
185. Blanchard, A.P., G. Guillemette, and G. Boulay, *Memantine potentiates agonist-induced Ca<sup>2+</sup> responses in HEK 293 cells*. Cell Physiol Biochem, 2008. **22**(1-4): p. 205-14.
186. Mony, L., et al., *Allosteric modulators of NR2B-containing NMDA receptors: molecular mechanisms and therapeutic potential*. Br J Pharmacol, 2009. **157**(8): p. 1301-17.
187. Parameshwaran, K., et al., *Amyloid beta-peptide Abeta(1-42) but not Abeta(1-40) attenuates synaptic AMPA receptor function*. Synapse, 2007. **61**(6): p. 367-74.
188. Chang, E.H., et al., *AMPA receptor downscaling at the onset of Alzheimer's disease pathology in double knockin mice*. Proc Natl Acad Sci U S A, 2006. **103**(9): p. 3410-5.
189. Flood, D.G., et al., *FAD mutant PS-1 gene-targeted mice: increased A beta 42 and A beta deposition without APP overproduction*. Neurobiol Aging, 2002. **23**(3): p. 335-48.
190. Chappell, A.S., et al., *AMPA potentiator treatment of cognitive deficits in Alzheimer disease*. Neurology, 2007. **68**(13): p. 1008-12.

191. Grigorev, V.V., O.A. Dranyi, and S.O. Bachurin, *Comparative study of action mechanisms of dimebon and memantine on AMPA- and NMDA-subtypes glutamate receptors in rat cerebral neurons*. Bull Exp Biol Med, 2003. **136**(5): p. 474-7.
192. Ueda, K., et al., *Amyloid beta protein potentiates  $Ca^{2+}$  influx through L-type voltage-sensitive  $Ca^{2+}$  channels: a possible involvement of free radicals*. J Neurochem, 1997. **68**(1): p. 265-71.
193. Anekonda, T.S. and J.F. Quinn, *Calcium channel blocking as a therapeutic strategy for Alzheimer's disease: the case for isradipine*. Biochim Biophys Acta, 2011. **1812**(12): p. 1584-90.
194. Lopez-Arrieta, J.M. and J. Birks, *Nimodipine for primary degenerative, mixed and vascular dementia*. Cochrane Database Syst Rev, 2002(3): p. CD000147.
195. Melnikova, I., *Therapies for Alzheimer's disease*. Nat Rev Drug Discov, 2007. **6**(5): p. 341-2.
196. Hung, C.H., Y.S. Ho, and R.C. Chang, *Modulation of mitochondrial calcium as a pharmacological target for Alzheimer's disease*. Ageing Res Rev, 2010. **9**(4): p. 447-56.
197. Yan, Z., et al., *Roscovitine: a novel regulator of P/Q-type calcium channels and transmitter release in central neurons*. J Physiol, 2002. **540**(Pt 3): p. 761-70.
198. Ferreira, E., C.R. Oliveira, and C. Pereira, *Involvement of endoplasmic reticulum  $Ca^{2+}$  release through ryanodine and inositol 1,4,5-triphosphate receptors in the neurotoxic effects induced by the amyloid-beta peptide*. J Neurosci Res, 2004. **76**(6): p. 872-80.
199. Buxbaum, J.D., et al., *Calcium regulates processing of the Alzheimer amyloid protein precursor in a protein kinase C-independent manner*. Proc Natl Acad Sci U S A, 1994. **91**(10): p. 4489-93.
200. Cedazo-Minguez, A., et al., *The presenilin 1 deltaE9 mutation gives enhanced basal phospholipase C activity and a resultant increase in intracellular calcium concentrations*. J Biol Chem, 2002. **277**(39): p. 36646-55.
201. Muller, M., et al., *Constitutive cAMP response element binding protein (CREB) activation by Alzheimer's disease presenilin-driven inositol trisphosphate receptor ( $InsP_3R$ )  $Ca^{2+}$  signaling*. Proc Natl Acad Sci U S A, 2011. **108**(32): p. 13293-8.

202. Chan, S.L., et al., *Presenilin-1 mutations increase levels of ryanodine receptors and calcium release in PC12 cells and cortical neurons*. J Biol Chem, 2000. **275**(24): p. 18195-200.
203. Chakroborty, S., et al., *Stabilizing ER Ca<sup>2+</sup> Channel Function as an Early Preventative Strategy for Alzheimer's Disease*. PLoS One, 2012. **7**(12): p. e52056.
204. Oules, B., et al., *Ryanodine receptor blockade reduces amyloid-beta load and memory impairments in Tg2576 mouse model of Alzheimer disease*. J Neurosci, 2012. **32**(34): p. 11820-11834.
205. Peng, J., et al., *Dantrolene ameliorates cognitive decline and neuropathology in Alzheimer triple transgenic mice*. Neurosci Lett, 2012. **516**(2): p. 274-9.
206. Radde, R., et al., *Abeta42-driven cerebral amyloidosis in transgenic mice reveals early and robust pathology*. EMBO Rep, 2006. **7**(9): p. 940-6.
207. Zhang, H., et al., *Role of presenilins in neuronal calcium homeostasis*. J Neurosci, 2010. **30**(25): p. 8566-80.
208. Mackrill, J.J., *Ryanodine receptor calcium channels and their partners as drug targets*. Biochem Pharmacol, 2010. **79**(11): p. 1535-43.
209. Mank, M. and O. Griesbeck, *Genetically encoded calcium indicators*. Chem Rev, 2008. **108**(5): p. 1550-64.
210. Zhao, Y., et al., *An expanded palette of genetically encoded Ca<sup>2+</sup> indicators*. Science, 2011. **333**(6051): p. 1888-91.
211. Miyawaki, A., et al., *Fluorescent indicators for Ca<sup>2+</sup> based on green fluorescent proteins and calmodulin*. Nature, 1997. **388**(6645): p. 882-7.
212. Nagai, T., et al., *Expanded dynamic range of fluorescent indicators for Ca<sup>2+</sup> by circularly permuted yellow fluorescent proteins*. Proc Natl Acad Sci U S A, 2004. **101**(29): p. 10554-9.
213. Garippa, R.J., et al., *High-throughput confocal microscopy for beta-arrestin-green fluorescent protein translocation G protein-coupled receptor assays using the Evotec Opera*. Methods Enzymol, 2006. **414**: p. 99-120.
214. De Strooper, B., T. Iwatsubo, and M.S. Wolfe, *Presenilins and gamma-Secretase: Structure, Function, and Role in Alzheimer Disease*. Cold Spring Harb Perspect Med, 2012. **2**(1): p. a006304.
215. Hass, M.R., et al., *Presenilin: RIP and beyond*. Semin Cell Dev Biol, 2009. **20**(2): p. 201-10.

216. Sherrington, R., et al., *Cloning of a gene bearing missense mutations in early-onset familial Alzheimer's disease*. Nature, 1995. **375**(6534): p. 754-60.
217. Levitan, D. and I. Greenwald, *Facilitation of lin-12-mediated signalling by sel-12, a Caenorhabditis elegans S182 Alzheimer's disease gene*. Nature, 1995. **377**(6547): p. 351-4.
218. Brunkan, A.L. and A.M. Goate, *Presenilin function and gamma-secretase activity*. J Neurochem, 2005. **93**(4): p. 769-92.
219. Sobhanifar, S., et al., *Structural investigation of the C-terminal catalytic fragment of presenilin 1*. Proc Natl Acad Sci U S A, 2010. **107**(21): p. 9644-9.
220. Ratovitski, T., et al., *Endoproteolytic processing and stabilization of wild-type and mutant presenilin*. J Biol Chem, 1997. **272**(39): p. 24536-41.
221. Kim, T.W., et al., *Endoproteolytic cleavage and proteasomal degradation of presenilin 2 in transfected cells*. J Biol Chem, 1997. **272**(17): p. 11006-10.
222. Ito, E., et al., *Internal Ca<sup>2+</sup> mobilization is altered in fibroblasts from patients with Alzheimer disease*. Proc Natl Acad Sci U S A, 1994. **91**(2): p. 534-8.
223. Guo, Q., et al., *Alzheimer's PS-1 mutation perturbs calcium homeostasis and sensitizes PC12 cells to death induced by amyloid beta-peptide*. Neuroreport, 1996. **8**(1): p. 379-83.
224. Leissring, M.A., et al., *Alzheimer's presenilin-1 mutation potentiates inositol 1,4,5-trisphosphate-mediated calcium signaling in Xenopus oocytes*. J Neurochem, 1999. **72**(3): p. 1061-8.
225. Schneider, I., et al., *Mutant presenilins disturb neuronal calcium homeostasis in the brain of transgenic mice, decreasing the threshold for excitotoxicity and facilitating long-term potentiation*. J Biol Chem, 2001. **276**(15): p. 11539-44.
226. Stutzmann, G.E., et al., *Dysregulated IP<sub>3</sub> signaling in cortical neurons of knock-in mice expressing an Alzheimer's-linked mutation in presenilin1 results in exaggerated Ca<sup>2+</sup> signals and altered membrane excitability*. J Neurosci, 2004. **24**(2): p. 508-13.
227. Kasri, N.N., et al., *Up-regulation of inositol 1,4,5-trisphosphate receptor type 1 is responsible for a decreased endoplasmic-reticulum Ca<sup>2+</sup> content in presenilin double knock-out cells*. Cell Calcium, 2006. **40**(1): p. 41-51.
228. Tu, H., et al., *Presenilins form ER Ca<sup>2+</sup> leak channels, a function disrupted by familial Alzheimer's disease-linked mutations*. Cell, 2006. **126**(5): p. 981-93.

229. Etcheberrigaray, R., et al., *Calcium responses in fibroblasts from asymptomatic members of Alzheimer's disease families*. Neurobiol Dis, 1998. **5**(1): p. 37-45.
230. Stutzmann, G.E., et al., *Enhanced ryanodine receptor recruitment contributes to  $Ca^{2+}$  disruptions in young, adult, and aged Alzheimer's disease mice*. J Neurosci, 2006. **26**(19): p. 5180-9.
231. Nelson, O., et al., *Mutagenesis mapping of the presenilin 1 calcium leak conductance pore*. J Biol Chem, 2011. **286**(25): p. 22339-47.
232. Shilling, D., et al., *Lack of evidence for presenilins as endoplasmic reticulum  $Ca^{2+}$  leak channels*. J Biol Chem, 2012. **287**(14): p. 10933-44.
233. Brunello, L., et al., *Presenilin-2 dampens intracellular  $Ca^{2+}$  stores by increasing  $Ca^{2+}$  leakage and reducing  $Ca^{2+}$  uptake*. J Cell Mol Med, 2009. **13**(9B): p. 3358-69.
234. McCombs, J.E., E.A. Gibson, and A.E. Palmer, *Using a genetically targeted sensor to investigate the role of presenilin-1 in ER  $Ca^{2+}$  levels and dynamics*. Mol Biosyst, 2010. **6**(9): p. 1640-9.
235. Cheung, K.H., et al., *Gain-of-function enhancement of  $IP_3$  receptor modal gating by familial Alzheimer's disease-linked presenilin mutants in human cells and mouse neurons*. Sci Signal, 2010. **3**(114): p. ra22.
236. Hayrapetyan, V., et al., *The N-terminus of presenilin-2 increases single channel activity of brain ryanodine receptors through direct protein-protein interaction*. Cell Calcium, 2008. **44**(5): p. 507-18.
237. Zhang, C., et al., *Presenilins are essential for regulating neurotransmitter release*. Nature, 2009. **460**(7255): p. 632-6.
238. Saura, C.A., et al., *Loss of presenilin function causes impairments of memory and synaptic plasticity followed by age-dependent neurodegeneration*. Neuron, 2004. **42**(1): p. 23-36.
239. Pratt, K.G., et al., *Presenilin 1 regulates homeostatic synaptic scaling through Akt signaling*. Nat Neurosci, 2011. **14**(9): p. 1112-4.
240. Jung, C.K., et al., *Role of presenilin 1 in structural plasticity of cortical dendritic spines in vivo*. J Neurochem, 2011. **119**(5): p. 1064-73.
241. Buxbaum, J.D., et al., *Calsenilin: a calcium-binding protein that interacts with the presenilins and regulates the levels of a presenilin fragment*. Nat Med, 1998. **4**(10): p. 1177-81.



242. Stabler, S.M., et al., *A myristoylated calcium-binding protein that preferentially interacts with the Alzheimer's disease presenilin 2 protein*. J Cell Biol, 1999. **145**(6): p. 1277-92.
243. Leissring, M.A., et al., *Calsenilin reverses presenilin-mediated enhancement of calcium signaling*. Proc Natl Acad Sci U S A, 2000. **97**(15): p. 8590-3.
244. Lee, S.Y., et al., *PS2 mutation increases neuronal cell vulnerability to neurotoxicants through activation of caspase-3 by enhancing of ryanodine receptor-mediated calcium release*. FASEB J, 2006. **20**(1): p. 151-3.
245. Yoo, A.S., et al., *Presenilin-mediated modulation of capacitative calcium entry*. Neuron, 2000. **27**(3): p. 561-72.
246. Herms, J., et al., *Capacitive calcium entry is directly attenuated by mutant presenilin-1, independent of the expression of the amyloid precursor protein*. J Biol Chem, 2003. **278**(4): p. 2484-9.
247. Bojarski, L., et al., *Presenilin-dependent expression of STIM proteins and dysregulation of capacitative Ca<sup>2+</sup> entry in familial Alzheimer's disease*. Biochim Biophys Acta, 2009. **1793**(6): p. 1050-7.
248. Hardy, J., *A hundred years of Alzheimer's disease research*. Neuron, 2006. **52**(1): p. 3-13.
249. Van Broeckhoven, C., *Presenilins and Alzheimer disease*. Nat Genet, 1995. **11**(3): p. 230-2.
250. Wolfe, M.S. and C. Haass, *The Role of presenilins in gamma-secretase activity*. J Biol Chem, 2001. **276**(8): p. 5413-6.
251. De Strooper, B. and W. Annaert, *Novel research horizons for presenilins and gamma-secretases in cell biology and disease*. Annu Rev Cell Dev Biol, 2010. **26**: p. 235-60.
252. De Strooper, B., et al., *Deficiency of presenilin-1 inhibits the normal cleavage of amyloid precursor protein*. Nature, 1998. **391**(6665): p. 387-90.
253. Mattson, M.P., *ER calcium and Alzheimer's disease: in a state of flux*. Sci Signal, 2010. **3**(114): p. pe10.
254. Annaert, W.G., et al., *Presenilin 1 controls gamma-secretase processing of amyloid precursor protein in pre-golgi compartments of hippocampal neurons*. J Cell Biol, 1999. **147**(2): p. 277-94.
255. Honarnejad, K. and J. Herms, *Presenilins: Role in calcium homeostasis*. Int J Biochem Cell Biol, 2012. **44**(11): p. 1983-1986.

256. Nelson, O., et al., *Familial Alzheimer disease-linked mutations specifically disrupt  $Ca^{2+}$  leak function of presenilin 1*. J Clin Invest, 2007. **117**(5): p. 1230-9.
257. Rybalchenko, V., et al., *The cytosolic N-terminus of presenilin-1 potentiates mouse ryanodine receptor single channel activity*. Int J Biochem Cell Biol, 2008. **40**(1): p. 84-97.
258. Jin, H., et al., *Presenilin-1 holoprotein is an interacting partner of sarco endoplasmic reticulum calcium-ATPase and confers resistance to endoplasmic reticulum stress*. J Alzheimers Dis, 2010. **20**(1): p. 261-73.
259. Giacomello, M., et al., *Reduction of  $Ca^{2+}$  stores and capacitative  $Ca^{2+}$  entry is associated with the familial Alzheimer's disease presenilin-2 T122R mutation and anticipates the onset of dementia*. Neurobiol Dis, 2005. **18**(3): p. 638-48.
260. Saito, T., et al., *Potent amyloidogenicity and pathogenicity of A $\beta$ 43*. Nat Neurosci, 2011. **14**(8): p. 1023-32.
261. Takahashi, H., et al., *Impaired proteolytic processing of presenilin-1 in chromosome 14-linked familial Alzheimer's disease patient lymphocytes*. Neurosci Lett, 1999. **260**(2): p. 121-4.
262. Prokop, S., et al., *Requirement of PEN-2 for stabilization of the presenilin N-/C-terminal fragment heterodimer within the gamma-secretase complex*. J Biol Chem, 2004. **279**(22): p. 23255-61.
263. Walter, J., et al., *The Alzheimer's disease-associated presenilins are differentially phosphorylated proteins located predominantly within the endoplasmic reticulum*. Mol Med, 1996. **2**(6): p. 673-91.
264. Braak, H., et al., *Staging of Alzheimer disease-associated neurofibrillary pathology using paraffin sections and immunocytochemistry*. Acta Neuropathol, 2006. **112**(4): p. 389-404.
265. Thinakaran, G., et al., *Endoproteolysis of presenilin 1 and accumulation of processed derivatives in vivo*. Neuron, 1996. **17**(1): p. 181-90.
266. Steiner, H., et al., *Amyloidogenic function of the Alzheimer's disease-associated presenilin 1 in the absence of endoproteolysis*. Biochemistry, 1999. **38**(44): p. 14600-5.
267. Fukumori, A., et al., *Three-amino acid spacing of presenilin endoproteolysis suggests a general stepwise cleavage of gamma-secretase-mediated intramembrane proteolysis*. J Neurosci, 2010. **30**(23): p. 7853-62.

268. Haass, C., *Take five - BACE and the gamma-secretase quartet conduct Alzheimer's amyloid beta-peptide generation*. EMBO J, 2004. **23**(3): p. 483-8.
269. Takasugi, N., et al., *The role of presenilin cofactors in the gamma-secretase complex*. Nature, 2003. **422**(6930): p. 438-41.
270. Xie, Z., D.M. Romano, and R.E. Tanzi, *Effects of RNAi-mediated silencing of PEN-2, APH-1a, and nicastrin on wild-type vs FAD mutant forms of presenilin 1*. J Mol Neurosci, 2005. **25**(1): p. 67-77.
271. Supnet, C. and I. Bezprozvanny, *The dysregulation of intracellular calcium in Alzheimer disease*. Cell Calcium, 2010. **47**(2): p. 183-9.
272. Zatti, G., et al., *Presenilin mutations linked to familial Alzheimer's disease reduce endoplasmic reticulum and Golgi apparatus calcium levels*. Cell Calcium, 2006. **39**(6): p. 539-50.
273. Zatti, G., et al., *The presenilin 2 M239I mutation associated with familial Alzheimer's disease reduces Ca<sup>2+</sup> release from intracellular stores*. Neurobiol Dis, 2004. **15**(2): p. 269-78.
274. Michno, K., et al., *Intracellular calcium deficits in Drosophila cholinergic neurons expressing wild type or FAD-mutant presenilin*. PLoS One, 2009. **4**(9): p. e6904.
275. Popescu, B.O., et al., *Gamma-secretase activity of presenilin 1 regulates acetylcholine muscarinic receptor-mediated signal transduction*. J Biol Chem, 2004. **279**(8): p. 6455-64.
276. Leissring, M.A., et al., *Subcellular mechanisms of presenilin-mediated enhancement of calcium signaling*. Neurobiol Dis, 2001. **8**(3): p. 469-78.
277. Kim, J.H., et al., *TGF-beta potentiates airway smooth muscle responsiveness to bradykinin*. Am J Physiol Lung Cell Mol Physiol, 2005. **289**(4): p. L511-20.
278. Liu, T.Y. and S.H. Chueh, *Carbachol but not bradykinin blocks the enkephalin-induced calcium transient in human neuroblastoma SK-N-SH cells*. Chin J Physiol, 1995. **38**(2): p. 75-80.
279. Willars, G.B. and S.R. Nahorski, *Quantitative comparisons of muscarinic and bradykinin receptor-mediated Ins (1,4,5)P<sub>3</sub> accumulation and Ca<sup>2+</sup> signalling in human neuroblastoma cells*. Br J Pharmacol, 1995. **114**(6): p. 1133-42.
280. White, C. and J.G. McGeown, *Carbachol triggers RyR-dependent Ca<sup>2+</sup> release via activation of IP<sub>3</sub> receptors in isolated rat gastric myocytes*. J Physiol, 2002. **542**(Pt 3): p. 725-33.

281. Tong, J., et al., *HEK-293 cells possess a carbachol- and thapsigargin-sensitive intracellular Ca<sup>2+</sup> store that is responsive to stop-flow medium changes and insensitive to caffeine and ryanodine*. *Biochem J*, 1999. **343 Pt 1**: p. 39-44.
282. Wang, J.M., et al., *A transmembrane motif governs the surface trafficking of nicotinic acetylcholine receptors*. *Nat Neurosci*, 2002. **5(10)**: p. 963-70.
283. Leissring, M.A., et al., *A physiologic signaling role for the gamma -secretase-derived intracellular fragment of APP*. *Proc Natl Acad Sci U S A*, 2002. **99(7)**: p. 4697-702.
284. Schor, N.F., *What the halted phase III gamma-secretase inhibitor trial may (or may not) be telling us*. *Ann Neurol*, 2011. **69(2)**: p. 237-9.
285. Coon, A.L., et al., *L-type calcium channels in the hippocampus and cerebellum of Alzheimer's disease brain tissue*. *Neurobiol Aging*, 1999. **20(6)**: p. 597-603.
286. Grynspan, F., et al., *Active site-directed antibodies identify calpain II as an early-appearing and pervasive component of neurofibrillary pathology in Alzheimer's disease*. *Brain Res*, 1997. **763(2)**: p. 145-58.
287. Young, L.T., et al., *Decreased brain [3H]inositol 1,4,5-trisphosphate binding in Alzheimer's disease*. *Neurosci Lett*, 1988. **94(1-2)**: p. 198-202.
288. Borghi, R., et al., *Upregulation of presenilin 1 in brains of sporadic, late-onset Alzheimer's disease*. *J Alzheimers Dis*, 2010. **22(3)**: p. 771-5.
289. Li, T., et al., *Increased expression of PS1 is sufficient to elevate the level and activity of gamma-secretase in vivo*. *PLoS One*, 2011. **6(11)**: p. e28179.
290. Weihl, C.C., et al., *Processing of wild-type and mutant familial Alzheimer's disease-associated presenilin-1 in cultured neurons*. *J Neurochem*, 1999. **73(1)**: p. 31-40.
291. Supnet, C. and I. Bezprozvanny, *Presenilins as endoplasmic reticulum calcium leak channels and Alzheimer's disease pathogenesis*. *Sci China Life Sci*, 2011. **54(8)**: p. 744-51.
292. Beher, D., et al., *In vitro characterization of the presenilin-dependent gamma-secretase complex using a novel affinity ligand*. *Biochemistry*, 2003. **42(27)**: p. 8133-42.
293. Holtzman, D.M., J.C. Morris, and A.M. Goate, *Alzheimer's disease: the challenge of the second century*. *Sci Transl Med*, 2011. **3(77)**: p. 77sr1.
294. Green, K.N., *Calcium in the initiation, progression and as an effector of Alzheimer's disease pathology*. *J Cell Mol Med*, 2009. **13(9A)**: p. 2787-99.

295. Mattson, M.P., M.G. Engle, and B. Rychlik, *Effects of elevated intracellular calcium levels on the cytoskeleton and tau in cultured human cortical neurons*. Mol Chem Neuropathol, 1991. **15**(2): p. 117-42.
296. Patzke, H. and L.H. Tsai, *Calpain-mediated cleavage of the cyclin-dependent kinase-5 activator p39 to p29*. J Biol Chem, 2002. **277**(10): p. 8054-60.
297. Coleman, P.D. and P.J. Yao, *Synaptic slaughter in Alzheimer's disease*. Neurobiol Aging, 2003. **24**(8): p. 1023-7.
298. Scheff, S.W., et al., *Hippocampal synaptic loss in early Alzheimer's disease and mild cognitive impairment*. Neurobiol Aging, 2006. **27**(10): p. 1372-84.
299. Mitterreiter, S., et al., *Bepridil and amiodarone simultaneously target the Alzheimer's disease beta- and gamma-secretase via distinct mechanisms*. J Neurosci, 2010. **30**(26): p. 8974-83.
300. Page, R.M., et al., *Generation of Abeta38 and Abeta42 is independently and differentially affected by familial Alzheimer disease-associated presenilin mutations and gamma-secretase modulation*. J Biol Chem, 2008. **283**(2): p. 677-83.
301. Lipinski, C.A., et al., *Experimental and computational approaches to estimate solubility and permeability in drug discovery and development settings*. Adv Drug Deliv Rev, 2001. **46**(1-3): p. 3-26.
302. Carmichael, J., et al., *Evaluation of a tetrazolium-based semiautomated colorimetric assay: assessment of chemosensitivity testing*. Cancer Res, 1987. **47**(4): p. 936-42.
303. Moreno-Navarrete, J.M., et al., *OCT1 Expression in adipocytes could contribute to increased metformin action in obese subjects*. Diabetes, 2010. **60**(1): p. 168-76.
304. Zhang, J.H., T.D. Chung, and K.R. Oldenburg, *A Simple Statistical Parameter for Use in Evaluation and Validation of High Throughput Screening Assays*. J Biomol Screen, 1999. **4**(2): p. 67-73.
305. Salminen, A. and K. Kaarniranta, *AMP-activated protein kinase (AMPK) controls the aging process via an integrated signaling network*. Ageing Res Rev, 2011. **11**(2): p. 230-41.
306. Hawley, S.A., et al., *Calmodulin-dependent protein kinase kinase-beta is an alternative upstream kinase for AMP-activated protein kinase*. Cell Metab, 2005. **2**(1): p. 9-19.

307. Woods, A., et al., *Ca<sup>2+</sup>/calmodulin-dependent protein kinase kinase-beta acts upstream of AMP-activated protein kinase in mammalian cells*. Cell Metab, 2005. **2**(1): p. 21-33.
308. Tokumitsu, H., et al., *STO-609, a specific inhibitor of the Ca<sup>2+</sup>/calmodulin-dependent protein kinase kinase*. J Biol Chem, 2002. **277**(18): p. 15813-8.
309. Monteith, G.R. and G.S. Bird, *Techniques: high-throughput measurement of intracellular Ca<sup>2+</sup> - back to basics*. Trends Pharmacol Sci, 2005. **26**(4): p. 218-23.
310. Ho, A. and J. Shen, *Presenilins in synaptic function and disease*. Trends Mol Med, 2011. **17**(11): p. 617-24.
311. Landfield, P.W., et al., *Mechanisms of neuronal death in brain aging and Alzheimer's disease: role of endocrine-mediated calcium dyshomeostasis*. J Neurobiol, 1992. **23**(9): p. 1247-60.
312. Bezprozvanny, I., *Calcium signaling and neurodegenerative diseases*. Trends Mol Med, 2009. **15**(3): p. 89-100.
313. Toescu, E.C. and A. Verkhratsky, *The importance of being subtle: small changes in calcium homeostasis control cognitive decline in normal aging*. Aging Cell, 2007. **6**(3): p. 267-73.
314. Herrup, K., *Reimagining Alzheimer's disease--an age-based hypothesis*. J Neurosci, 2010. **30**(50): p. 16755-62.
315. Li, D., et al., *Mutations of presenilin genes in dilated cardiomyopathy and heart failure*. Am J Hum Genet, 2006. **79**(6): p. 1030-9.
316. Chadwick, W., et al., *Therapeutic targeting of the endoplasmic reticulum in Alzheimer's disease*. Curr Alzheimer Res, 2012. **9**(1): p. 110-9.
317. Mantovani, J. and R. Roy, *Re-evaluating the general(ized) roles of AMPK in cellular metabolism*. FEBS Lett, 2011. **585**(7): p. 967-72.
318. Park, S., T.L. Scheffler, and D.E. Gerrard, *Chronic high cytosolic calcium decreases AICAR-induced AMPK activity via calcium/calmodulin activated protein kinase II signaling cascade*. Cell Calcium, 2011. **50**(1): p. 73-83.
319. Reznick, R.M., et al., *Aging-associated reductions in AMP-activated protein kinase activity and mitochondrial biogenesis*. Cell Metab, 2007. **5**(2): p. 151-6.
320. Vingtdeux, V., et al., *AMP-activated protein kinase signaling activation by resveratrol modulates amyloid-beta peptide metabolism*. J Biol Chem, 2010. **285**(12): p. 9100-13.

321. Won, J.S., et al., *Involvement of AMP-activated-protein-kinase (AMPK) in neuronal amyloidogenesis*. *Biochem Biophys Res Commun*, 2010. **399**(4): p. 487-91.
322. Donmez, G., et al., *SIRT1 suppresses beta-amyloid production by activating the alpha-secretase gene ADAM10*. *Cell*, 2010. **142**(2): p. 320-32.
323. Kuhn, P.H., et al., *ADAM10 is the physiologically relevant, constitutive alpha-secretase of the amyloid precursor protein in primary neurons*. *EMBO J*, 2010. **29**(17): p. 3020-32.
324. Lu, J., et al., *Quercetin activates AMP-activated protein kinase by reducing PP2C expression protecting old mouse brain against high cholesterol-induced neurotoxicity*. *J Pathol*, 2010. **222**(2): p. 199-212.
325. Ho, M., et al., *Effect of Metal Chelators on gamma-Secretase Indicates That Calcium and Magnesium Ions Facilitate Cleavage of Alzheimer Amyloid Precursor Substrate*. *Int J Alzheimers Dis*, 2011. **2011**: p. 950932.
326. Labuzek, K., et al., *Metformin increases phagocytosis and acidifies lysosomal/endosomal compartments in AMPK-dependent manner in rat primary microglia*. *Naunyn Schmiedebergs Arch Pharmacol*, 2010. **381**(2): p. 171-86.
327. Vingtdeux, V., et al., *Novel synthetic small-molecule activators of AMPK as enhancers of autophagy and amyloid-beta peptide degradation*. *FASEB J*, 2011. **25**(1): p. 219-31.
328. Greco, S.J., et al., *Leptin inhibits glycogen synthase kinase-3beta to prevent tau phosphorylation in neuronal cells*. *Neurosci Lett*, 2009. **455**(3): p. 191-4.
329. Thornton, C., et al., *AMP-activated protein kinase (AMPK) is a tau kinase, activated in response to amyloid beta-peptide exposure*. *Biochem J*, 2011. **434**(3): p. 503-12.
330. Huang, Y. and L. Mucke, *Alzheimer mechanisms and therapeutic strategies*. *Cell*, 2012. **148**(6): p. 1204-22.
331. Smith, I.F., et al., *Enhanced caffeine-induced Ca<sup>2+</sup> release in the 3xTg-AD mouse model of Alzheimer's disease*. *J Neurochem*, 2005. **94**(6): p. 1711-8.
332. Honarnejad, K., et al., *FRET-based calcium imaging: a tool for high-throughput/content phenotypic drug screening in Alzheimer disease*. *J Biomol Screen*, 2013. **18**(10): p. 1309-20.

333. Lammich, S., et al., *Presenilin-dependent intramembrane proteolysis of CD44 leads to the liberation of its intracellular domain and the secretion of an Abeta-like peptide*. J Biol Chem, 2002. **277**(47): p. 44754-9.
334. Honarnejad, K., et al., *Involvement of presenilin holoprotein upregulation in calcium dyshomeostasis of Alzheimer's disease*. J Cell Mol Med, 2013. **17**(2): p. 293-302.
335. Scaduto, R.C., Jr. and L.W. Grotyohann, *Measurement of mitochondrial membrane potential using fluorescent rhodamine derivatives*. Biophys J, 1999. **76**(1 Pt 1): p. 469-77.
336. Colombo, A., et al., *Constitutive alpha- and beta-secretase cleavages of the amyloid precursor protein are partially coupled in neurons, but not in frequently used cell lines*. Neurobiol Dis, 2012. **49C**: p. 137-147.
337. Honarnejad, K., et al., *Development and implementation of a high-throughput compound screening assay for targeting disrupted ER calcium homeostasis in Alzheimer's disease*. PLoS One, 2013. **8**(11): p. e80645.
338. Lebedzinska, M., et al., *Interactions between the endoplasmic reticulum, mitochondria, plasma membrane and other subcellular organelles*. Int J Biochem Cell Biol, 2009. **41**(10): p. 1805-16.
339. Area-Gomez, E., et al., *Upregulated function of mitochondria-associated ER membranes in Alzheimer disease*. EMBO J, 2012. **31**(21): p. 4106-23.
340. Eckert, G.P., et al., *Mitochondrial dysfunction – a pharmacological target in Alzheimer's disease*. Mol Neurobiol, 2012. **46**(1): p. 136-50.
341. Peters, O.M., et al., *Chronic administration of dimebon ameliorates pathology in TauP301S transgenic mice*. J Alzheimers Dis, 2012.
342. Doody, R.S., et al., *Effect of dimebon on cognition, activities of daily living, behaviour, and global function in patients with mild-to-moderate Alzheimer's disease: a randomised, double-blind, placebo-controlled study*. Lancet, 2008. **372**(9634): p. 207-15.
343. Gauthier, S., *Dimebon improves cognitive function in people with mild to moderate Alzheimer's disease*. Evid Based Ment Health, 2009. **12**(1): p. 21.
344. Eckert, S.H., et al., *Dimebon ameliorates amyloid-beta induced impairments of mitochondrial form and function*. J Alzheimers Dis, 2012. **31**(1): p. 21-32.
345. Kern, A. and C. Behl, *The unsolved relationship of brain aging and late-onset Alzheimer disease*. Biochim Biophys Acta, 2009. **1790**(10): p. 1124-32.



346. Toescu, E.C., A. Verkhratsky, and P.W. Landfield, *Ca<sup>2+</sup> regulation and gene expression in normal brain aging*. Trends Neurosci, 2004. **27**(10): p. 614-20.
347. Puzianowska-Kuznicka, M. and J. Kuznicki, *The ER and ageing II: calcium homeostasis*. Ageing Res Rev, 2009. **8**(3): p. 160-72.
348. Ibarreta, D., R. Parrilla, and M.S. Ayuso, *Altered Ca<sup>2+</sup> homeostasis in lymphoblasts from patients with late-onset Alzheimer disease*. Alzheimer Dis Assoc Disord, 1997. **11**(4): p. 220-7.
349. Ma, Z., et al., *Calcium homeostasis modulator 1 (CALHM1) is the pore-forming subunit of an ion channel that mediates extracellular Ca<sup>2+</sup> regulation of neuronal excitability*. Proc Natl Acad Sci U S A, 2012. **109**(28): p. E1963-71.
350. Decuyper, J.P., et al., *IP<sub>3</sub> receptors, mitochondria, and Ca<sup>2+</sup> signaling: implications for aging*. J Aging Res, 2011. **2011**: p. 920178.
351. Trimmer, P.A., et al., *Abnormal mitochondrial morphology in sporadic Parkinson's and Alzheimer's disease cybrid cell lines*. Exp Neurol, 2000. **162**(1): p. 37-50.
352. Yang, L.B., et al., *Elevated beta-secretase expression and enzymatic activity detected in sporadic Alzheimer disease*. Nat Med, 2003. **9**(1): p. 3-4.
353. Li, R., et al., *Amyloid beta peptide load is correlated with increased beta-secretase activity in sporadic Alzheimer's disease patients*. Proc Natl Acad Sci U S A, 2004. **101**(10): p. 3632-7.
354. Ferreira, E., et al., *An endoplasmic-reticulum-specific apoptotic pathway is involved in prion and amyloid-beta peptides neurotoxicity*. Neurobiol Dis, 2006. **23**(3): p. 669-78.
355. Thatthiah, A. and B. De Strooper, *The role of G protein-coupled receptors in the pathology of Alzheimer's disease*. Nat Rev Neurosci, 2011. **12**(2): p. 73-87.
356. Clader, J.W. and Y. Wang, *Muscarinic receptor agonists and antagonists in the treatment of Alzheimer's disease*. Curr Pharm Des, 2005. **11**(26): p. 3353-61.
357. Tsang, S.W., et al., *Impaired coupling of muscarinic M1 receptors to G-proteins in the neocortex is associated with severity of dementia in Alzheimer's disease*. Neurobiol Aging, 2006. **27**(9): p. 1216-23.
358. Popovics, P. and A.J. Stewart, *Phospholipase C- $\eta$  activity may contribute to Alzheimer's disease-associated calciumopathy*. J Alzheimers Dis, 2012. **30**(4): p. 737-44.

359. Alkadhi, K. and J. Eriksen, *The complex and multifactorial nature of Alzheimer's disease*. *Curr Neuropharmacol*, 2012. **9**(4): p. 586.
360. Akoury, E., et al., *Mechanistic basis of phenothiazine-driven inhibition of Tau aggregation*. *Angew Chem Int Ed Engl*, 2013. **52**(12): p. 3511-5.
361. Darvesh, S., I.R. Macdonald, and E. Martin, *Selectivity of phenothiazine cholinesterase inhibitors for neurotransmitter systems*. *Bioorg Med Chem Lett*, 2013. **23**(13): p. 3822-5.
362. Bulic, B., et al., *Tau protein and tau aggregation inhibitors*. *Neuropharmacology*, 2010. **59**(4-5): p. 276-89.
363. Drachman, D.A., *The amyloid hypothesis, time to move on: Amyloid is the downstream result, not cause, of Alzheimer's disease*. *Alzheimers Dement*, 2014.
364. Takeda, T., et al., *Presenilin 2 regulates the systolic function of heart by modulating Ca<sup>2+</sup> signaling*. *FASEB J*, 2005. **19**(14): p. 2069-71.

## 10 Acknowledgments

On September 7<sup>th</sup> 2001, a 20 year old boy came to Germany to study Biotechnology, hoping that he would become a scientist one day! I still cannot believe that this boy is me and how far life has brought him in the past 11 years! Now that I am about to get my PhD degree, I wish to use this opportunity to thank numerous people who provided their invaluable help, support, love, guidance and mentorship throughout all these years. First and foremost, I wish to express my profoundest gratitude to my parents Rahim and Rouhi, and my brother Saman for their unconditional love and support throughout this entire journey! Without them, this thesis would not have been possible!

Next, I would like to especially thank all those nice people who helped over the last 5 years, during which I was carrying out my PhD project in Munich! Particularly, I would like to thank my supervisor, mentor, motivator, boss, Prof. Dr. Jochen Herms, for giving me the opportunity to carry out this amazing AD drug discovery project in his lab, for constantly supporting and encouraging me during the ups and downs of the project, giving me the freedom to run the project in my way, while at the same time showing his faith in me, which always reassured me that I can successfully complete this challenging task! Last but not least, I wish to appreciate his absolute support outside of the scientific realm, which went way beyond standard employer-employee relationship! I would also like to give a big thank to Prof. Dr. Jacek Kuźnicki, both as a close collaboration partner and also as my external PhD project advisor for his long-lasting support and engagement, and especially for his unique way of being sincere, kind, and at the same time showing the highest level of professionalism! Furthermore, I wish to thank the other members of my thesis advisory committee, Prof. Dr. Stephan Kröger and Dr. Martin Fuhrmann for their support and guidance. I wish to also express my appreciation to Prof. Dr. Franz Bracher and André Gehring for the fruitful collaboration and to other PhD examination committee members, Prof. Dr. Armin Giese and Prof. Dr. Kai Bötzel. I am particularly grateful to the Graduate School of Systemic Neurosciences of LMU, to which I was affiliated as a PhD student, which provided excellent educational and supportive atmosphere!

Of course, it was the greatest pleasure to work together with so many great colleagues and fellow PhD students at the friendly atmosphere of ZNP! I sincerely appreciate all the

helpful comments, remarks and suggestions by each and every of them! In particular, I wish to thank Alex for the close collaboration we maintained which mutually benefitted the success of our PhD projects. Furthermore, I would like to appreciate the invaluable assistance provided by Tobias, Julia, Olga and Eric. My time in Munich would have not been so great without the countless great friends I made here, which I cannot even possibility think of listing them all! However, I would like to express my greatest appreciation to Eli for her constant support, understanding, and motivation over the last four years.

## 11 Curriculum Vitae

---



---

### PERSONAL INFORMATION

---



---

First Name: **Kamran**  
 Last Name: **Honarnejad**  
 Birth Place: **Tehran**  
 Birth Date: **17 June 1981**

---



---

### UNIVERSITY EDUCATION

---



---

2008 – 2014 **PhD in Systemic Neurosciences**  
 Graduate School of Systemic Neurosciences, Munich Center for  
 Neurosciences, Ludwig Maximilian University, Munich, Germany

2006 – 2007 **MSc Biotechnology**  
 Mannheim University of Applied Sciences, Germany

2001 – 2006 **BSc (Hons) in Biotechnology**  
 Mannheim University of Applied Sciences, Germany

---



---

### RESEARCH AND PROFESSIONAL EXPERIENCE

---



---

**PhD Project:** **High-throughput screening and identification of drugs targeting calciumopathy in Alzheimer's disease**

16 Nov. 2007 – 30 Apr. 2013 German Center for Neurodegenerative Diseases (DZNE), Munich site  
 Center for Neuropathology and Prion Research (ZNP)  
 Ludwig Maximilian University of Munich, Germany  
 Prof. Dr. Jochen Herms

**Masters Project:** **Identification and characterization of required factors for active DNA demethylation**

01 Oct. 2006 – 31 May 2007 German Cancer Research Center (DKFZ)  
 Molecular Embryology Department, Heidelberg, Germany  
 Prof. Dr. Christof Niehrs

**Bachelors Project:** **Expression profiling of astroglial-induced neurotransdifferentiation of human multipotent adult progenitor Cells (MAPCs) using MELK**

01 Sep. 2004 – 31 May 2005 Center for Molecular Biology Heidelberg (ZMBH), University of Heidelberg,  
 Germany  
 Prof. Dr. Tobias Hartmann and Prof. Dr. Konrad Beyreuther

**Internships:**

- 09 Jul. 2007 –  
06 Aug. 2007      **Computational studies on functional aspects of chromatin organization in a set of 41 hormone-inducible human genes**  
Ctr. for Genomic Regulation (CRG), Genome Bioinformatics, Barcelona, Spain  
Prof. Dr. Roderic Guigó
- 01 Nov. 2005 – 31  
May 2006      **Characterization of responsive and initiative genes in Alzheimer's disease triggered by alterations of the A $\beta$ 42/A $\beta$ 40 ratio**  
Ctr. for Molecular Biology Heidelberg (ZMBH), University of Heidelberg, Germany  
Prof. Dr. Tobias Hartmann
- 24 Jul. 2005 – 03  
Sep. 2005      **Studies on gene expression in individual rat cerebral artery endothelial cells using RT-PCR**  
Neurosurgery Research Institute, University Hospital Mannheim, Germany  
Prof. Dr. Dr. Lothar Schilling
- 01 Aug. 2003 – 31  
Dec. 2003      **Cloning, expression, and purification of *drosophila* MSL-1 and MSL-2**  
EMBL (European Molecular Biology Laboratory), Heidelberg, Germany  
Dr. Asifa Akhtar
- 15 Jul. 2002 –  
30 Sep. 2002      **Molecular Characterization of the *Arabis mosaic nepovirus***  
Centre for Green Genetic Engineering (CGG), Neustadt an der Weinstraße, Germany  
Dr. Gabi Krczal

---

---

**PRESENTATIONS AT CONGRESSES**

---

---

- Poster presentation at the 3<sup>rd</sup> annual conference of the Society for Laboratory Automation & Screening (SLAS), January 18 – 22, 2014, San Diego, CA, USA
- Poster presentation at the MipTec – The Leading European Event for Drug Discovery ; September 24 – 26, 2013, Basel, Switzerland
- Oral presentation at the 6<sup>th</sup> Interact symposium; March 22, 2013, Munich, Germany
- Poster presentation at the 11<sup>th</sup> International Congress on Alzheimer's & Parkinson's Diseases (AD/PD); March 6 –10, 2013, Florence, Italy
- Poster presentation at the 2<sup>nd</sup> annual conference of the Society for Laboratory Automation & Screening (SLAS), January 12 – 16, 2013, Orlando, FL, USA
- Oral presentation at the MipTec – The Leading European Event for Drug Discovery; September 23 – 26, 2012, Basel, Switzerland
- Oral presentation at the BioVaria 2012; Europe's Next Top Technologies; May 15, 2012, Munich, Germany
- Poster presentation at the MipTec – The Leading European Event for Drug Discovery; October 19 – 22, 2011, Basel, Switzerland
- Poster presentation at the 10<sup>th</sup> International Congress on Alzheimer's & Parkinson's Diseases (AD/PD); March 9 –13, 2011, Barcelona, Spain
- Poster presentation at the 40<sup>th</sup> Annual Meeting of the Society for Neuroscience; November 13 – 17, 2010, San Diego, CA, USA
- Poster presentation at the MipTec – The Leading European Event for Drug Discovery ; September 20 – 24, 2010, Basel, Switzerland
- Poster presentation at the 39<sup>th</sup> Annual Meeting of the Society for Neuroscience; October 17– 21, 2009, Chicago, IL, USA
- Poster presentation at the MipTec – The Leading European Event for Drug Discovery ; October 13 – 15, 2009, Basel, Switzerland
- Oral presentation at the International Conference on Alzheimer's Disease (ICAD); 11-16 July 2009, Vienna, Austria

---

---

**AWARDS**

---

---

- The top student poster award at the at the 2<sup>nd</sup> annual conference of the Society for Laboratory Automation & Screening (SLAS2013), Orlando, FL, USA
- Young Scientist Award of the Society for Laboratory Automation & Screening (SLAS), MipTec 2012, Basel, Switzerland
- Poster award of the Graduate School of Systemic Neurosciences, Ludwig Maximilian University of Munich, 2012

## PUBLICATIONS AND PATENTS

- Kamran Honarnejad, Alexander Daschner, Armin Giese, André Gehring, Franz Bracher, Aleksandra Szybinska, Jacek Kuznicki, Jochen Herms. “*Identification of tetrahydrocarbazoles as novel multifactorial drug candidates in the treatment of Alzheimer’s disease*”. (Manuscript under review in Translational Psychiatry)
- Kamran Honarnejad, Achim K. Kirsch, Alexander Daschner, Aleksandra Szybinska, Jacek Kuznicki, Jochen Herms. “*FRET-Based Calcium Imaging: A Tool for High-Throughput/Content Phenotypic Drug Screening in Alzheimer Disease*” (J Biomol Screen. 2013 Dec;18(10):1309-20); doi: 10.1177/1087057113502672
- Kamran Honarnejad, Alexander Daschner, Armin Giese, Andrea Zall, Boris Schmidt, Aleksandra Szybinska, Jacek Kuznicki, Jochen Herms. “*Development and Implementation of a High-throughput Compound Screening Assay for Targeting Disrupted ER Calcium Homeostasis in Alzheimer’s Disease*”. (PLoS One. 2013 Nov 15;8(11):e80645); doi:10.1371/journal.pone.0080645
- Kamran Honarnejad, Sven Lammich, Christian K.E. Jung, Thomas Arzberger, Hans Kretschmar, Jochen Herms. “*Involvement of presenilin holoprotein upregulation in calcium dyshomeostasis of Alzheimer’s disease*”. (J Cell Mol Med. 2013 Feb;17(2):293-302); doi: 10.1111/jcmm.12008
- Kamran Honarnejad, Jochen Herms. “*Presenilins: role in calcium homeostasis*” (Int J Biochem Cell Biol. 2012 Nov;44(11):1983-6); doi: 10.1016/j.biocel.2012.07.019
- Kamran Honarnejad, Alexander Daschner, Jochen Herms, Franz Bracher, Jacek Kuźnicki, André P. Gehring. “*Novel means and methods for treating diseases of the central nervous system, metabolic and cardiac diseases and aging*”. (Priority European Patent Application EP 12160864, 22 March 2012; PCT Patent Application PCT/EP2013/055969, 21 March 2013; Pub. No. WO/2013/139929, 26 Sep 2013)
- Christian K. E. Jung, Martin Fuhrmann, Kamran Honarnejad, Fred Van Leuven, Jochen Herms. “*Role of Presenilin1 in Structural Plasticity of Cortical Dendritic Spines in vivo*” (2011 Dec;119(5):1064-73); doi: 10.1111/j.1471-4159.2011.07503.x
- Kamran Honarnejad, Lukasz Bojarski, Jacek Kuznicki, Jochen Herms. “*Dysregulated Endoplasmic Reticulum calcium release in Alzheimer’s disease: A paradigm for high throughput drug/siRNA screens*” (Alzheimer’s & Dementia Vol. 5, Issue 4, ICAD Conference Suppl., July 2009); doi: 10.1016/j.jalz.2009.04.500
- Markus Uhrig, Peter Brechlin, Olaf Jahn, Yuri Knyazev, Annette Weninger, Laura Busia, Kamran Honarnejad, Markus Otto, Tobias Hartmann. “*Upregulation of CRABP1 in human neuroblastoma cells overproducing the Alzheimer-typical Abeta42 reduces their differentiation potential.*” (BMC Med. 2008 Dec 16;6:38); doi: 10.1186/1741-7015-6-38



**Eidesstattliche Versicherung/Affidavit**

Hiermit versichere ich an Eides statt, dass ich die vorliegende Dissertation "*Discovery and characterization of novel drugs for treatment of Alzheimer's disease from a high-throughput compound screen*" selbstständig angefertigt habe, mich außer der angegebenen keiner weiteren Hilfsmittel bedient und alle Erkenntnisse, die aus dem Schrifttum ganz oder annähernd übernommen sind, als solche kenntlich gemacht und nach ihrer Herkunft unter Bezeichnung der Fundstelle einzeln nachgewiesen habe.

I hereby confirm that the dissertation "*Discovery and characterization of novel drugs for treatment of Alzheimer's disease from a high-throughput compound screen*" is the result of my own work and that I have only used sources or materials listed and specified in the dissertation.

München, 29 April 2014

Munich, 29 April 2014

Kamran Honarnejad



The author of this doctoral thesis has majorly contributed to chapter 3 (cumulative thesis: based on paper I) by completely writing the manuscript and preparing the figures.

The author of this doctoral thesis has majorly contributed chapter 5 (cumulative thesis: based on paper II) of this thesis by conceiving, designing and performing the experiments, analyzing the data, writing the entire manuscript and designing all the figures.

The author of this doctoral thesis has majorly contributed to chapter 6 (cumulative thesis: paper based on III) of this thesis by conceiving, designing and performing the experiments, analyzing parts of the data, preparing the figures and entirely writing the manuscript.

The author of this doctoral thesis has majorly contributed to chapter 7 (cumulative thesis: based on paper IV) of this thesis by conceiving, designing and performing the experiments, analyzing the data, preparing the figures and entirely writing the manuscript.

Munich, 29 April 2014

Kamran Honarnejad

Prof. Dr. Jochen Herms